DOT/FAA/AR-03/55

Office of Aviation Research
Washington, D.C. 20591

Investigation of Type II and Type IV Aircraft Ground Anti-Icing Fluid Aerodynamic Certification Standards

July 2003

Final Report

This document is available to the U.S. public through the National Technical Information Service (NTIS), Springfield, Virginia 22161.



U.S. Department of Transportation
Federal Aviation Administration

NOTICE

This document is disseminated under the sponsorship of the U.S. Department of Transportation in the interest of information exchange. The United States Government assumes no liability for the contents or use thereof. The United States Government does not endorse products or manufacturers. Trade or manufacturer's names appear herein solely because they are considered essential to the objective of this report. This document does not constitute FAA certification policy. Consult your local FAA aircraft certification office as to its use.

This report is available at the Federal Aviation Administration William J. Hughes Technical Center's Full-Text Technical Reports page: actlibrary.tc.faa.gov in Adobe Acrobat portable document format (PDF).

Technical Report Documentation Page

1. Report No.	2. Government Accession No.	3. Recipient's Catalog No.
DOT/FAA/AR-03/55		

4. Title and Subtitle	5. Report Date
INVESTIGATION OF TYPE II AND TYPE IV AIRCRAFT GROUND ANTI-ICING FLUID AERODYNAMIC CERTIFICATION STANDARDS	July 2003
	6. Performing Organization Code

7. Author(s)	8. Performing Organization Report No.
Arlene Beisswenger, Guy Fortin, and Jean-Louis Laforte	

9. Performing Organization Name and Address	10. Work Unit No. (TRAIS)
Anti-icing Materials International Laboratory University of Quebec at Chicoutimi 555 University Boulevard Chicoutimi, Quebec G7H 2B1	11. Contract or Grant No. DTFA0302P10157

12. Sponsoring Agency Name and Address	13. Type of Report and Period Covered
U.S. Department of Transportation Federal Aviation Administration Office of Aviation Research Washington, DC 20591	Final Report
	14. Sponsoring Agency Code AFS-200, ANM-111N

15. Supplementary Notes

The Federal Aviation Administration William J. Hughes Technical Center COTR was Charles Masters.

16. Abstract

The certification process for aircraft ground anti-icing fluids involves flat-plate wind tunnel aerodynamic flow-off tests. This test method was developed in 1990 from flight and wind tunnel test results of full-scale and model airfoils and flat plates. The resulting lift losses were then correlated to the Boundary Layer Displacement Thickness (BLDT) on a flat plate. This correlation was made for Type II fluids existing at the time. Since the introduction of Type IV fluids in 1994, with significantly longer anti-icing endurance times, the same test procedure was applied. However, Type IV fluids are generally more viscous than Type II fluids of the same concentration. At the Federal Aviation Administration's request, a study was undertaken to determine if aerodynamic certification testing should be different for Type IV fluids compared to Type II. A comparison of existing certification BLDT data showed no significant differences between fluids, nor, more specifically, between Type II and Type IV fluids. Tests on five commercial fluids, two typical Type II and three typical Type IV fluids, with initial thicknesses of 1, 2, and 4 mm showed that the thickness had little effect on BLDT and fluid elimination data, with the exception of one fluid. This effect manifested itself near the end of the temperature range at which this fluid is acceptable. Examination of energy data showed that more energy was required by the wind tunnel to move the Type II fluids compared to Type IV fluids. When these fluids were tested using an identical fixed fan speed profile at 0°, -10°, and -25°C, little difference was seen in the BLDTs compared to those generated by a certification profile adjusted to obtain the same acceleration. These preliminary tests suggest that the aerodynamic certification method developed for Type II fluids is adequate for assessing Type IV fluids.

17. Key Words	18. Distribution Statement
Aircraft anti-icing fluid, Type II, Type IV fluids, Takeoff, Flow-off, Certification, Deicing	This document is available to the public through the National Technical Information Service (NTIS), Springfield, Virginia 22161.

19. Security Classif. (of this report)	20. Security Classif. (of this page)	21. No. of Pages	22. Price
Unclassified	Unclassified	100	

TABLE OF CONTENTS

		Page
EXECUTIVE SUMMARY		xiii
1.	INTRODUCTION	1
1.1	Objective	2
1.2	Scope	2
2.	TASK 1: BLDT COMPARISONS	3
2.1	Test Fluids	4
2.2	Boundary Layer Displacement Thickness at 30 Seconds	5
2.3	Boundary Layer Displacement Thickness at 30 Seconds With Respect to the Acceptance Criteria	7
2.4	Maximum BLDT	11
2.5	Estimate of the Maximum BLDT Possible	13
2.5.1	Methodology	15
2.5.2	Boundary Layer Displacement Thickness at Station 3	18
2.5.3	Boundary Layer Displacement Thickness Evaluated at x Meters	18
2.5.4	Dry Boundary Layer Displacement Thickness	19
2.5.5	Results	20
2.5.5.1	Merging Position Estimation	20
2.5.5.2	Merging Position Correlation	20
2.5.5.3	Boundary Layer Thickness Correlation	21
2.5.5.4	Box Height for Required Merging	22
2.5.6	Boundary Layer Displacement Thickness Merging	22
2.6	Time of Maximum BLDT	23
2.7	Fluid Elimination	26
2.8	Boundary Layer Displacement Thickness at 50 Seconds	28
2.9	Boundary Layer Displacement Thickness Comparisons—Conclusions	29
3.	TASK 2: DIFFERENT INITIAL FLUID THICKNESSES	29
3.1	Test Fluids	30
3.2	Results	31
3.2.1	Kilfrost ABC-3	32

3.2.2 Clariant Safewing MPII 1951 35
3.2.3 Octagon Process MaxFlight 38
3.2.4 SPCA AD-480 41
3.2.5 Dow Ultra+ 44

3.3 Maximum Wave Height 47
3.4 Different Initial Fluid Thicknesses—Conclusion 48

4. TASK 3: ENERGY REQUIRED 48

4.1 Energy Depending on the Fan Frequency 49

4.1.1 Equations 49
4.1.2 Dry (No Fluid) Test Data 50
4.1.3 Dry and Reference Military Fluid Test Data 51
4.1.4 Energy Input for Test Fluids 54
4.1.5 Energy Input for Different Initial Fluid Thicknesses 57

4.1.5.1 Kilfrost ABC-3 57

4.1.5.2 Clariant Safewing MPII 1951 59

4.1.5.3 Octagon Process MaxFlight 62

4.1.5.4 SPCA AD-480 64

4.1.5.5 Dow Ultra+ 67

4.1.5.6 Energy Input for Different Initial Fluid Thicknesses—Summary 69

4.2 Fixed Fan Acceleration Profile 70

4.2.1 Kilfrost ABC-3 70
4.2.2 Clariant Safewing MPII 1951 73
4.2.3 Octagon Process MaxFlight 76
4.2.4 SPCA AD-480 79
4.2.5 Dow Ultra+ 82
4.2.6 Fixed Fan Acceleration Profile—Summary 84

5. CONCLUSIONS 84

5.1 Boundary Layer Displacement Thickness Comparisons 84
5.2 Different Initial Fluid Thicknesses 85
5.3 Energy Required 85

6. RECOMMENDATIONS 85

7. REFERENCES 86

LIST OF FIGURES

Figure		Page
1	Flat Plate Elimination Test Data Sheet for a Military Fluid at -10°C	3
2	Flat Plate Elimination Test Run	4
3	Boundary Layer Displacement Thickness at 30 sec., All Fluid Dilutions	5
4	Boundary Layer Displacement Thickness at 30 sec., Neat Fluids	6
5	Boundary Layer Displacement Thickness at 30 sec., 75/25 Dilutions	6
6	Boundary Layer Displacement Thickness at 30 sec., 50/50 Dilutions	7
7	Example of Results of an Aerodynamic Certification for an AMS1428 Fluid	8
8	Boundary Layer Displacement Thickness at 30 sec. With Respect to MIL Fluid, All Fluid Dilutions	9
9	Boundary Layer Displacement Thickness at 30 sec. With Respect to MIL Fluid, Neat Fluids	9
10	Boundary Layer Displacement Thickness at 30 sec. With Respect to MIL Fluid, 75/25 Dilutions	10
11	Boundary Layer Displacement Thickness at 30 sec. With Respect to MIL Fluid, 50/50 Dilutions	10
12	Maximum BLDT, All Fluid Dilutions	11
13	Maximum BLDT, Neat Fluids	12
14	Maximum BLDT, 75/25 Dilutions	12
15	Maximum BLDT, 50/50 Dilutions	13
16	Test Section Boundary Layers	13
17	Test Section Box in Wind Tunnel	14
18	Luan Phan Refrigerated Wind Tunnel	14

19	Velocity and BLDT at 1.55 and 0.53 meters	16
20	Velocity and BLDT at 1.55 and 0.83 meters	16
21	Velocity and BLDT at 1.55 and 1.03 meters	17
22	Velocity and BLDT at 1.55 and 1.28 meters	17
23	Merging Position Estimation Results	21
24	Time of Maximum BLDT, All Fluid Dilutions	23
25	Time of Maximum BLDT, Neat Fluids	24
26	Time of Maximum BLDT, 75/25 Dilutions	24
27	Time of Maximum BLDT, 50/50 Dilutions	25
28	Test Data Sheet for FPET of TIV-5 Fluid	25
29	Fluid Elimination Percent, All Dilutions	26
30	Fluid Elimination Percent, Neat Fluids	27
31	Fluid Elimination Percent, 75/25 Dilutions	27
32	Fluid Elimination Percent, 50/50 Dilutions	28
33	Boundary Layer Displacement Thickness at 50 sec., All Fluids, Neat and Diluted	29
34	Aerodynamic Test Results for Kilfrost ABC-3 With Three Different Initial Fluid Thicknesses	32
35	Percentage Fluid Elimination For Kilfrost ABC-3	34
36	Final Fluid Thickness for Kilfrost ABC-3	34
37	Aerodynamic Test Results for Clariant Safewing MPII 1951 With Three Different Initial Fluid Thicknesses	35
38	Percentage Fluid Elimination for Clariant Safewing MPII 1951	37
39	Final Fluid Thickness for Clariant Safewing MPII 1951	37
40	Aerodynamic Test Results for Octagon Process MaxFlight With Three Different Initial Fluid Thickness	38
41	Percentage Fluid Elimination for Octagon Process MaxFlight	40

42	Final Fluid Thickness for Octagon Process MaxFlight	40
43	Aerodynamic Test Results for SPCA AD-480 With Three Different Initial Fluid Thicknesses	42
44	Percentage Fluid Elimination for SPCA AD-480	43
45	Final Fluid Thickness for SPCA AD-480	43
46	Aerodynamic Test Results for Dow Ultra+ With Three Different Initial Fluid Thicknesses	44
47	Percentage Fluid Elimination for Dow Ultra+	46
48	Final Fluid Thickness for Dow Ultra+	46
49	Maximum Wave Height for 1-mm Initial Fluid Thickness	47
50	Maximum Wave Height for 2-mm Initial Fluid Thickness	47
51	Maximum Wave Height for 4-mm Initial Fluid Thickness	48
52	Test Data From a Dry Test Run	50
53	Power and Energy Required for the Dry Test	51
54	Energy After 30 sec. for Dry Run and Military Fluid	52
55	Energy Factor After 30 sec. for Dry Run and Military Fluid	52
56	Energy After 50 sec. for Dry Run and Military Fluid	53
57	Energy Factor After 50 sec. for Dry Run and Military Fluid	53
58	Energy Input After 30 sec. for Test Fluids	54
59	Energy Input After 50 sec. for Test Fluids	55
60	Energy Factor After 30 sec. for Test Fluids	56
61	Energy Factor After 50 sec. for Test Fluids	56
62	Energy Input After 30 sec. for Different Initial Fluid Thicknesses of Kilfrost ABC-3	57
63	Energy Input After 50 sec. for Different Initial Fluid Thicknesses of Kilfrost ABC-3	58

64 Energy Factor After 30 sec. for Different Initial Fluid Thicknesses of Kilfrost ABC-3 58

65 Energy Factor After 50 sec. for Different Initial Fluid Thicknesses of Kilfrost ABC-3 59

66 Energy Input After 30 sec. for Different Initial Fluid Thicknesses of Clariant Safewing MPII 1951 60

67 Energy Input After 50 sec. for Different Initial Fluid Thicknesses of Clariant Safewing MPII 1951 60

68 Energy Factor After 30 sec. for Different Initial Fluid Thicknesses of Clariant Safewing MPII 1951 61

69 Energy Factor After 50 sec. for Different Initial Fluid Thicknesses of Clariant Safewing MPII 1951 61

70 Energy Input After 30 sec. for Different Initial Fluid Thicknesses of Octagon Process MaxFlight 62

71 Energy Input After 50 sec. for Different Initial Fluid Thicknesses of Octagon Process MaxFlight 63

72 Energy Factor After 30 sec. for Different Initial Fluid Thicknesses of Octagon Process MaxFlight 63

73 Energy Factor After 50 sec. for Different Initial Fluid Thicknesses of Octagon Process MaxFlight 64

74 Energy Input After 30 sec. for Different Initial Fluid Thicknesses of SPCA AD-480 65

75 Energy Input After 50 sec. for Different Initial Fluid Thicknesses of SPCA AD-480 65

76 Energy Factor After 30 sec. for Different Initial Fluid Thicknesses of SPCA AD-480 66

77 Energy Factor After 50 sec. for Different Initial Fluid Thicknesses of SPCA AD-480 66

78 Energy Input After 30 sec. for Different Initial Fluid Thicknesses of Dow Ultra+ 67

79 Energy Input After 50 sec. for Different Initial Fluid Thicknesses of Dow Ultra+ 68

80 Energy Factor After 30 sec. for Different Initial Fluid Thicknesses of Dow Ultra+ 68

81 Energy Factor After 50 sec. for Different Initial Fluid Thicknesses of Dow Ultra+ 69

82 Fan Acceleration Profile for Kilfrost ABC-3 at -10°C 70

83	Boundary Layer Displacement Thickness Aerodynamic Performance for Kilfrost ABC-3	71
84	Fluid Elimination for Kilfrost ABC-3	72
85	Maximum Wave Heights for Both Ramps, Kilfrost ABC-3	72
86	Boundary Layer Displacement Thickness Aerodynamic Performance for Clariant Safewing MPII 1951	74
87	Fluid Elimination for Clariant Safewing MPII 1951	74
88	Example of Fixed Ramp Test at 0°C—Clariant Safewing MPII 1951	75
89	Example of Fixed Ramp Test at -25°C—Clariant Safewing MPII 1951	75
90	Maximum Wave Heights for Both Ramps, Clariant Safewing MPII 1951	76
91	Boundary Layer Displacement Thickness Aerodynamic Performance for Octagon Process MaxFlight	77
92	Fluid Elimination for Octagon Process MaxFlight	78
93	Maximum Wave Heights for Both Ramps, Octagon Process MaxFlight	78
94	Boundary Layer Displacement Thickness Aerodynamic Performance for SPCA AD-480	80
95	Fluid Elimination for SPCA AD-480	80
96	Example of Fixed Ramp Test at 0°C—SPCA AD-480	81
97	Maximum Wave Heights for Both Ramps, SPCA AD-480	81
98	Boundary Layer Displacement Thickness Aerodynamic Performance for Dow Ultra+	83
99	Fluid Elimination for Dow Ultra+	83
100	Maximum Wave Heights for Both Ramps, Dow Ultra+	84

LIST OF TABLES

Table		Page
1	Fluid Data Used for Comparison	5
2	Position and Section	19
3	Results for Positions	20
4	Average Results for Each Position Measured	20
5	Fluid Identification	30
6	WSET Times of Fluids Tested	31
7	Brookfield Viscosity (mPa•s)	31
8	Aerodynamic Performance Test Data for Kilfrost ABC-3	33
9	Aerodynamic Performance Test Data for Clariant Safewing MPII 1951	36
10	Aerodynamic Performance Test Data for Octagon Process MaxFlight	39
11	Aerodynamic Performance Test Data for SPCA AD-480	41
12	Aerodynamic Performance Test Data for Dow Ultra+	45
13	Summary of Energy and Energy Factor for the Different Thicknesses of the Fluids Tested	69
14	Aerodynamic Performance Test Data With Fixed Ramp for Kilfrost ABC-3	71
15	Aerodynamic Performance Test Data With Fixed Ramp for Clariant Safewing MPII 1951	73
16	Aerodynamic Performance Test Data With Fixed Ramp for Octagon Process MaxFlight	77
17	Aerodynamic Performance Test Data With Fixed Ramp for SPCA AD-480	79
18	Aerodynamic Performance Test Data With Fixed Ramp for Dow Ultra+	82

LIST OF SYMBOLS AND ACYRONYMS

AMIL	Anti-icing Materials International Laboratory
AMS	Aerospace Material Specification
BLDT	Boundary Layer Displacement Thickness
FIE	First Icing Event
FPET	Flat Plate Elimination Test
SAE	Society of Automotive Engineers
WSET	Water Spray Endurance Test
A	Cross-sectional area at the test section box input
B_2	Width at station 2
B_3	Width at station 3
C_3	Perimeter at station 3
δ^*	Boundary layer displacement thickness
δ_{dry}	Dry boundary layer thickness
D_0	Upper limit of BLDT at 0°C
D_{20}	Upper limit of BLDT at 20°C
E	Wind tunnel energy
H	Shape factor
H_3	Height at station 3
H_2	Height at station 2
λ	Power factor
l_{cone}	Cone length at the box input
μ_a	Dynamic viscosity
P_1	Static pressure at station 1 in test section
P_2	Static pressure at station 2 in test section
P_3	Static pressure at station 3 in test section
P	Motor power
ρ_{air}, ρ_a	Air density
R_e	Reynolds number
r.h.	Relative humidity
S_2	Tests duct cross-section area at station 2
S_3	Tests duct cross-section area at station 3
t	Time, sec
t_o	t_{end}
T	Time
T_a	Average Air Temperature
T_f	Average Fluid Temperature
U	Velocity in the test section box
U_∞	Free stream speed
V	Velocity
x	Position
Λ	Energy factor

EXECUTIVE SUMMARY

It had been brought to the attention of the Society of Automotive Engineers SAE G-12 Fluids subcommittee that certain airlines had experienced aerodynamic abnormalities when using Type IV aircraft ground anti-icing fluids compared to Type II fluids. The concerns related to the apparent reduction in aerodynamic performance of aircraft treated with Type IV anti-icing fluids compared to Type II anti-icing fluids. The tentative conclusion was that the Type IV fluid performance reduction, compared to the Type II fluid, is unknown and that the certification process of Type IV fluids, which is equal to that of Type II fluids, may not be justified.

The certification process for all thickened fluids includes the Flat Plate Elimination Test (FPET) of Annex B and C of AMS1428, which is based on fluid elimination on a flat surface. The test procedure was developed in 1990, before the introduction of Type IV fluids. Later, when Type IV fluids with significantly longer anti-icing endurance times were introduced in 1994, the same test procedure, proven for Type II fluids, was applied to the Type IV fluids. However, Type IV fluids are generally more viscous than Type II fluids with the same concentration and, therefore, when applied to an aircraft wing may have different flow-off characteristics and leave a thicker residue.

The higher-viscosity, modified flow-off behavior, and the potential greater residue thickness could imply that an aircraft wing may require more shearing forces to displace a Type IV fluid compared to a Type II fluid. Therefore, at the Federal Aviation Administration's request, the Anti-icing Materials International Laboratory was tasked to run preliminary aerodynamic tests as part of a plan to resolve this issue.

The objective of this study was to conduct high-speed ramp investigations and tests, including FPET to determine boundary layer displacement thickness (BLDT), conduct fluid thickness comparisons, flow-off characteristic differences for various Type II and Type IV fluids, and the sensitivity of fluid thickness on the results of the FPET.

The main objective of these comparative tests was to determine if there was a significant difference between Type II and Type IV anti-icing fluids that would support different aerodynamic testing and certification testing for Type IV fluids compared to Type II fluids.

The project was divided into three tasks:

- The first task consisted of using existing certification FPET data to compare information such as the maximum BLDT and the time at which this occurs to ascertain if there are differences between the Type II and Type IV fluids.

- The second task consisted of running FPET tests using initial fluid thicknesses of 1, 2, and 4 mm to compare the BLDTs, the energy required to move the fluid, and the amount of fluid remaining. A normal certification FPET is run with 2-mm initial fluid thickness.

- Different fan speed profiles are used during certification of different fluids at different temperatures to achieve the required takeoff acceleration profile. Therefore, the third task consisted of conducting the necessary tests and investigations to (1) determine the power and energy required to eliminate different fluids, depending on the fan frequency

(speed) and (2) determine whether, if the same fan acceleration profile is used for all fluids, the same peak BLDT is obtained.

BLDT Comparisons

Comparisons of (1) the BLDT at 30 sec., (2) the BLDT at 30 sec. (with respect to the acceptance criteria limit), (3) the maximum BLDT, (4) time of maximum BLDT, (5) the fluid elimination, and (6) the BLDT at 50 sec. showed no clear difference between Type II and Type IV fluids.

A parallel study made on the merging of the upper and lower boundary layers showed that, for a sample fluid, the test section merged 1.16 m from its entry. It also showed that at station 3, where the BLDT is measured for a certification FPET 1.55 m from the entry, the maximum BLDT that can be measured is 17 mm. To ensure that the boundary layer thicknesses do not merge, the required box height at the output would be 117.42 mm, 8 mm higher than it currently is. However, to measure the BLDT at 30 sec. for a certification test, the value is usually below about 10 mm to be acceptable, and therefore, the current box height is more than adequate.

Different Initial Fluid Thicknesses

Examination of BLDT and elimination data from FPET testing on two Type II and three Type IV commercial fluids with initial fluid thicknesses of 1, 2, and 4 mm showed that for four of the five fluids the initial fluid thickness had little or no effect on the BLDT and fluid elimination. However, for one of the Type IV fluids, there was some difference with the 4-mm initial thickness at -25°C, where higher BLDT measurements and more fluid remaining on the test section floor following the test were noted. These higher BLDT values may partially be due to the fact that, for this fluid, -25°C is very near to its acceptable temperature limit, a point at which all fluids tend to show much variation in BLDT measurements. Therefore, the initial fluid thickness may only have an effect on a fluid at critical temperatures, near the fluid's acceptable temperature limit.

Energy Required

The amount of energy and the energy factor, which takes into account the energy lost outside the test section insert, of Type II and Type IV fluids were compared. The results showed that more energy was required to move the Type II fluids compared to the Type IV fluids.

The energy required to move the test fluids with three different initial thicknesses was calculated. The data showed that, in most cases, the 4-mm thickness required the most energy. For some cases, there was no difference. In most cases, the 4-mm thickness required about 5% more energy, except for one Type IV fluid that used a 10% higher energy factor.

FPET were run using the same fan acceleration profile for all fluids at all temperatures. For three of the five fluids tested with the fixed ramp, there was little difference seen in the BLDT at 30 sec., fluid elimination, and maximum wave heights when compared to the certification ramp, where the fan frequency was adjusted, depending on fluid and temperature, to obtain the same acceleration profile. The two other fluids had slightly higher BLDT values for the fixed ramp, possibly within error.

1. INTRODUCTION.

It had been brought to the attention of the Society of Automotive Engineers SAE G-12 Fluids Subcommittee that certain airlines had experienced aerodynamic abnormalities when using Type IV aircraft ground anti-icing fluids compared to Type II fluids. The concerns were related to the apparent reduction in aerodynamic performance of these aircraft when treated with Type IV anti-icing fluids compared to Type II anti-icing fluids. A presentation given by the airlines [1] described flight tests conducted with different Type IV fluids and thicknesses and one Type II fluid. The results of the flight tests [2] indicated that for Type IV fluids there was an apparent

- increase in stick force to rotate aircraft,
- reduction in elevator control tab effectiveness,
- reduction in elevator effectiveness,
- reduction in pitch moment due to less effective elevator power, and
- perceived increase in total aircraft drag (aircraft felt sluggish, less responsive, and there was a slight roll tendency during initial climb).

The tentative conclusion was that the Type IV fluid performance reduction, compared to the Type II fluid, is unknown and that the certification process of Type IV fluids, which is equal to that of the Type II fluids, may not be justified.

The certification process for all thickened fluids includes the Flat Plate Elimination Test (FPET) of Annex B and C of AMS1428 [3], or now the proposed AS5900 [4], which is based on fluid elimination on a flat surface. The test procedure was developed in 1990 [5, 6, and 7] before the introduction of Type IV fluids. Supporting technical documents included flight tests and wind tunnel test results on full-scale and model airfoils and flat plates. The resulting lift losses were then correlated to the Boundary Layer Displacement Thickness (BLDT) on a flat plate. This correlation was made for the Type II fluids existing at that time.

When Type IV fluids were introduced in 1994, with significantly longer anti-icing endurance times, the same test procedure proven for Type II fluids was applied to Type IV fluids. However, Type IV fluids are generally more viscous than Type II fluids of the same concentration and, therefore, when applied to an aircraft wing may have different flow-off characteristics and leave a thicker residue.

The apparent higher-viscosity, modified flow-off behavior, and the greater residue thickness could imply that an aircraft wing may require more shearing forces to displace a Type IV fluid versus a Type II fluid. Therefore, the Federal Aviation Administration (FAA), with the aerodynamics working group of the SAE G-12 Fluids Subcommittee, tasked the Anti-icing Materials International Laboratory (AMIL) [8] to investigate this concern. AMIL conducted preliminary tests using its wind tunnel to examine various fluid thicknesses on plates and investigated fluid flow-off characteristics, shear forces required to eliminate the fluid, and the

sensitivity of fluid thickness in elimination of the fluids. Also at the FAA's request, AMIL ran tests based upon existing FPET and high-speed ramp tests on different brands of Type II and IV fluids.

1.1 OBJECTIVE.

The objective of this effort was to conduct high-speed ramp investigations and tests, including FPET to determine various BLDTs, fluid thickness comparisons, and flow-off characteristic differences for various Type II and Type IV fluids, and the sensitivity of fluid thickness on the results of the FPET.

The main objective of these comparative tests was to determine if there was a significant difference between Type II and Type IV anti-icing fluid behavior that would support different aerodynamic testing and certification testing for Type IV and Type II fluids.

1.2 SCOPE.

The project was divided into three tasks:

1. BLDT Comparisons

   During a certification wind tunnel FPET run, all BLDT data are measured during the course of the test run. However, the BLDT used to calculate fluid acceptance is only at 30 sec., once the acceleration from 5 to 65 m/s is complete. This is considered to be equivalent to takeoff rotation speed time.

   The first task used existing certification FPET data to examine the maximum BLDT and the time at which this occurs to ascertain if there are differences between the Type II and Type IV fluids.

2. Different Initial Fluid Thicknesses

   Currently, certification tests are run with an initial fluid thickness of 2 mm. The question arose in the Aerodynamics Workgroup [5] meeting as to whether the thicknesses have increased with the use of Type IV fluids, which are generally more viscous, and therefore, more fluid remains on an aircraft wing after application.

   Therefore, tests were conducted using initial fluid thicknesses of 1, 2, and 4 mm at temperatures of 0°, -10°, and -25°C to obtain three data points per temperature and fluid thickness combination.

3. Energy Required

   Currently, during a certification FPET, the speed of the fan is initially adjusted to obtain the required 5 m/s velocity. The fan frequency is then increased to obtain a linear wind speed acceleration of 2.6 m/s² for 25 sec., levelling off at 65 m/s (figure 1). To obtain this profile on different fluids with different viscosities, the acceleration of the fan

frequency (speed) is adjusted, depending on the fluid and temperature. Therefore, this task consisted of conducting the necessary tests and investigations to

a. determine the power and energy required to eliminate different fluids, depending on the fan frequency (speed).

b. determine whether, if the same fan acceleration profile is used for all fluids, the same peak BLDT is obtained.

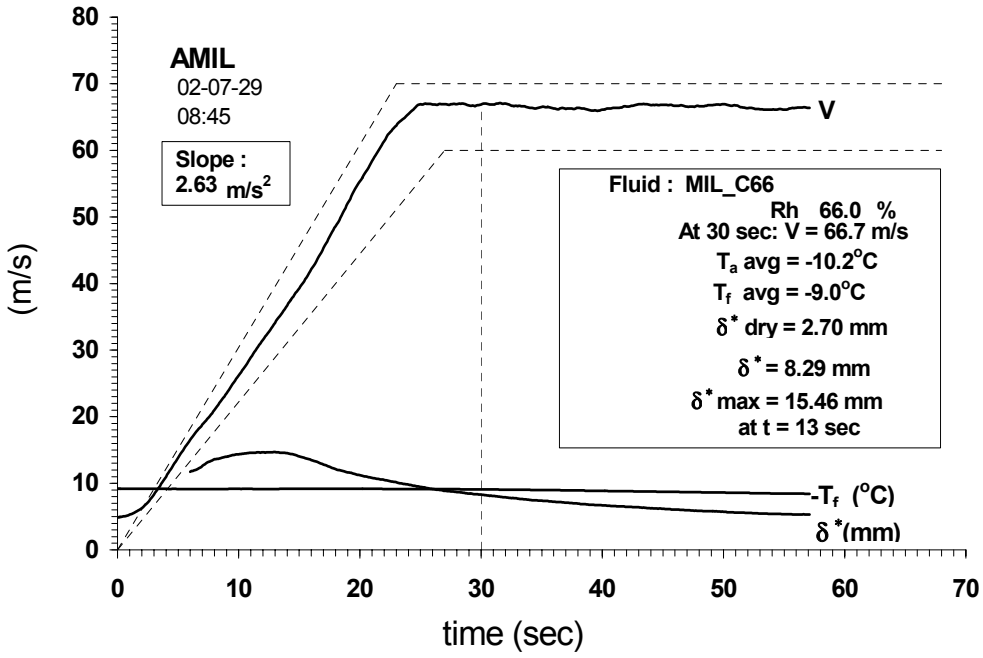

FIGURE 1. FLAT PLATE ELIMINATION TEST DATA SHEET FOR A MILITARY FLUID AT -10°C

2. TASK 1: BLDT COMPARISONS.

Currently, AMIL is the only laboratory accredited to certify deicing and anti-icing fluids for aerodynamic acceptance. Therefore, all commercial deicing and anti-icing fluids have been tested at AMIL, and AMIL has retained the test data.

This task used existing aerodynamic acceptance certification data at AMIL to compare variables such as BLDT at 30 sec., maximum BLDT, time at which the maximum BLDT occurs, fluid elimination, and BLDT at 50 sec. to determine whether there is a difference between Type II and Type IV fluids.

A typical FPET consists of pouring 1 liter of fluid onto the test duct floor of the wind tunnel. After 5 minutes of wind at 5 m/s, to equilibrate the fluid to the air temperature, the wind is accelerated to 65 m/s over a nominal 25 sec. period at an acceleration of 2.6 m/s² (figure 1)

according to Annex B of AMS1424 and AMS1428 [3], now AS5900 [4]. The 65 m/s speed is maintained for 30 sec.

For a certification FPET test, the BLDT at 30 sec. is recorded. This is considered a representative takeoff time for large transport type jet aircraft [5]. At this time, the BLDT must be below an acceptable limit based on a reference military fluid, which is tested simultaneously. However, each fluid can have a different BLDT at each temperature interval, as long as it is below the limit. The first comparison involves comparing the different BLDT values at the 30 sec. mark.

For the same test, a maximum BLDT will be obtained sometime before the 30-sec. mark. The maximum will occur as the fluid begins to move down the test plate (figure 2). Then the BLDT levels out as the acceleration ends.

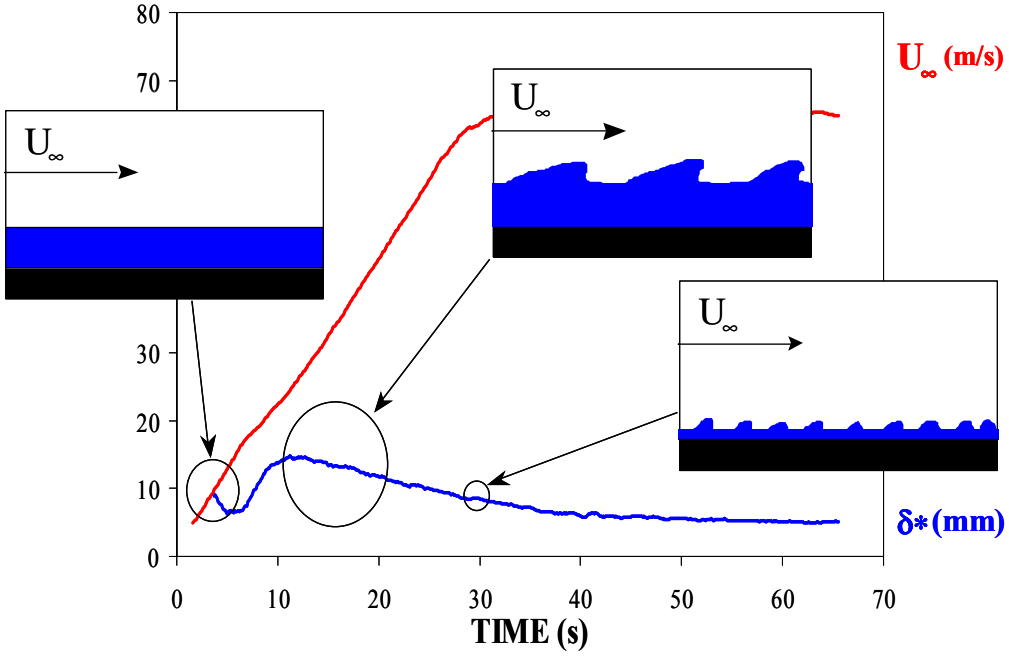

FIGURE 2. FLAT PLATE ELIMINATION TEST RUN

Therefore, the maximum BLDT and the time at which it occurs can be compared to determine if there are notable differences between different fluids, more specifically, between Type II and Type IV fluids.

The fluid elimination and the BLDT at 50 sec. were also compared.

2.1 TEST FLUIDS.

This task used existing certification data, therefore, data from all certified fluids were used. Since the data used was from confidential certification reports, the fluids are not identified, only whether they are a Type II or Type IV fluid. A list of the fluids studied is presented in table 1.

TABLE 1. FLUID DATA USED FOR COMPARISON

Company	Fluid	Type
Clariant	Safewing MPII 1951	II
Kilfrost	ABC-3	II
Kilfrost	ABC-II Plus	II
SPCA	AD-104/N	II
SPCA	Ecowing 26	II
Clariant	Safewing MPIV 1957	IV
Clariant	Safewing MPIV 2001	IV
Clariant	Safewing MPIV Four	IV
Clariant	Safewing MPIV Protect 2012	IV
Dow	Ultra+	IV
Kilfrost	ABC-S	IV
Octagon	MaxFlight	IV
SPCA	AD 480	IV

2.2 BOUNDARY LAYER DISPLACEMENT THICKNESS AT 30 SECONDS.

For a certification FPET test, the BLDT at 30 sec. is recorded as the BLDT for that test. Although the BLDT at 30 sec. must be below the acceptance criteria limit, it can be anywhere below. Figure 3 presents a compilation of the BLDT at 30 sec. data for all fluids, neat, 75/25, and 50/50 dilution. For all graphs, solid symbols represent the Type II fluids, and the open symbols and shapes represent Type IV fluids. Figure 4 shows the neat fluid data, figure 5 shows the 75/25 dilution, and figure 6 shows the 50/50 dilution.

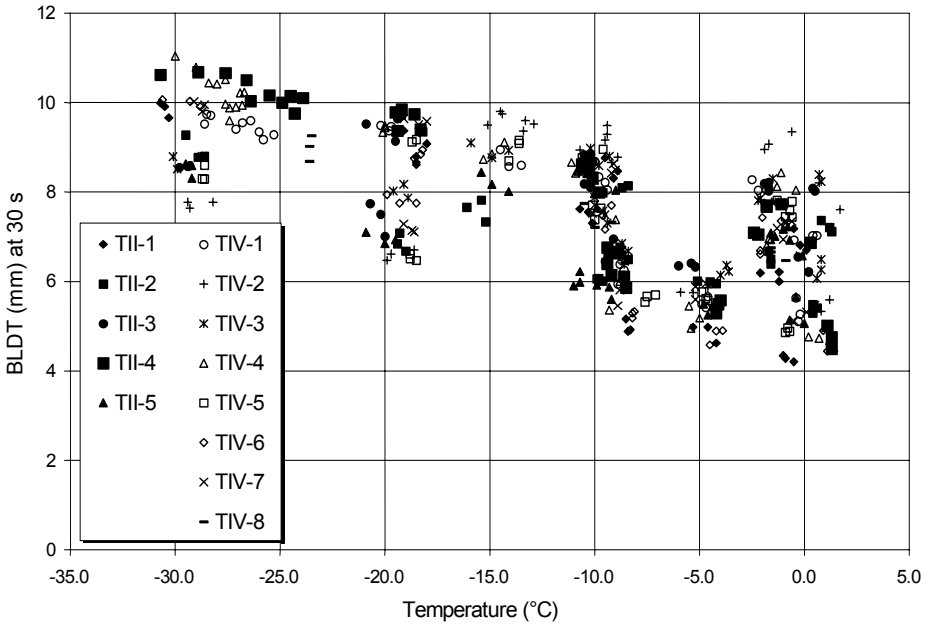

FIGURE 3. BOUNDARY LAYER DISPLACEMENT THICKNESS AT 30 sec., ALL FLUID DILUTIONS

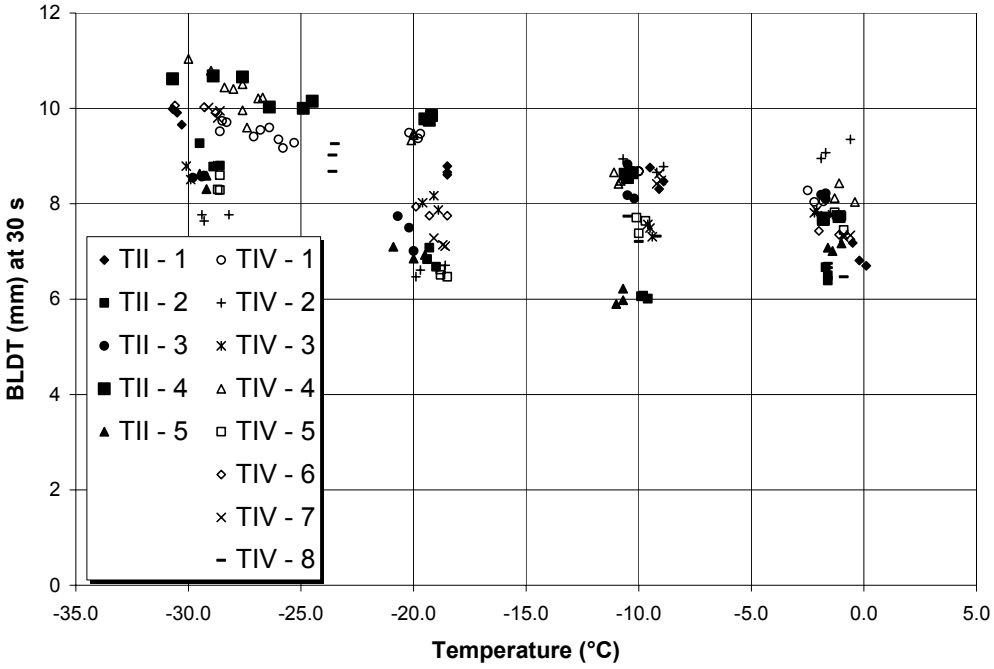

FIGURE 4. BOUNDARY LAYER DISPLACEMENT THICKNESS AT 30 sec., NEAT FLUIDS

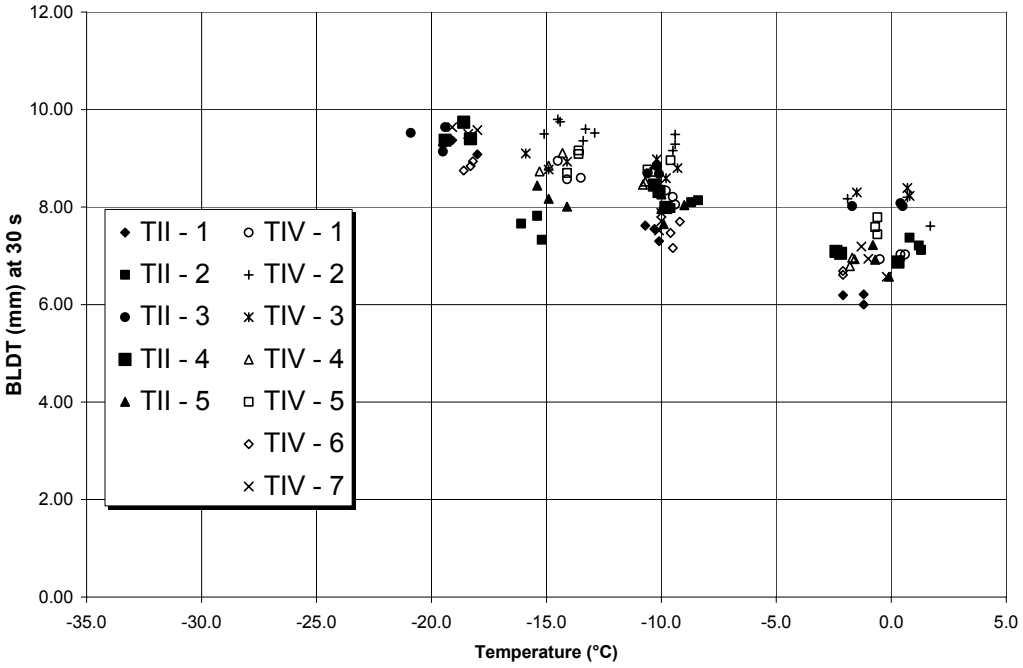

FIGURE 5. BOUNDARY LAYER DISPLACEMENT THICKNESS AT 30 sec., 75/25 DILUTIONS

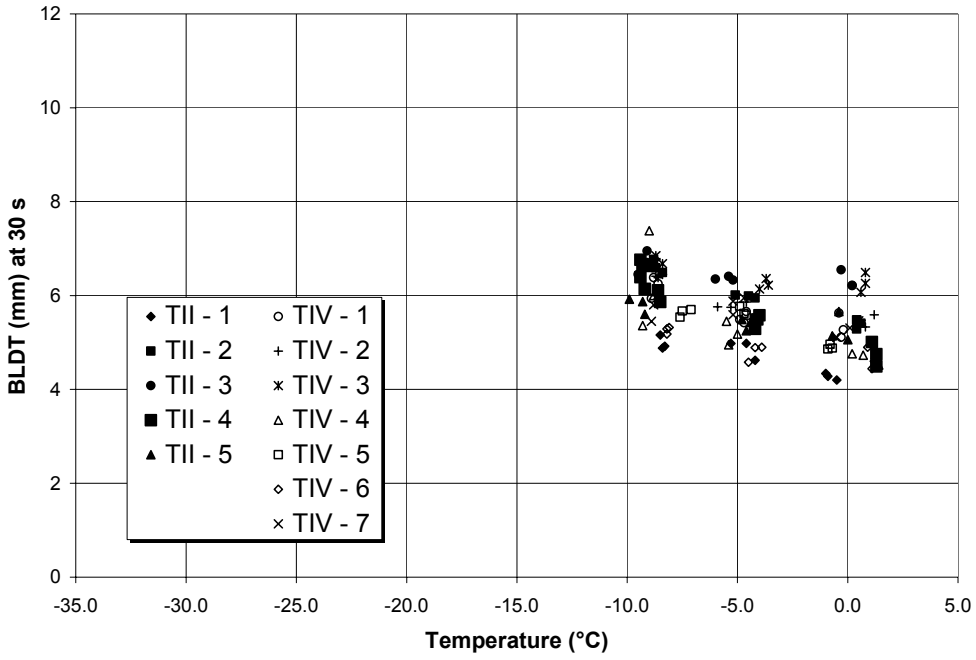

FIGURE 6. BOUNDARY LAYER DISPLACEMENT THICKNESS AT 30 sec., 50/50 DILUTIONS

All the graphs show an increase in BLDT with decreasing temperature, with an average scatter of 2 mm at each temperature interval for each dilution. The data shows no clear difference for the BLDT at 30 sec. between the Type II and Type IV fluids.

2.3 BOUNDARY LAYER DISPLACEMENT THICKNESS AT 30 SECONDS WITH RESPECT TO THE ACCEPTANCE CRITERIA.

Figure 7 shows an example of the results of an AMS1428 fluid certification, i.e., a Type II or Type IV fluid. A fluid is considered acceptable at a test temperature if "none of the independent BLDT measurements is greater than the acceptance criteria." [3] The figure shows how all the data is compared to the acceptance criteria or limit, which is based on data measured simultaneously for the reference military fluid, MIL-A-8243. The maximum acceptable BLDT value as a function of temperature is established according to dry and reference fluid results. Values of D_{20} and D_0 are used as the upper limit for BLDT values. These values are defined as

$$D_0 = \delta_r^* + 0.71\left(\delta_r^* - \delta_d^*\right) \text{ at } 0°\text{C} \quad (1)$$

$$D_{20} = \delta_r^* - 0.18\left(\delta_r^* - \delta_d^*\right) \text{ at } -20°\text{C} \quad (2)$$

where

δ_r^* = the reference BLDT value at 0°C in equation 1 and at -20°C in equation 2, obtained by interpolation from a straight line fitting of the reference BLDT values measured at 0°, -10°, -20°, and -25°C

δ_d^* = the average of all dry BLDT values measured

D_{20} = the limit for below -20°C, usually around 10 mm, can vary between 9.5 and 10.5 mm.

D_0 = the limit at 0°C can vary more, usually between 8.0 and 9.5 mm.

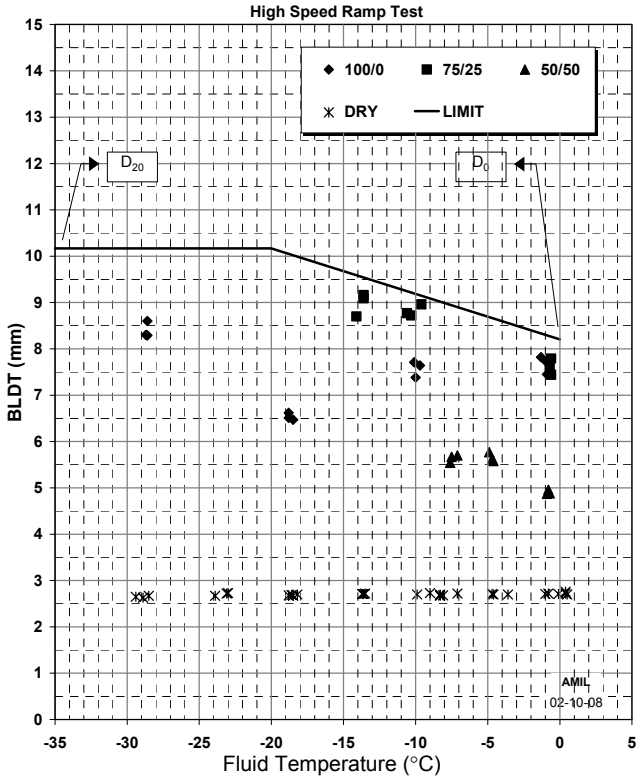

FIGURE 7. EXAMPLE OF RESULTS OF AN AERODYNAMIC CERTIFICATION FOR AN AMS1428 FLUID

Since a candidate fluid will always be tested with respect to the military fluid, a comparison between fluids should be made compared to its acceptance criteria.

Figure 8 shows a comparison of the BLDT at 30 sec. for all fluids, neat, and their dilutions. The x axis represents the test temperature and the y axis values are the BLDT at 30 sec. of the fluids minus the acceptance criteria value at that temperature, i.e., the difference between the BLDT and the acceptance criteria.

The data is then separated according to fluid dilution in figures 9 through 11 for the neat fluid, 75/25 dilution, and 50/50 dilution respectively.

Since these values were compared to the acceptance criteria and based on its shape (figure 7), the distribution with temperature seen in section 2.2 is not seen here. Much variation can be seen for the neat fluid, which can be up to 4 mm. For most, the variation is in the 2-mm range. None of the three graphs show a clear difference between Type II and Type IV fluids.

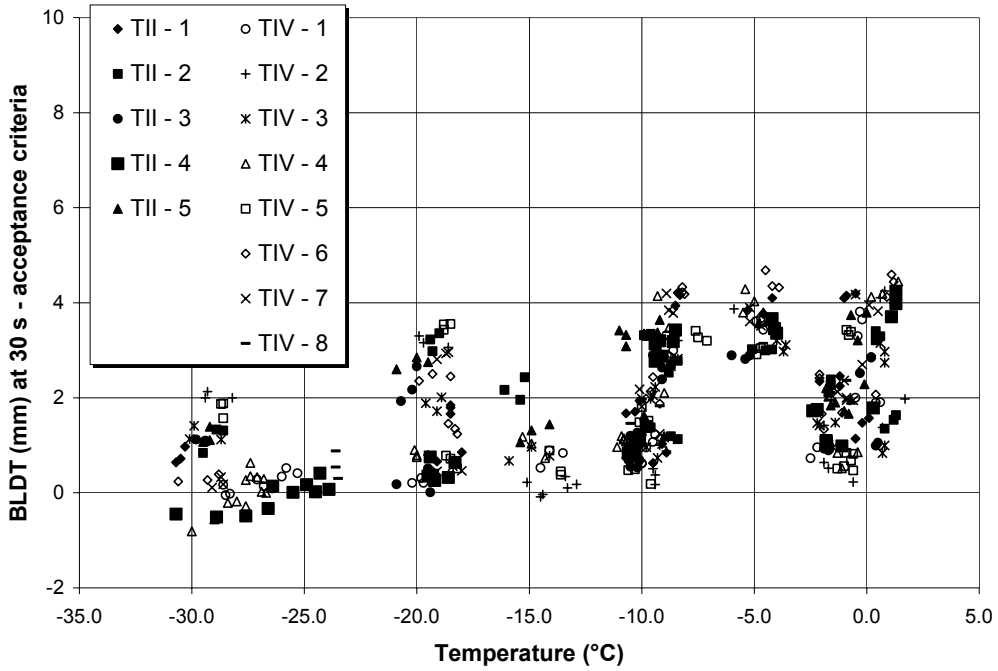

FIGURE 8. BOUNDARY LAYER DISPLACEMENT THICKNESS AT 30 sec. WITH RESPECT TO MIL FLUID, ALL FLUID DILUTIONS

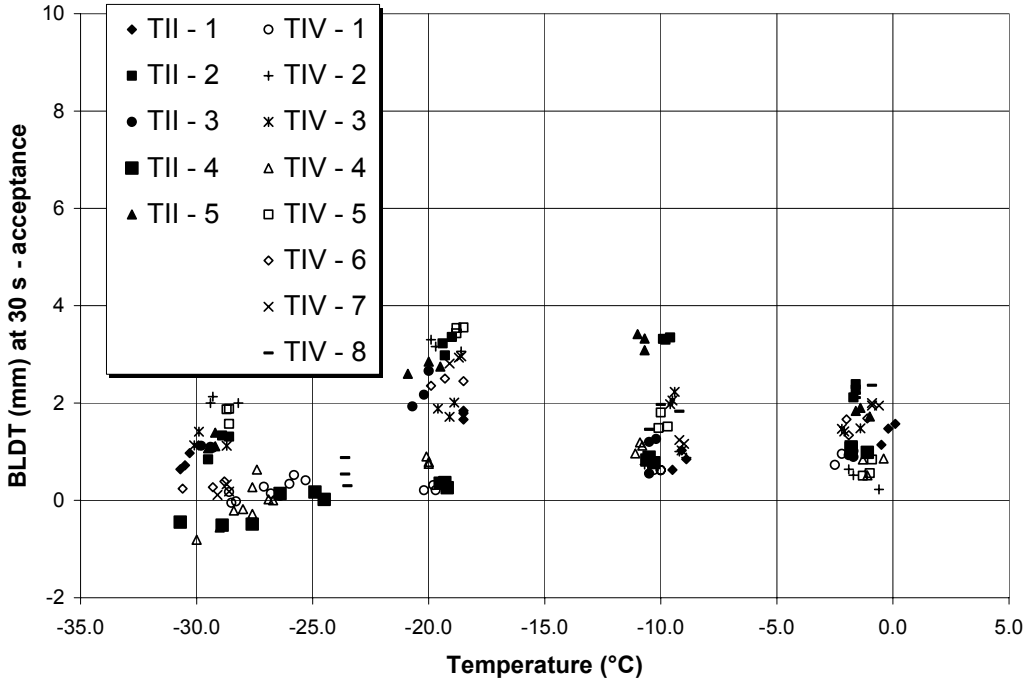

FIGURE 9. BOUNDARY LAYER DISPLACEMENT THICKNESS AT 30 sec. WITH RESPECT TO MIL FLUID, NEAT FLUIDS

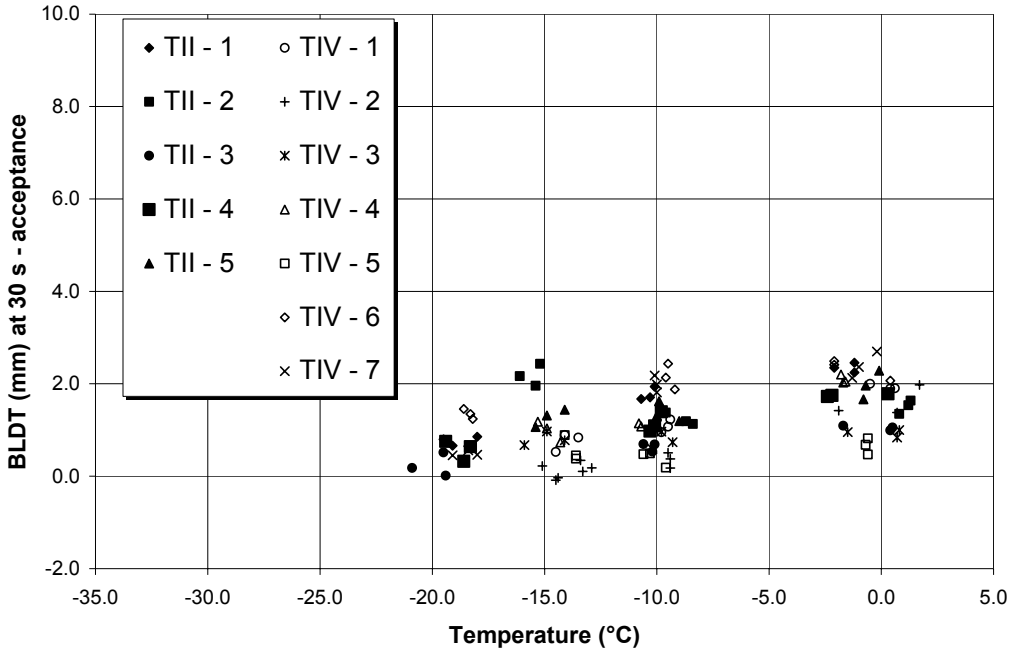

FIGURE 10. BOUNDARY LAYER DISPLACEMENT THICKNESS AT 30 sec. WITH RESPECT TO MIL FLUID, 75/25 DILUTIONS

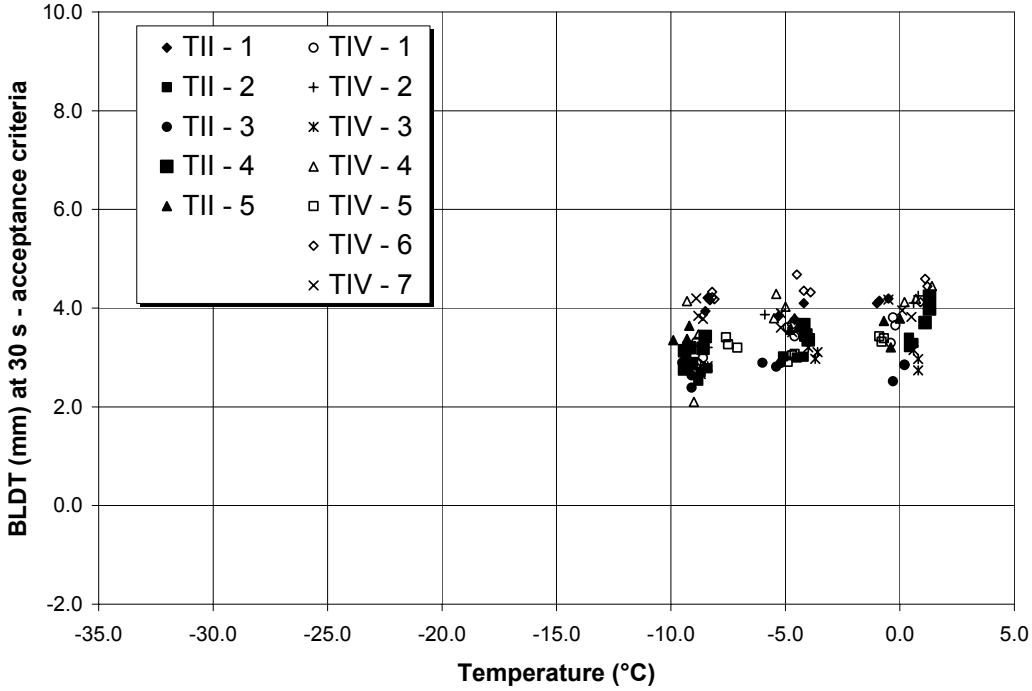

FIGURE 11. BOUNDARY LAYER DISPLACEMENT THICKNESS AT 30 sec. WITH RESPECT TO MIL FLUID, 50/50 DILUTIONS

2.4 MAXIMUM BLDT.

All fluids must have an acceptable BLDT at 30 sec., which is considered the time of rotation following takeoff acceleration. But the maximum BLDT attained prior to the 30 sec. (figure 2) can have any value. For example, figure 1 shows a maximum BLDT of 15.4 mm at ~13 sec. This section compares the maximum BLDT of the test fluids.

Figure 12 presents the maximum BLDT data for all fluids neat and diluted, figure 13 shows the neat fluid, figure 14 shows the 75/25 dilution, and figure 15 shows the 50/50 dilution. The figures show that the maximum BLDT measured for all fluids at all temperatures is between 12 and 16 mm, with only a slight decrease in maximum BLDT with decreasing temperature.

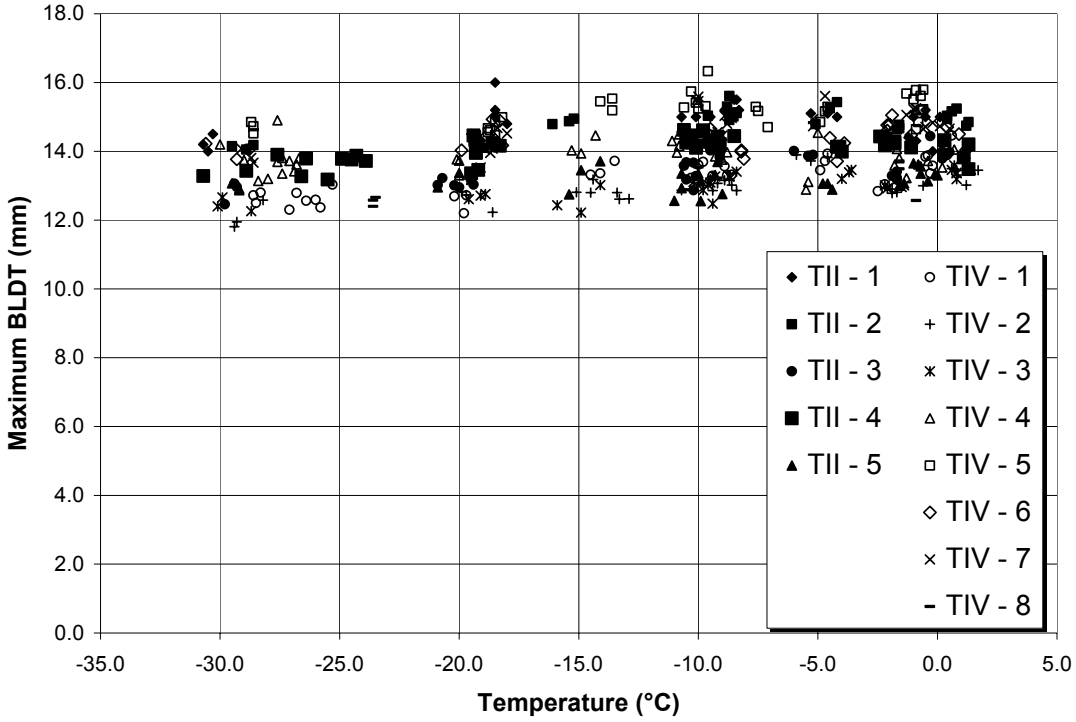

FIGURE 12. MAXIMUM BLDT, ALL FLUID DILUTIONS

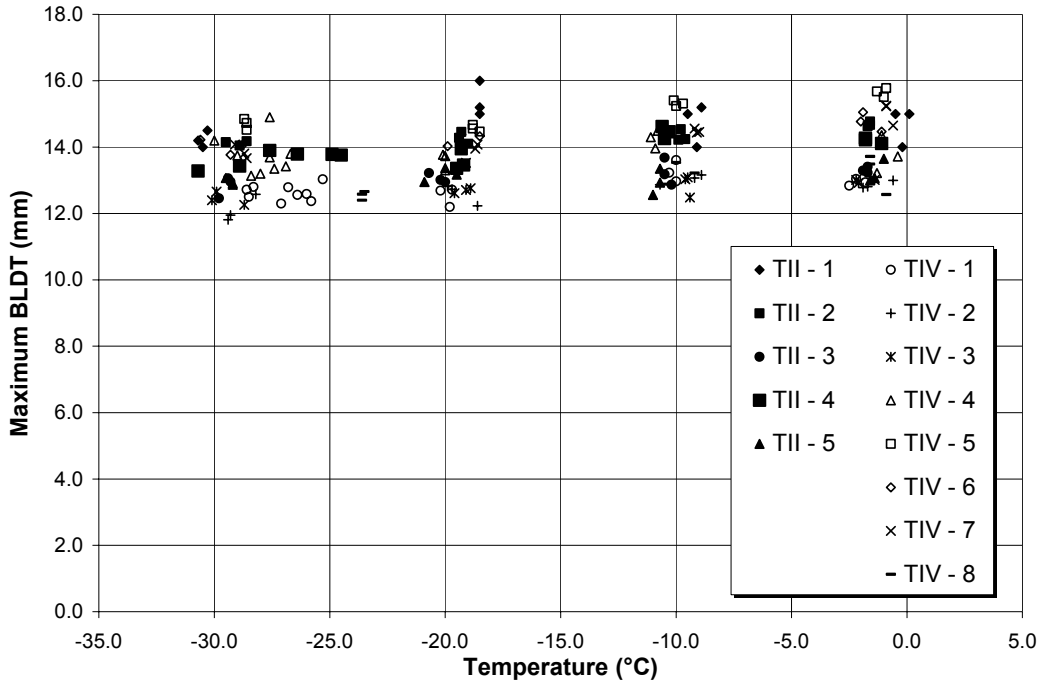

FIGURE 13. MAXIMUM BLDT, NEAT FLUIDS

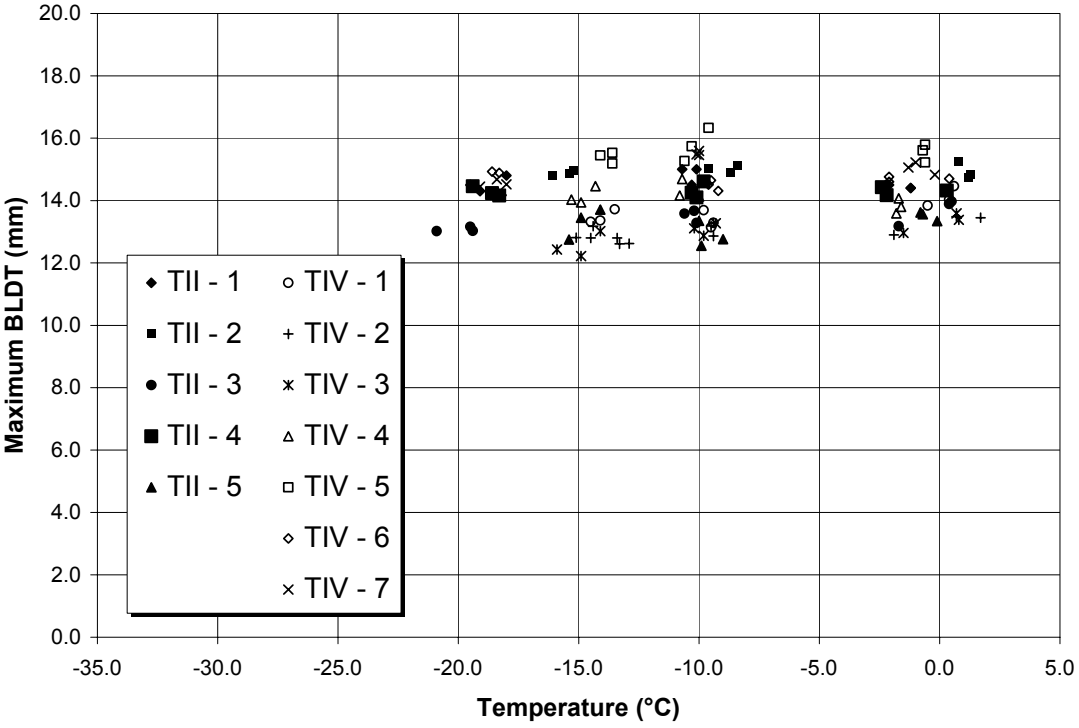

FIGURE 14. MAXIMUM BLDT, 75/25 DILUTIONS

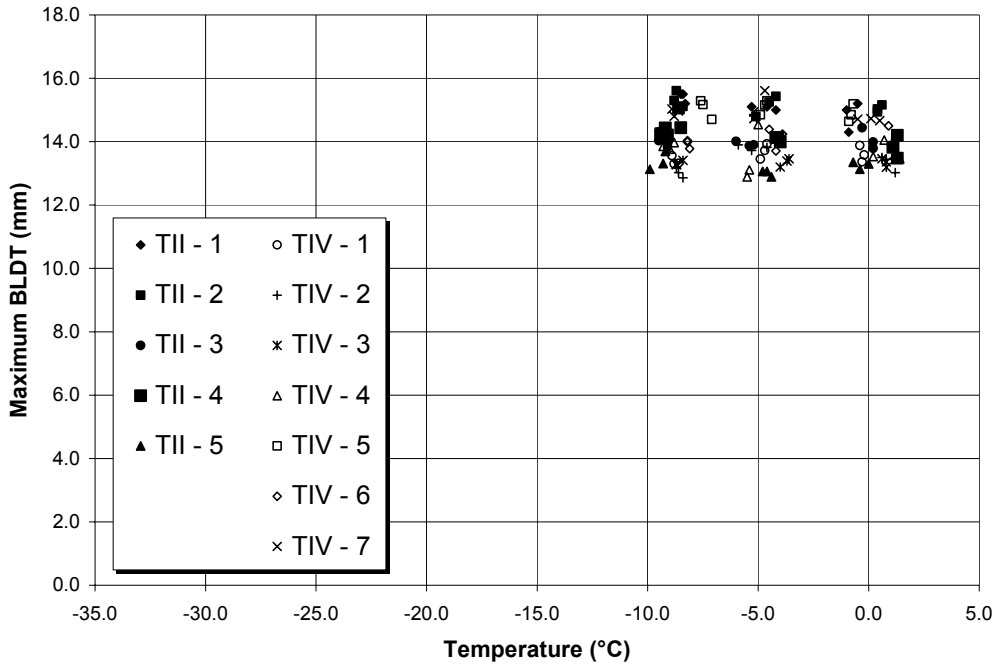

FIGURE 15. MAXIMUM BLDT, 50/50 DILUTIONS

2.5 ESTIMATE OF THE MAXIMUM BLDT POSSIBLE.

Since the maximum BLDTs are similar for all fluids, it is possible that there is a maximum measurable BLDT value. This maximum may be the result of the merging of the upper and lower boundary layers in the test section (figure 16). The test section box and the convergent and divergent cones are inserted into the test section part of the wind tunnel (figures 17 and 18) to perform FPET on deicing and anti-icing fluids according to AMS 1424/1428. Therefore, a parallel study was conducted to determine whether the boundary layer in the test box merges, and if so, where.

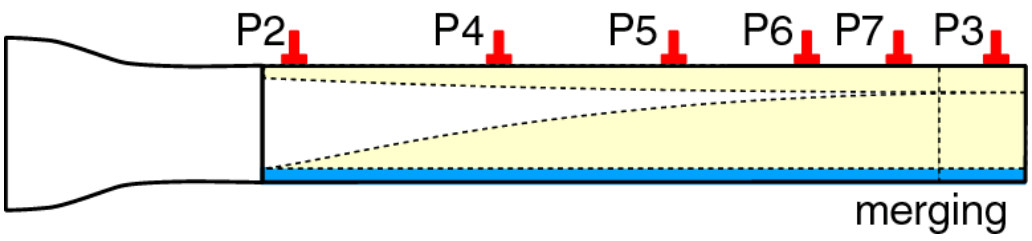

FIGURE 16. TEST SECTION BOUNDARY LAYERS

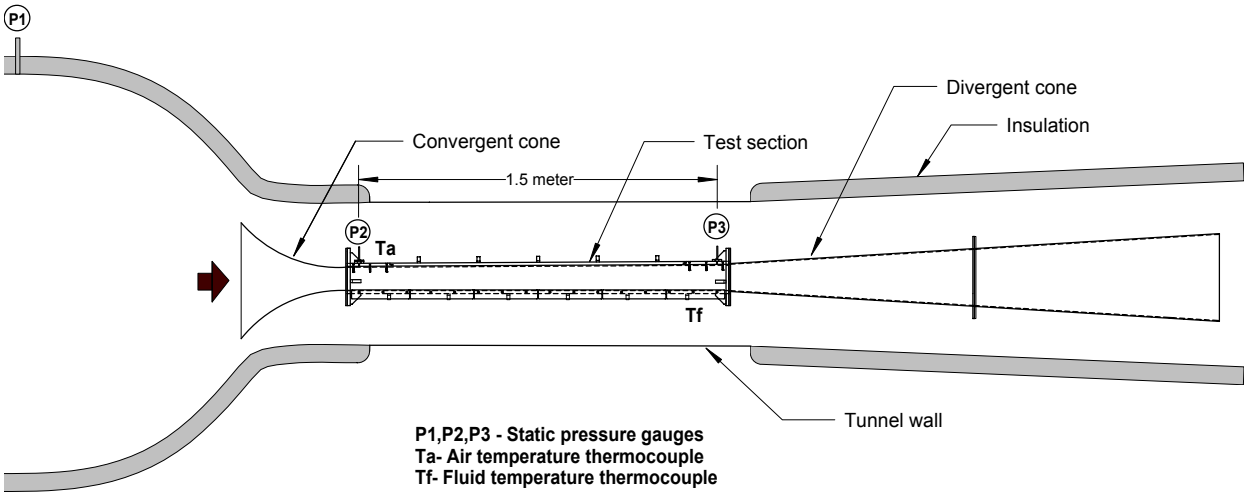

FIGURE 17. TEST SECTION BOX IN WIND TUNNEL

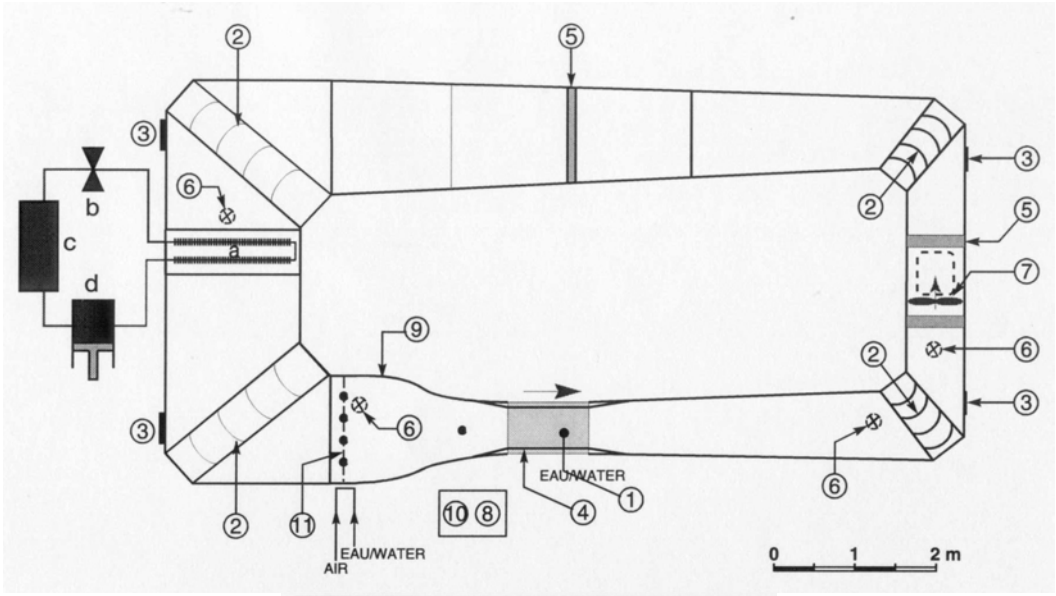

1	SECTION D'ESSAI TEST SECTION		SYSTÈME DE RÉFRIGÉRATION REFRIGERING SYSTEM
2	DÉFLECTEURS DE COIN CORNER VANES	a	ÉVAPORATEUR EVAPORATOR
3	PORTES D'ACCÈS ACCESS DOORS	b	SOUPAPE DE DÉTENTE EXPANSION VALVE
4	PANNEAUX D'ACCÈS ACCESS PANELS	c	CONDENSEUR CONDENSOR
5	JOINTS FLEXIBLES THERMAL EXPANSION JOINTS	d	COMPRESSEUR (75 hp) COMPRESSOR (75 hp)
6	DRAINS DRAINS		
7	MOTEUR ET VENTILATEUR FAN AND MOTOR		
8	PANNEAU DE CONTRÔLE MOTOR CONTROL PANEL		
9	CONVERGENT CONTRACTION CONE		
10	CONSOLE DE CONTRÔLE CONTROL CONSOLE		
11	GICLEURS SPRAY NOZZLES		

FIGURE 18. LUAN PHAN REFRIGERATED WIND TUNNEL

2.5.1 Methodology.

First, the boundary layer displacement thickness was evaluated at 0.83 m from the entry of the test section using an existing orifice in the test box cover (position P5, figure 16). This orifice is normally used for calibration in the same way that the BLDT is normally measured for certification at 1.55 m (position P3, figure 16). The merging position can then be estimated by considering the BLDT in a turbulent regime for a smooth flat plate [7], according to

$$\delta^* \alpha x^{0.8} \Rightarrow \delta^* = C_s \cdot x^{0.8} \tag{3}$$

where

δ^* = the BLDT
x = the position in meters
C_s = a constant

Second, the merging position was determined empirically by evaluating the boundary layer displacement thickness at 0.53, 0.83, 1.03, and 1.28 meters. For this, orifices were drilled into the test box cover to estimate the merging position. A power law curve fit was used to find the BLDT correlation in a turbulent regime for a rough flat plate according to

$$\delta^* = C_s \cdot x^n \tag{4}$$

For each position, three tests, according to the certification FPET procedure, were performed with a fluid at 0°C, and three static gauge pressure measurements were taken simultaneously (station 3, position 5, and position 4, 6, or 7). Figures 19 through 22 show typical results for all positions. The fluid selected for these tests was Kilfrost ABC-3, the only fluid still in production from the original Boeing study [5].

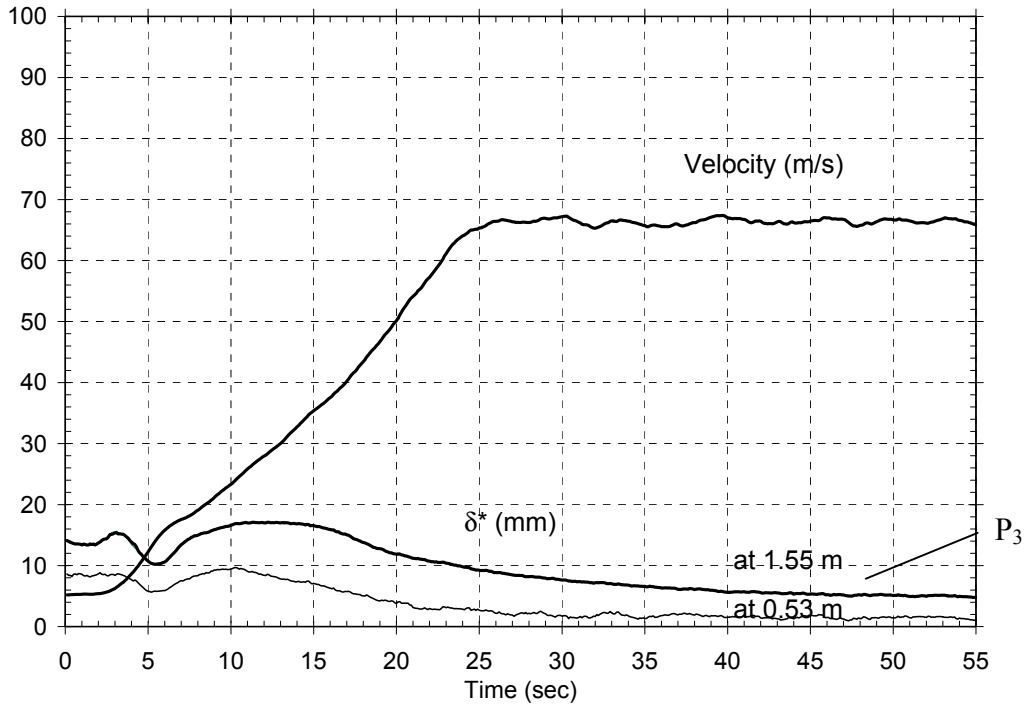

FIGURE 19. VELOCITY AND BLDT AT 1.55 AND 0.53 meters

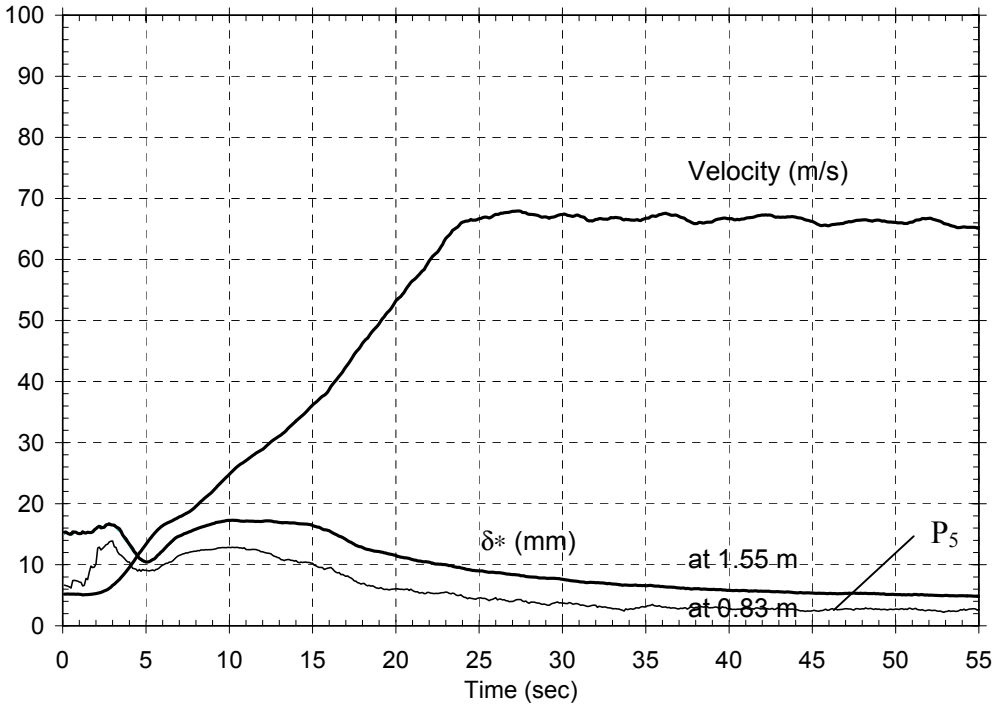

FIGURE 20. VELOCITY AND BLDT AT 1.55 AND 0.83 meters

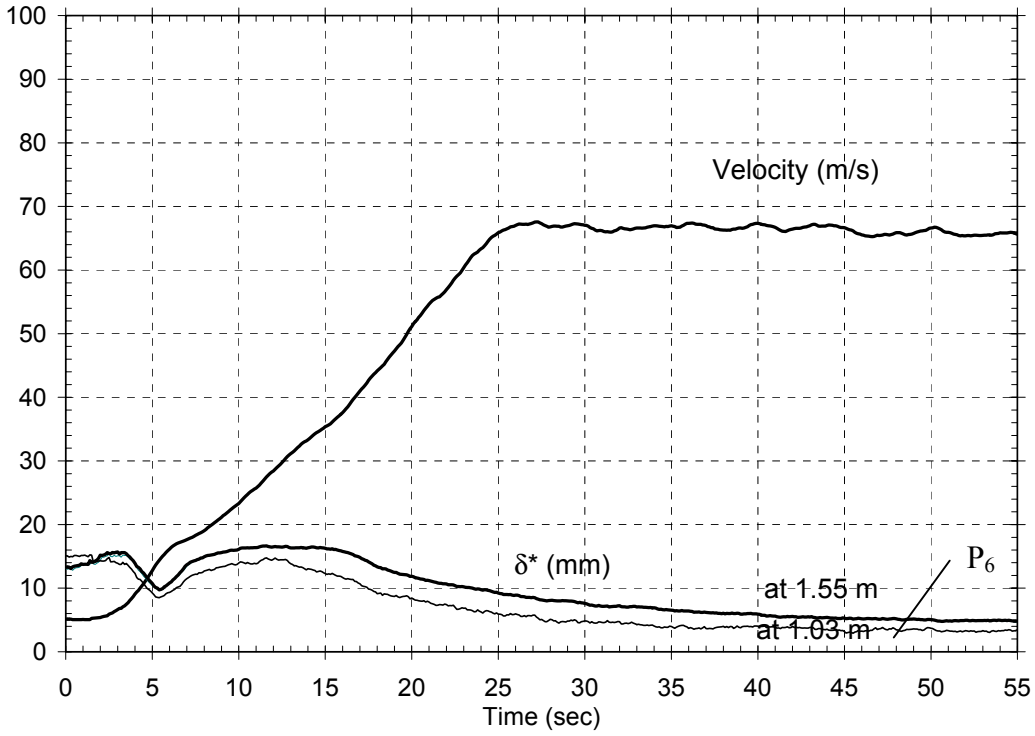

FIGURE 21. VELOCITY AND BLDT AT 1.55 AND 1.03 meters

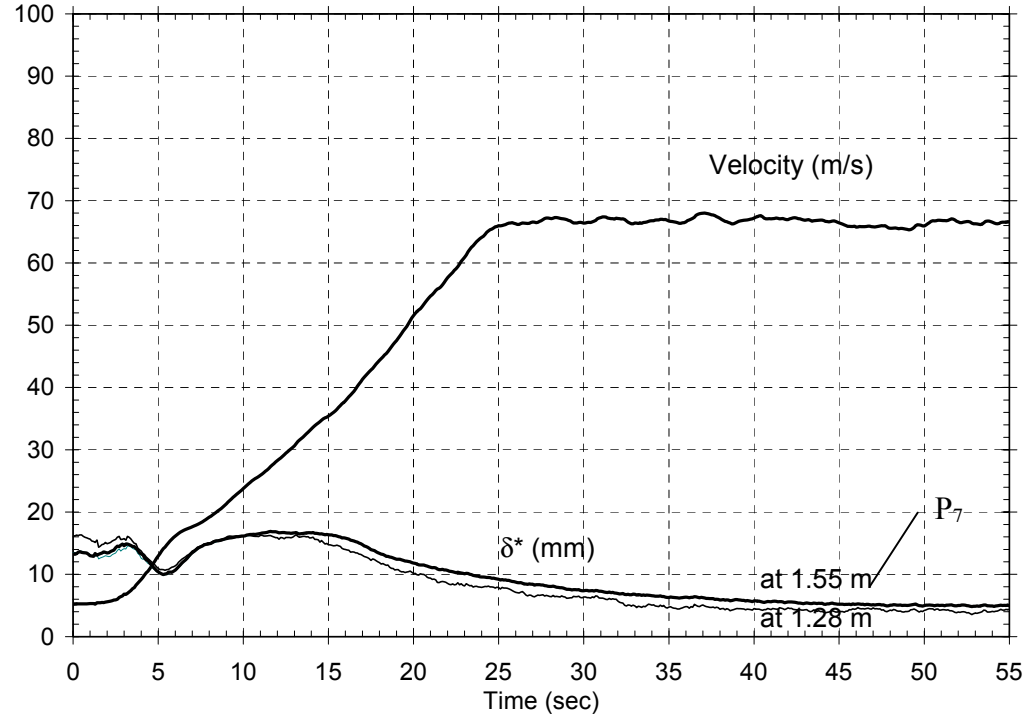

FIGURE 22. VELOCITY AND BLDT AT 1.55 AND 1.28 meters

2.5.2 Boundary Layer Displacement Thickness at Station 3.

For a standard FPET certification test, the BLDT is evaluated at station 3 by measuring the static pressure at 1.55 meters from the input with a static pressure gauge and using equations B2 and B3 of AMS1428 [4] as a certification test

$$\delta^*_{1.55} = \frac{1}{b_3} \cdot \left[S_3 - S_2 \cdot \sqrt{\frac{P_1 - P_2}{P_1 - P_2 + P_2 - P_3}} \right] - \frac{c_3 - b_3}{c_3} \cdot \delta^*_{1.55dry} \tag{5}$$

where

b_2 = the width (301.82 mm) at station 2
h_2 = the height (101.30 mm) at station 2
S_2 = the area (30574.37 mm^2) at station 2
b_3 = the width (301.82 mm) at station 3
h_3 = the height (109.64 mm) at station 3
c_3 = the perimeter (822.92 mm) at station 3
S_3 = the area (33091.54 mm^2) at station 3
P_1 = the static pressure at station 1
P_2 = the static pressure at station 2
P_3 = the static pressure at station 3

The dry BLDT is evaluated at station 3 without fluid by measuring the static pressure at 1.55 meters from the input with a static pressure gauge and by using

$$\delta^*_{1.55dry} = \frac{1}{b_3} \cdot \left[S_3 - S_2 \cdot \sqrt{\frac{P_1 - P_2}{P_1 - P_2 + P_2 - P_3}} \right] \tag{6}$$

2.5.3 Boundary Layer Displacement Thickness Evaluated at x Meters.

In the same way, a static pressure gauge was placed at position i (x meters from the input) and the BLDT was evaluated using

$$\delta^*_X = \frac{1}{b_i} \cdot \left[S_i - S_2 \cdot \sqrt{\frac{P_1 - P_2}{P_1 - P_2 + P_2 - P_i}} \right] - \frac{c_4 - b_i}{c_i} \cdot \delta^*_{Xdry}$$

The dry BLDT was evaluated at position i without fluid by measuring the static pressure at x meters from the input with a static pressure gauge and by using

$$\delta^*_{Xdry} = \frac{1}{b_i} \cdot \left[S_i - S_2 \cdot \sqrt{\frac{P_1 - P_2}{P_1 - P_2 + P_2 - P_i}} \right]$$

The position and section characteristics are listed in table 2.

TABLE 2. POSITION AND SECTION

Station Position	x (m)	B (mm)	H (mm)	C (mm)	S ($mm^{2)}$	δ^*_{xdry}
2*	0.05	301.82	101.30	806.24	30574.37	0.11
4	0.53	301.82	103.97	811.58	31379.86	1.03
5	0.83	301.82	105.90	815.44	31962.74	1.55
6	1.03	301.82	106.75	817.14	32218.92	1.88
7	1.28	301.82	108.14	819.92	32638.45	2.29
3*	1.55	301.82	109.64	822.92	33091.54	2.71

* The standard measures taken for a fluid certification FPET.

2.5.4 Dry Boundary Layer Displacement Thickness.

The static gauge pressure sensors were calibrated using a smooth, flat-plate BLDT in a turbulent regime, where δ^*_{xdry} is in meters

$$\delta^*_{Xdry} = \frac{H-1}{H+1} \cdot \delta_{dry}(x) \tag{7}$$

where

H = the shape factor and is 1.3 for a turbulent flat plate [9]
δ^*_{dry} = the dry BLDT
δ = the dry boundary layer thickness

$$\delta_{dry}(x) = 0.368 \cdot \frac{x + l_{cone}}{R_{e\,x+l_{cone}}^{0.2}} - 0.368 \cdot \frac{l_{cone}}{R_{e\,l_{cone}}^{0.2}} \tag{8}$$

where

$$R_e(x_t I_{cone}) = \frac{\rho_a}{\mu_a}(x_t I_{cone}) U_\infty \tag{9}$$

where

ρ_a = the air density
μ_a = the dynamic viscosity
U_∞ = the free-stream speed
l_{cone} = the cone length at the input box
R_e = the Reynolds number

2.5.5 Results.

2.5.5.1 Merging Position Estimation.

Table 3 shows the results for position 5 (at 0.83 meters).

TABLE 3. RESULTS FOR POSITIONS

Measurement No.	$\delta^*_{0.83}$ mm (Position 5)	$\delta^*_{1.55}$ mm (Station 3)
1	13.38	16.75
2	12.88	16.98
3	12.87	17.26
Average	13.04	16.99

By considering $\delta^* \propto x^{0.8}$ and that the BLDT at station 3 is the maximum value, the estimated merging position is

$$x_s = \left(\frac{\delta^*_s}{\delta^*_{0.83}}\right)^{5/4} \cdot x_{0.83} = \left(\frac{\delta^*_{1.55}}{\delta^*_{0.83}}\right)^{5/4} \cdot x_{0.83} = \left(\frac{16.99}{13.04}\right)^{5/4} \cdot 0.83 = 1.16 \text{ m} \qquad (10)$$

2.5.5.2 Merging Position Correlation.

Table 4 shows the average results for each position measured.

TABLE 4. AVERAGE RESULTS FOR EACH POSITION MEASURED

Position	x (m)	δ^*_X (mm)	$\delta^*_{0.83}$ (mm)	$\delta^*_{1.55}$ (mm)
4	0.53	10.16	13.08	17.06
5	0.83	13.04	13.04	16.99
6	1.03	14.55	13.09	16.70
7	1.28	16.57	13.13	16.96

The power law curve fit equation is

$$\delta^* = 14.4225 \cdot x^{0.55} \qquad (11)$$

with this result, the merging position is

$$x = \left(\frac{16.99}{14.4225}\right)^{1/0.55} = 1.35 \text{m}$$

All the results are presented in figure 23.

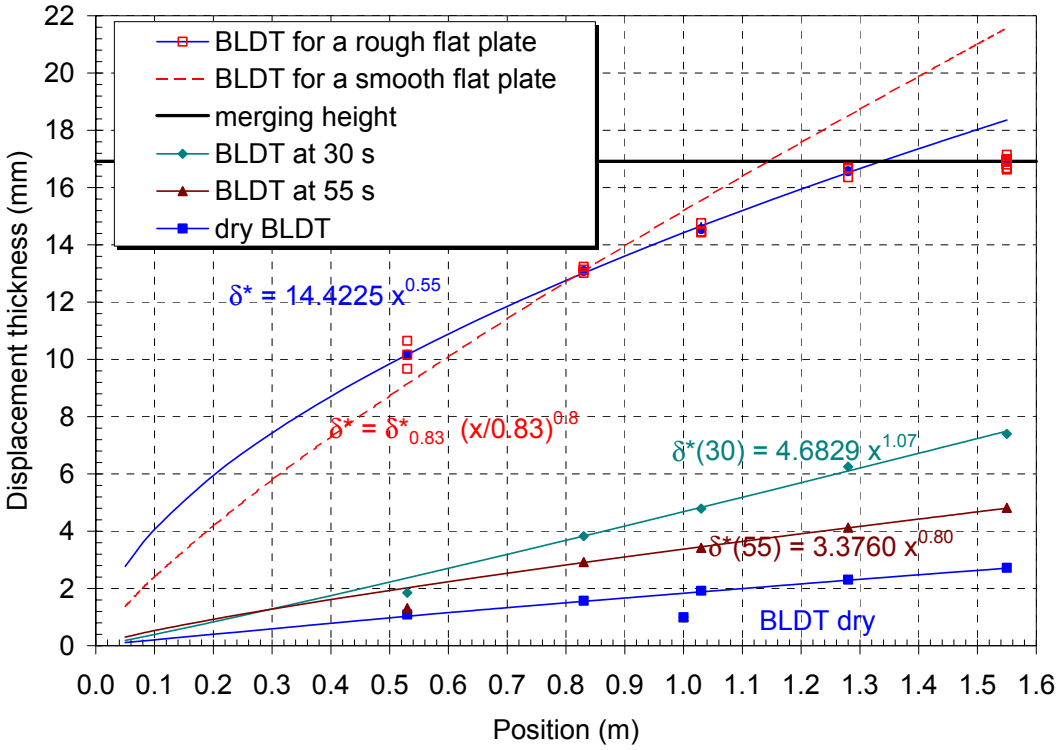

FIGURE 23. MERGING POSITION ESTIMATION RESULTS

2.5.5.3 Boundary Layer Thickness Correlation.

Using equation 7

$$\delta^*_X = \frac{H-1}{H+1} \cdot \delta(x)$$

and the fact that the BLDT at 1.33 meters from the input is the maximum value, the H value can be estimated using the box height h_x at this position (108.42 mm)

$$h_X - \delta_{dry}(x) = \delta(x) = \frac{H+1}{H-1} \cdot \delta^*_X$$

$$H = \frac{h_X - \delta_{dry}(x) + \delta^*_X}{h_X - \delta_{dry}(x) - \delta^*_X}$$

$$H = \frac{108.42 - 18.97 + 16.91}{108.42 - 18.97 - 16.91} = 1.47$$

The power law curve fit is

$$\delta^* = \frac{H-1}{H+1}\cdot\delta(x) = \frac{H-1}{H+1}\cdot\frac{c}{\left(\frac{\rho_a}{\mu_a}\cdot U_\infty\right)^n}\cdot x^{1-n} = 14.4\cdot x^{0.55}$$

where c is

$$c = 14.4\cdot\frac{H+1}{H-1}\cdot\left(\frac{\rho_a}{\mu_a}\cdot U_\infty\right)^n \text{ mm}$$

The boundary layer is

$$\delta(x) = 75.8\cdot\frac{x}{Re_x^{0.45}} \text{ m}$$

where

$$Re_x = \frac{\rho_a}{\mu_a}\cdot x\cdot U_\infty$$

2.5.5.4 Box Height for Required Merging.

For this fluid, Kilfrost ABC-3, the estimated maximum BLDT is 18.38 mm and merging will not happen if the box height is

$$h_{1.55} = \delta_{dry}(1.55) + \delta(1.55) = \delta_{dry1.55} + \frac{1.47+1}{1.47-1}\cdot\delta^*_{1.55} = 21.66 + 5.26\cdot 18.38 = 118.34 \text{ mm} \qquad (12)$$

The existing box height at 1.55 meters is 109.64 mm and, therefore, is short by 7.78 mm.

The difference between the input and the output for the existing box test section is 8.34 mm, the new difference is about double (16.12 mm).

2.5.6 Boundary Layer Displacement Thickness Merging.

For the AMIL test section, the measured BLDT cannot be more than 17 mm because it is limited by the box height at the output. For the fluid tested, Kilfrost ABC-3, the estimated BLDT maximum was 18.4 mm.

For the fluid tested, the box height at the output needs to be 117.42 mm (8 mm higher) so that the BLDT would not merge.

The BLDT correlation is a characteristic of the fluid tested and the correlation depends on the wave height or surface roughness. The BLDT from 30 to 60 sec. are not affected by the box

height since the BLDTs are well below 17 mm. However, a comparison of the maximum BLDT of section 2.4 may not be relevant because the boundary layers in the box probably have merged.

2.6 TIME OF MAXIMUM BLDT.

Another comparison made between fluids was with the time of the maximum BLDT. For example, for the test of figure 1, this is equivalent to 13 sec. Figure 24 shows the time the maximum BLDT was reached for all fluids and their dilutions. Figures 25 through 27 show the same data separated into the neat fluid, 75/25, and 50/50 dilutions respectively.

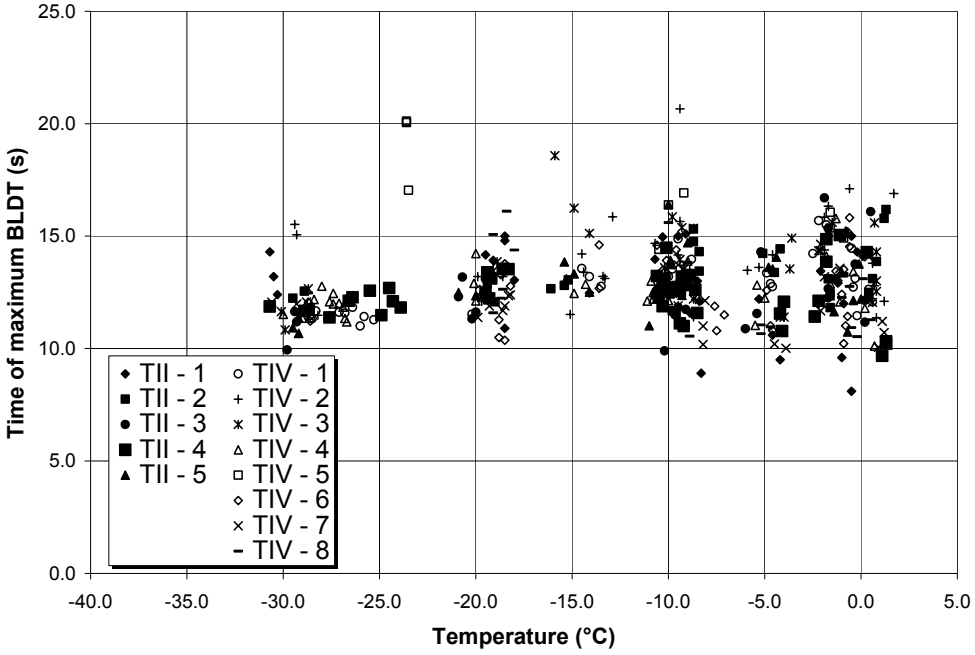

FIGURE 24. TIME OF MAXIMUM BLDT, ALL FLUID DILUTIONS

The results can show considerable variation for the same fluid at the same temperature interval. For example, in figure 25 fluid TIV-5 around -23°C has a maximum BLDT at 17 or 20 sec. Figure 28 shows a test data sheet of the FPET for this fluid. It shows an extended maximum BLDT whose maximum could be anywhere between 16 and 21 sec. The actual maximum is determined by computer software.

Figure 25 shows the time of maximum BLDT versus the temperature for the neat fluids. The graph shows that most of the data falls in the 10- and 17-sec. range. The times also tend to decrease with decreasing temperatures. Figure 26 shows the time of maximum BLDT versus temperature for the 75/25 dilution. The graph shows that most of the values occur in the 11- to 17-sec. range. There is no apparent trend with respect to temperature. Figure 27 shows the time of maximum BLDT versus temperature for the 50/50 dilution. The graph shows that the values generally occur in the 9- and 15-sec. range. The values tend to increase with decreasing temperature. In all cases, there were no clear differences between fluid with respect to Type II versus Type IV fluids.

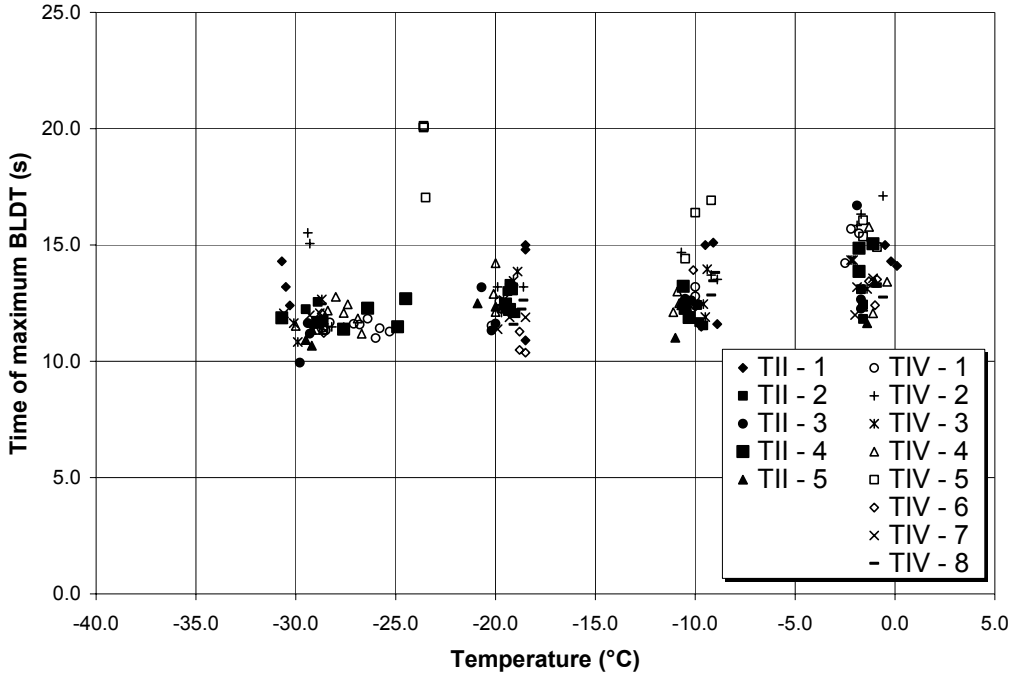

FIGURE 25. TIME OF MAXIMUM BLDT, NEAT FLUIDS

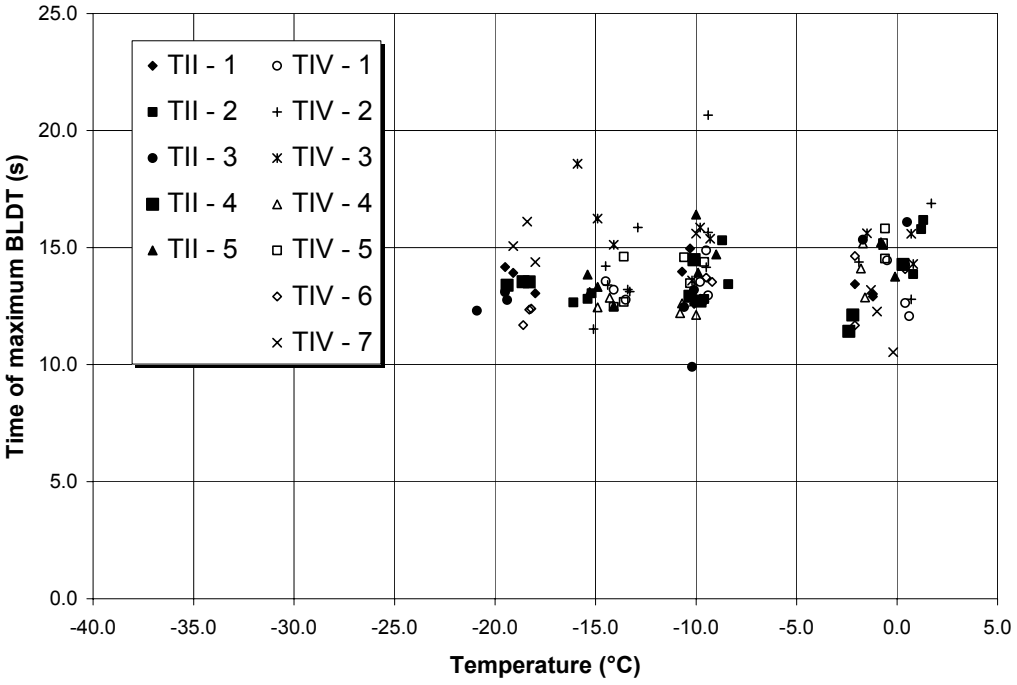

FIGURE 26. TIME OF MAXIMUM BLDT, 75/25 DILUTIONS

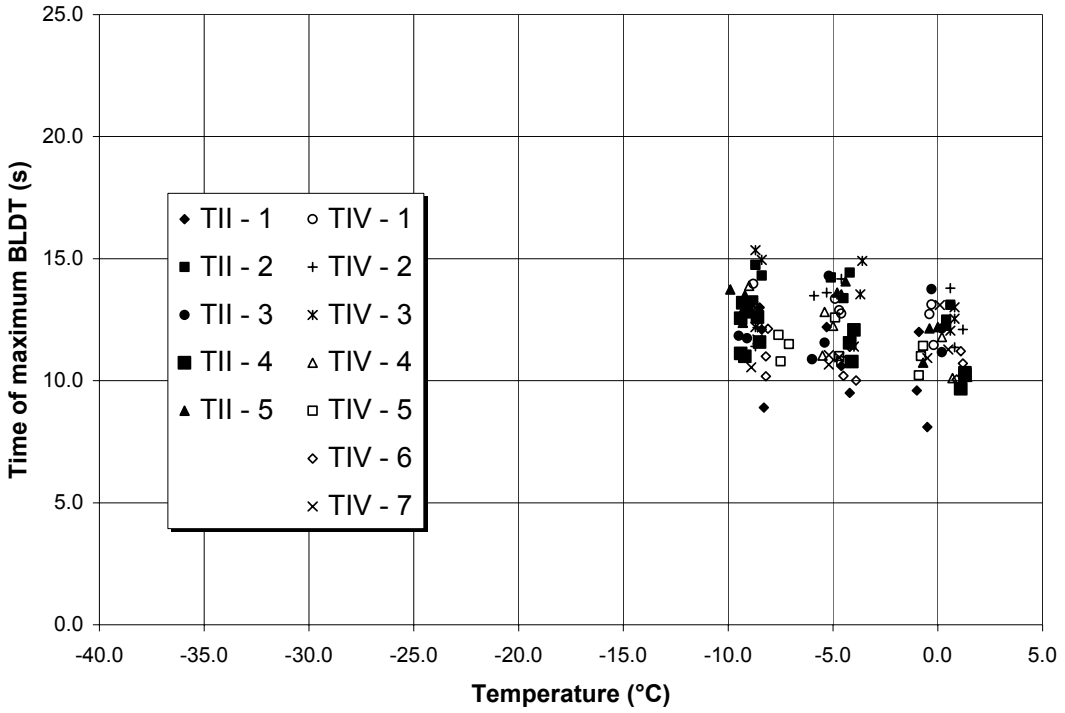

FIGURE 27. TIME OF MAXIMUM BLDT, 50/50 DILUTIONS

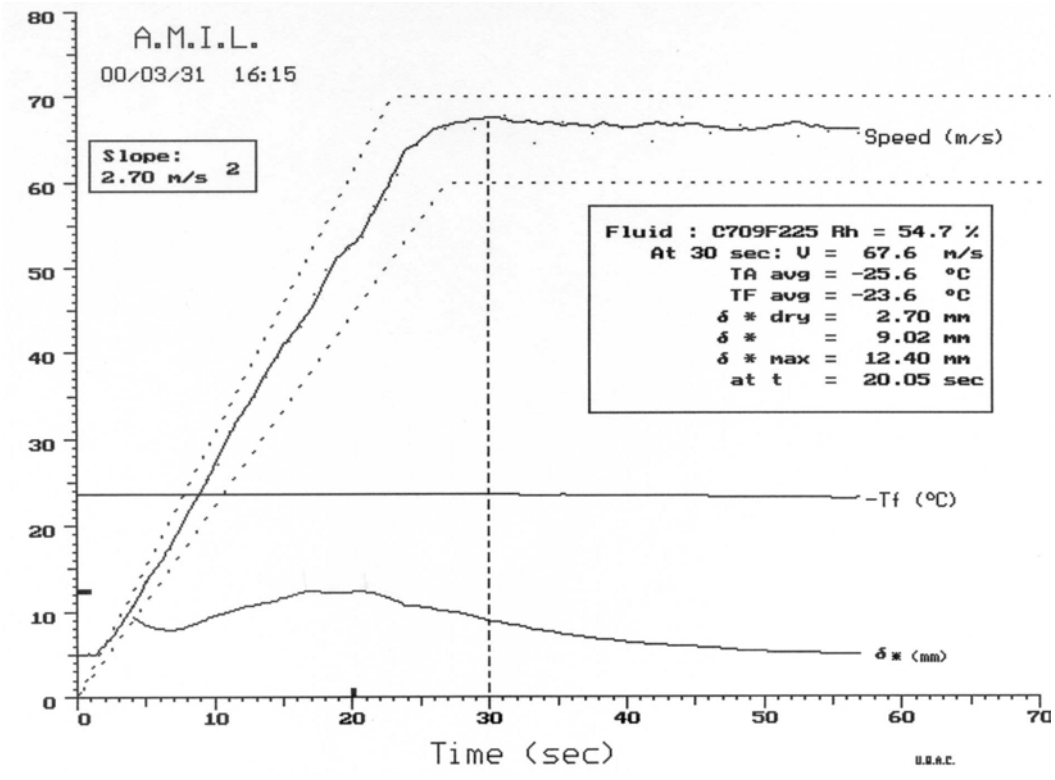

FIGURE 28. TEST DATA SHEET FOR FPET OF TIV-5 FLUID

2.7 FLUID ELIMINATION.

As required by AMS1428 [3], the fluid elimination must be greater than 74%, based on an initial thickness of 2 mm of fluid on the test duct floor. This section investigates whether the different fluids, and more specifically the Type II and Type IV fluids, have different quantities of fluid elimination.

Figure 29 presents the fluid elimination for all fluid dilutions. The data is separated with figure 30 representing the neat fluid, figure 31 representing the 75/25 dilution, and figure 32 representing the 50/50 dilution.

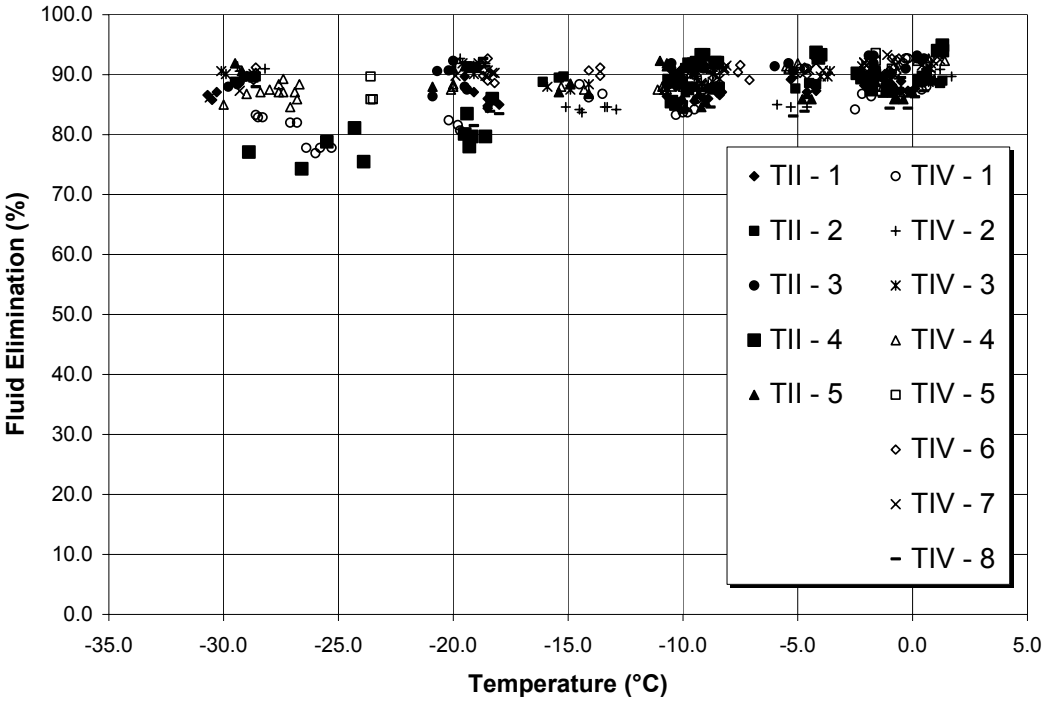

FIGURE 29. FLUID ELIMINATION PERCENT, ALL DILUTIONS

Figure 29 shows that for all fluids and all dilutions, the elimination percentage is usually between 85% and 95% and decreases for some fluids with decreasing temperature. The figure shows that there is more scatter below -20°C. Below -20°C, the Type IV fluids have lower fluid elimination percentages than the Type II fluids with the exception of fluid TII-4, which has the lowest elimination value.

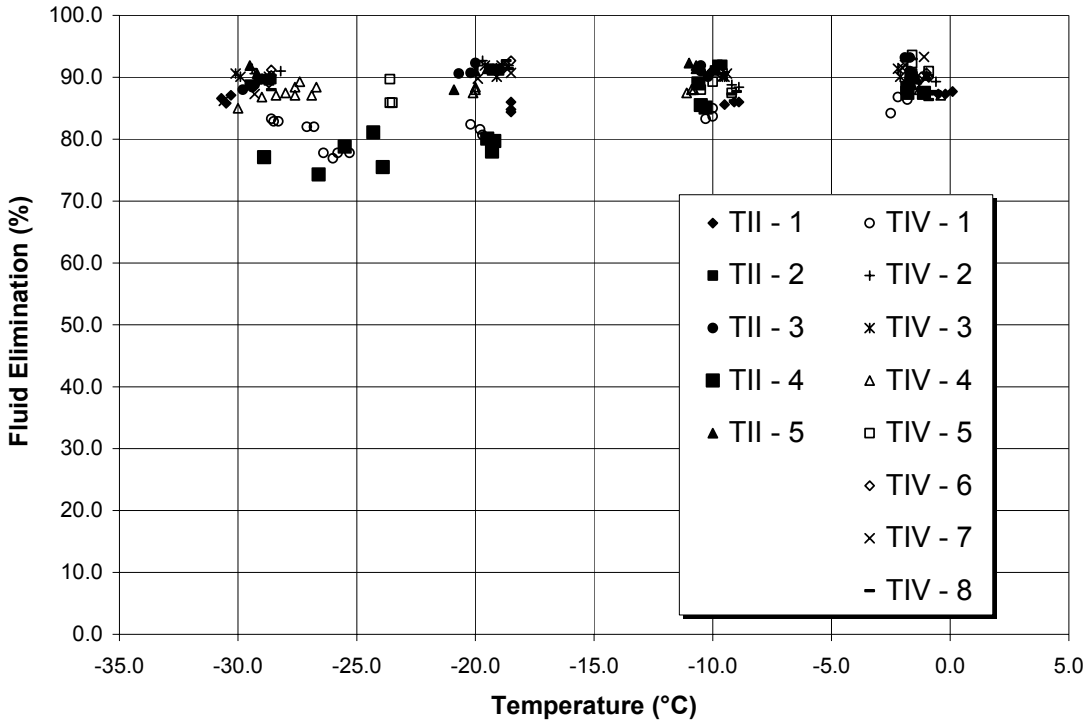

FIGURE 30. FLUID ELIMINATION PERCENT, NEAT FLUIDS

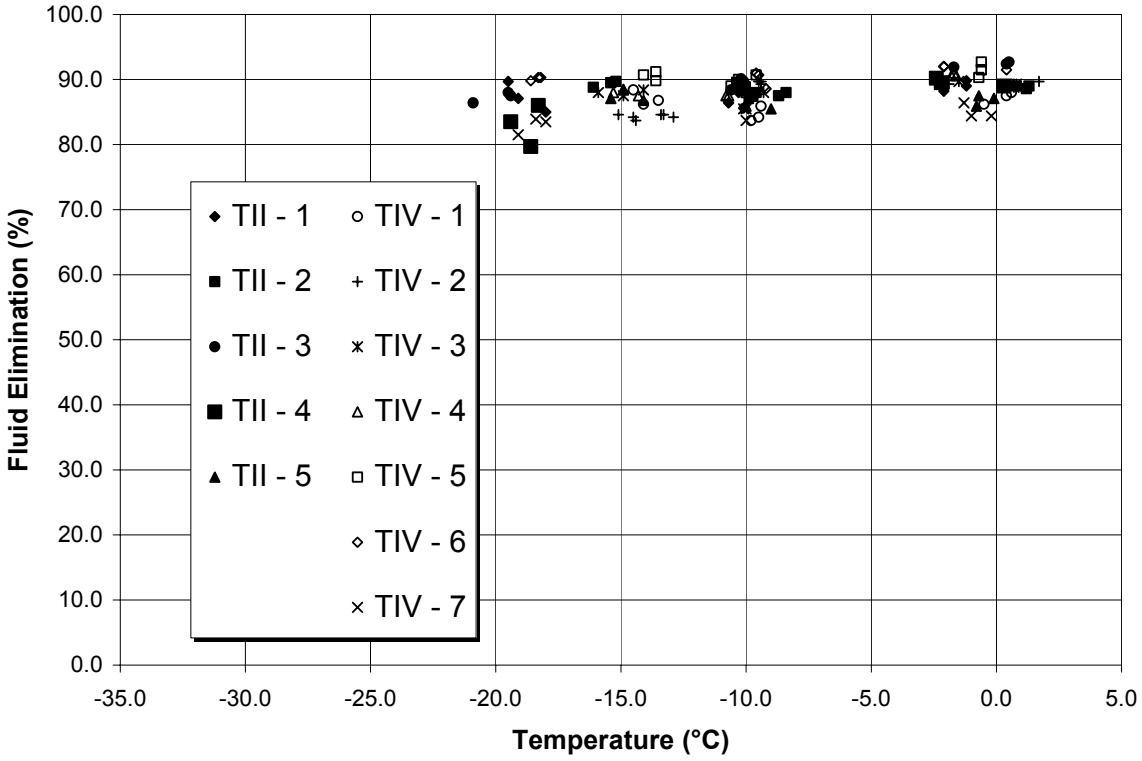

FIGURE 31. FLUID ELIMINATION PERCENT, 75/25 DILUTIONS

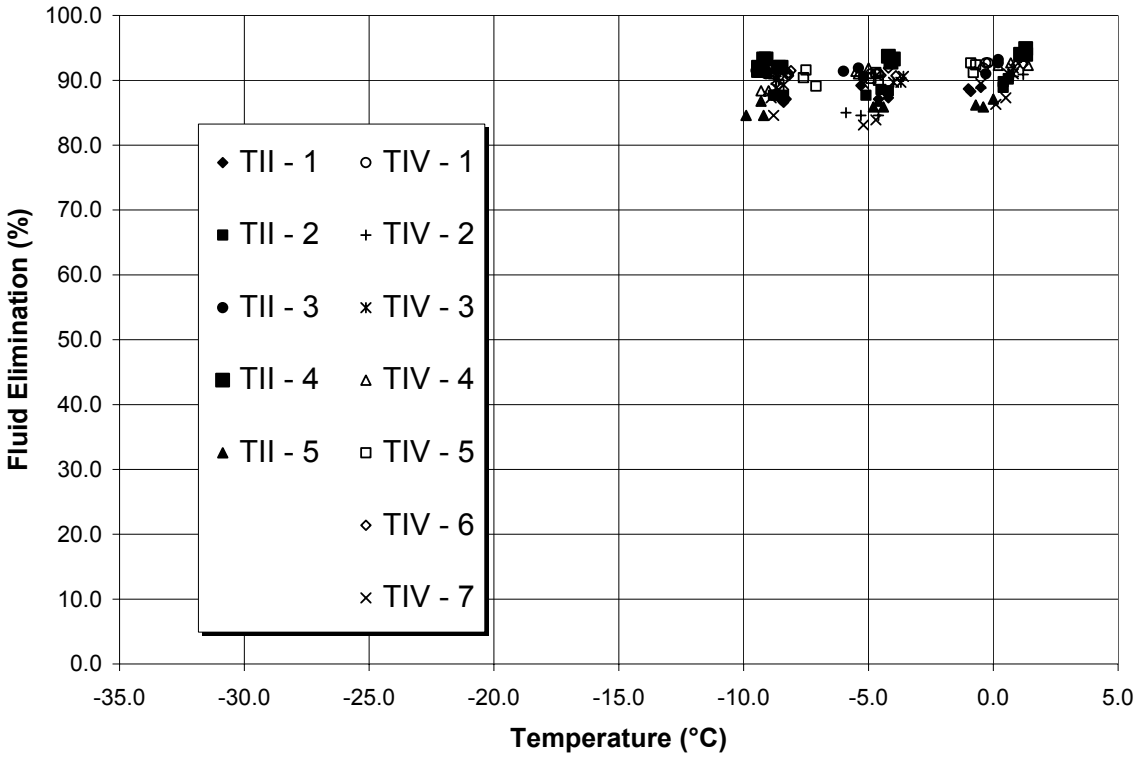

FIGURE 32. FLUID ELIMINATION PERCENT, 50/50 DILUTIONS

2.8 BOUNDARY LAYER DISPLACEMENT THICKNESS AT 50 SECONDS.

During an FPET, following the acceleration from 5 to 65 m/s, the 65 m/s speed is maintained for 30 sec. to complete a test run (figure 1). The BLDT at 50 sec. (near the end of the test) was compared. The comparison for all fluids, neat and diluted, is presented in figure 33. Since the computer software did not automatically generate these values, they were measured off the test data graphs similar to figure 1; therefore, all values could only be determined to a 0.5-mm precision. The figure shows that the values increase with decreasing temperature, but there is no clear difference to be seen with respect to Type II and Type IV fluids.

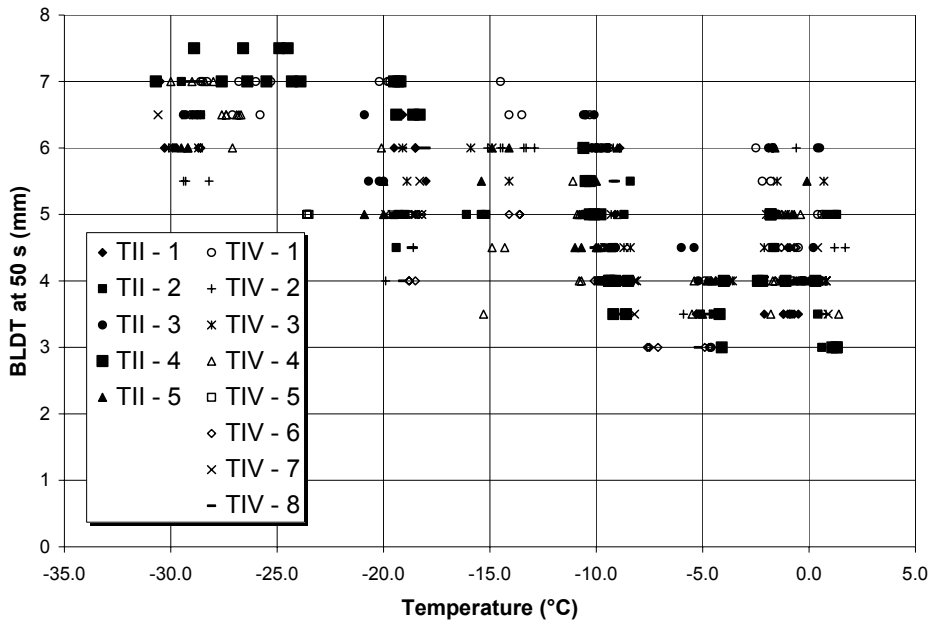

FIGURE 33. BOUNDARY LAYER DISPLACEMENT THICKNESS AT 50 sec., ALL FLUIDS, NEAT AND DILUTED

2.9 BOUNDARY LAYER DISPLACEMENT THICKNESS COMPARISONS—CONCLUSIONS.

Comparisons of the BLDT at 30 sec. (with respect to the limit), maximum BLDT, time of maximum BLDT, fluid elimination, and BLDT at 50 sec. all showed no clear difference between Type II and Type IV fluids.

A parallel study made on the merging of the upper and lower boundary layers showed, for a sample fluid, the test section merged at 1.16 m from its entry. At station 3, where the BLDT is measured for a certification FPET, 1.55 m from the entry, the maximum BLDT was 17 mm. To ensure that the boundary layer thicknesses do not merge, the required box height at the output would be 117.42 mm, 8 mm higher than it currently is. However, to measure the BLDT at 30 sec. for certification FPET, which is usually below about 10 mm to be acceptable, the current box height is more than adequate.

3. TASK 2: DIFFERENT INITIAL FLUID THICKNESSES.

Currently, certification tests are run with an initial thickness of 2 mm (AMS1428 [3]). Although a 2-mm initial thickness may not be representative of the quantity of fluid applied on an aircraft, it is this 2-mm thickness that was equated to lift, and therefore lift loss, in the original Boeing study [5].

However, the Boeing study [5] was conducted on Type II fluids before Type IV fluids existed. Type IV fluids tend to be thicker, which results in longer anti-icing endurance time tests, and therefore, more fluid remains on an aircraft after application.

The objective of this section was to look at different fluid thicknesses and to determine their effect on the BLDT and fluid elimination.

3.1 TEST FLUIDS.

For this task, testing was limited to five fluids: two Type II fluids and three Type IV fluids, listed in table 5.

TABLE 5. FLUID IDENTIFICATION

Company Name	Fluid	Type	Color	AMIL Label	Reception Date
Kilfrost Limited	ABC-3 lot # H/296/2/02	II	colorless	E607	2002-03-21
Clariant GMBH	Safewing MPII 1951 lot # DEGE144062	II	colorless	E618	2002-03-22
Octagon Process Inc.	MaxFlight lot # F-21395C	IV	green	E583	2001-03-13
SPCA	AD-480 lot # M025	IV	green	E007	2001-01-29
Dow Chemical Company	Ultra+ lot# 200103528-53	IV	green	E629	2002-03-28

Kilfrost ABC-3 was chosen since it was employed in the original Boeing investigation [5]. Clariant Safewing MPII 1951 was chosen since it is a typical Type II fluid that has been in use for several years. The three Type IV fluids were chosen since they represent different but typical Type IV fluids that have been in use for several years, and together with the Type II fluids, all manufacturers of thickened fluids are represented. Specifically, Octagon Process MaxFlight was selected since it is a relatively low-viscosity Type IV fluid and Dow Ultra+ since it is the only ethylene glycol-based Type IV fluid.

Table 6 shows the Water Spray Endurance Test (WSET) times determined at AMIL for the five samples received. The WSETs were conducted according to Annex A of AMS1428 [3] where three plates coated with fluid were exposed to precipitation at 5 $g/dm^2/h$ ±0.2. Both the air and plate temperatures were at -5°C. The WSET time is defined as the first icing event (FIE), which is time for the first ice crystal to reach the failure zone: 25 mm below the upper edge of the test plate and 5 mm in from either side of the test plate.

TABLE 6. WSET TIMES OF FLUIDS TESTED

Company Name	Fluid	Type	AMIL Label	WSET (FIE)
Kilfrost Limited	ABC-3 lot # H/296/2/02	II	E607	33 min ±0 sec
Clariant GMBH	Safewing MPII 1951 lot # DEGE144062	II	E618	27 min 42 sec ±10 sec
Octagon Process Inc.	MaxFlight lot # F-21395C	IV	E583	87 min 3 sec ±2 min 8 sec
SPCA	AD-480 lot # M025	IV	E007	88 min ±1 min 57 sec
Dow Chemical Company	Ultra+ lot# 200103528-53	IV	E629	95 min 57 sec ±1 min 32 sec

Table 7 shows the Brookfield viscosity measurement performed at AMIL for the same samples. The Brookfield viscosity measurements were performed according to ASTM D 2196.

TABLE 7. BROOKFIELD VISCOSITY (mPa•s)

Fluid	Temp (°C)	0.3 rpm		6 rpm		30 rpm	
		Viscosity	Accuracy	Viscosity	Accuracy	Viscosity	Accuracy
E607 ABC-3	20	5 000	1000[31]	925	50[31]	461	10[31]
	0	5 100	1000[31]	1 340	50[31]	746	10[31]
Fluid	Temp (°C)	0.3 rpm		6 rpm		30 rpm	
		Viscosity	Accuracy	Viscosity	Accuracy	Viscosity	Accuracy
E618 MPII 1951	20	4 500	1000[31]	535	50[31]	243	10[31]
	0	5 400	1000[31]	1 025	50[31]	480	10[31]
Fluid	Temp (°C)	0.3 rpm		6 rpm		30 rpm	
		Viscosity	Accuracy	Viscosity	Accuracy	Viscosity	Accuracy
E007 AD-480	20	18 400	1000[31]	1 860	50[31]	602	10[31]
	0	19 200	1000[31]	1 635	50[31]	608	10[31]
Fluid	Temp (°C)	0.3 rpm		6 rpm		30 rpm	
		Viscosity	Accuracy	Viscosity	Accuracy	Viscosity	Accuracy
E583 MaxFlight	20	7 100	1000[31]	1 130	50[31]	510	10[31]
	0	45 500	1000[31]	3 835	50[31]	1 278	20[34]
Fluid	Temp (°C)	0.3 rpm		6 rpm		30 rpm	
		Viscosity	Accuracy	Viscosity	Accuracy	Viscosity	Accuracy
E629 Ultra+	20	32 300	1000[31]	2 325	50[31]	678	10[31]
	0	56 100	1000[31]	3 370	50[31]	1 346	10[31]

Note: [31] and [34] = spindle number.

3.2 RESULTS.

For this section of tests, FPETs were run according to Annex B of AMS1428 [3] but with initial fluid thicknesses of 1, 2, and 4 mm. Normal certification FPET tests are run with the 2-mm

initial fluid thickness. Additionally, video tape recordings of the tests were examined to measure the maximum wave height and the time at which it occurred.

3.2.1 Kilfrost ABC-3.

Figure 34 and table 8 show the results for Kilfrost ABC-3 tested with 1-, 2-, and 4-mm initial fluid thicknesses. The graph shows that there is little difference in the measured BLDT at 30 sec. between the different initial fluid thicknesses at each temperature interval. Table 8 shows the maximum wave heights for each initial thickness. The wave heights are highest for the 4-mm initial thickness followed by the 2- and 1-mm thicknesses. Despite this, the BLDT measurements at 30 sec. are all relatively the same as in figure 34.

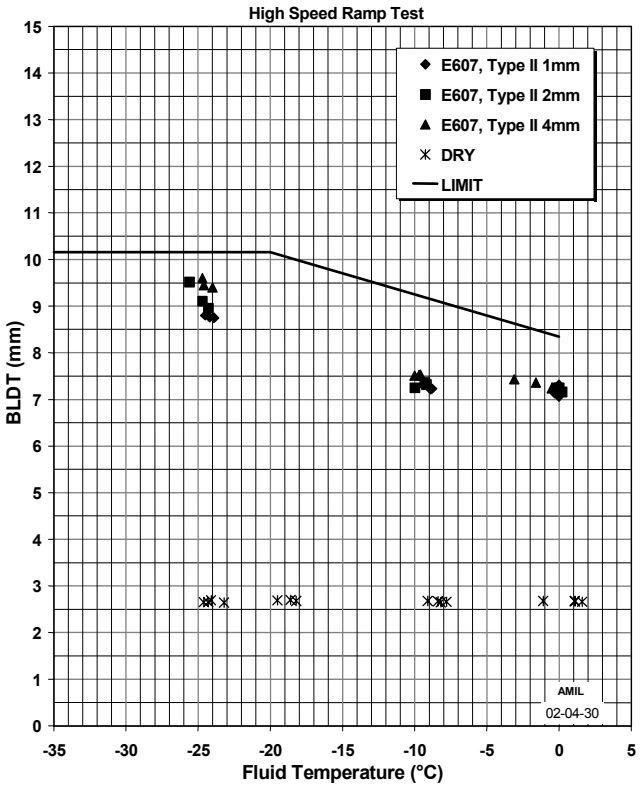

FIGURE 34. AERODYNAMIC TEST RESULTS FOR KILFROST ABC-3 WITH THREE DIFFERENT INITIAL FLUID THICKNESSES

Figure 35 presents the fluid elimination as a percentage for Kilfrost ABC-3 with 1-, 2-, and 4-mm initial thicknesses as well as the reference military fluid. The graph shows greater elimination percentage for the 4–mm initial thickness, followed by the 2-mm thickness, then the 1-mm initial thickness.

Figure 36 presents the same data in terms of final fluid thickness. This graph shows that the final thickness is in the order of 200 to 250 μm at all temperature intervals and is relatively independent of the initial fluid thickness.

TABLE 8. AERODYNAMIC PERFORMANCE TEST DATA FOR KILFROST ABC-3

Fluid Code	Test Code	T_a (°C)	T_f (°C)	r.h. (%)	t_o[(1)] (μm)	t_{end}[(2)] (μm)	F.E. [(3)] (%)	W.C. [(4)] (%)	V[(5)] (m/s)	δ* (mm)	δ max (mm)	t[(6)] (sec)	Maximum Wave Height (mm)
E-607	FP-668	0.1	0.0	82.0	1100	196	82.2	1.39	68.5	7.06	13.24	12	3
E-607	FP-669	1.0	0.0	83.2	1100	221	79.9	1.22	67.8	7.31	13.13	13	2
E-607	FP-670	-0.4	-0.3	79.0	1143	221	81.5	1.39	66.8	7.13	13.27	13	3
E-607	FP-686	-9.7	-8.8	79.9	1058	203	80.8	0.35	67.9	7.23	13.26	14	3
E-607	FP-688	-9.1	-8.9	78.2	1100	221	79.9	0.17	67.1	7.22	13.13	12	3
E-607	FP-687	-10.8	-9.2	70.1	1058	211	80.1	0.17	67.4	7.34	13.13	13	3
E-607	FP-706	-25.6	-23.9	53.1	1100	203	81.5	-0.69	66.2	8.75	12.94	10	4
E-607	FP-705	-25.7	-24.2	53.8	1058	211	80.1	0.17	66.9	8.76	13.28	13	3
E-607	FP-704	-26.5	-24.5	54.8	997	211	78.9	0.35	66.8	8.80	13.49	13	3
E-607	FP-671	0.6	0.2	86.2	2000	211	89.5	1.22	67.9	7.16	16.27	14	5
E-607	FP-673	-0.1	0.0	83.5	2000	229	88.6	1.04	67.2	7.25	16.64	12	6
E-607	FP-672	-1.4	-0.2	75.2	1975	211	89.3	0.87	67.0	7.25	16.39	13	5
E-607	FP-691	-9.9	-9.2	70.1	2000	221	89.0	0.52	66.8	7.32	16.65	12	5
E-607	FP-690	-9.0	-9.3	73.4	2000	211	89.5	0.87	66.9	7.36	16.38	13	5
E-607	FP-689	-11.1	-10.0	68.0	2000	211	89.5	0.69	67.0	7.25	16.39	12	4
E-607	FP-709	-25.9	-24.3	54.0	1975	221	88.8	-0.52	67.1	8.96	16.22	12	7
E-607	FP-708	-25.4	-24.7	61.4	1975	196	90.1	-1.56	67.0	9.11	15.70	13	4
E-607	FP-707	-28.1	-25.6	51.7	1975	221	88.8	-0.69	66.7	9.52	16.94	10	4
E-607	FP-674	0.2	-0.5	81.5	4000	229	94.3	0.69	67.2	7.24	21.33	14	8
E-607	FP-675	0.9	-1.6	83.0	4000	246	93.8	0.52	67.1	7.36	20.88	12	9
E-607	FP-676	-1.6	-3.1	73.7	4000	203	94.9	4.51	66.7	7.43	21.00	11	8
E-607	FP-694	-10.0	-9.6	66.6	4000	211	94.7	0.52	67.0	7.53	20.54	13	8
E-607	FP-693	-9.3	-9.7	72.1	4000	236	94.1	0.35	66.7	7.52	20.35	n.m.	n.m.
E-607	FP-692	-9.9	-10.0	68.4	4000	211	94.7	0.52	66.8	7.51	20.52	11	8
E-607	FP-712	-25.7	-24.0	53.0	4000	221	94.5	-1.56	66.4	9.40	20.08	13	n.m.
E-607	FP-711	-25.5	-24.6	53.1	4000	203	94.9	-0.69	66.2	9.45	20.10	12	7
E-607	FP-710	-26.4	-24.7	51.9	4000	229	94.3	-2.43	66.3	9.60	20.31	12	7

n.m. = not measured

Acceptance Criteria for Type II Fluid Series: D_0 = 8.34 mm, D_{-10} = 9.25 mm, D_{-15} = 9.70 mm, D_{-20} = 10.16 mm

(1) Thickness of the fluid measured at the beginning of the test.
(2) Thickness of the fluid measured at the end of the test.
(3) Fluid Elimination.
(4) Water Change.
(5) Air velocity 30 seconds after the beginning of the test.
(6) Time of maximum wave height.

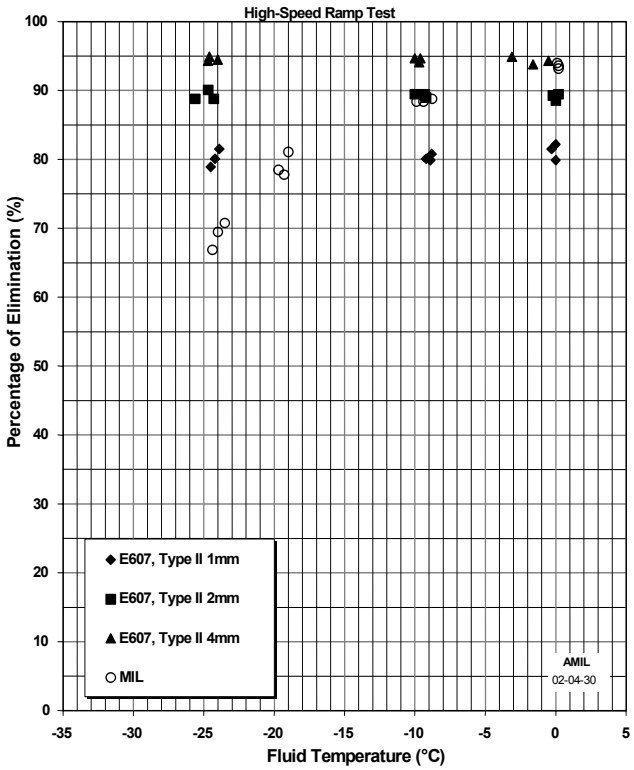

FIGURE 35. PERCENTAGE FLUID ELIMINATION FOR KILFROST ABC-3

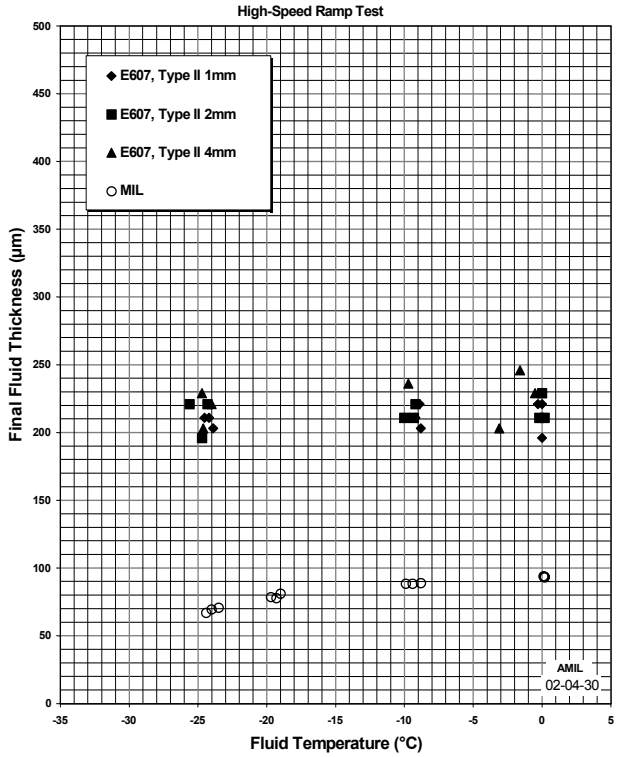

FIGURE 36. FINAL FLUID THICKNESS FOR KILFROST ABC-3

3.2.2 Clariant Safewing MPII 1951.

Figure 37 and table 9 show the results for Clariant Safewing MPII 1951 tested with 1-, 2-, and 4-mm initial fluid thicknesses. The graph shows that there is little difference in the measured BLDT at 30 sec. between the different initial fluid thicknesses at each temperature interval. Table 9 shows the maximum wave heights for each initial thickness. The wave heights are highest for the 4-mm initial thickness and in the same order as the Kilfrost ABC-3 (section 3.2.1), followed by the 2- and 1-mm thicknesses. Despite this, the BLDT measurements at 30 sec. are all relatively the same as seen in figure 37.

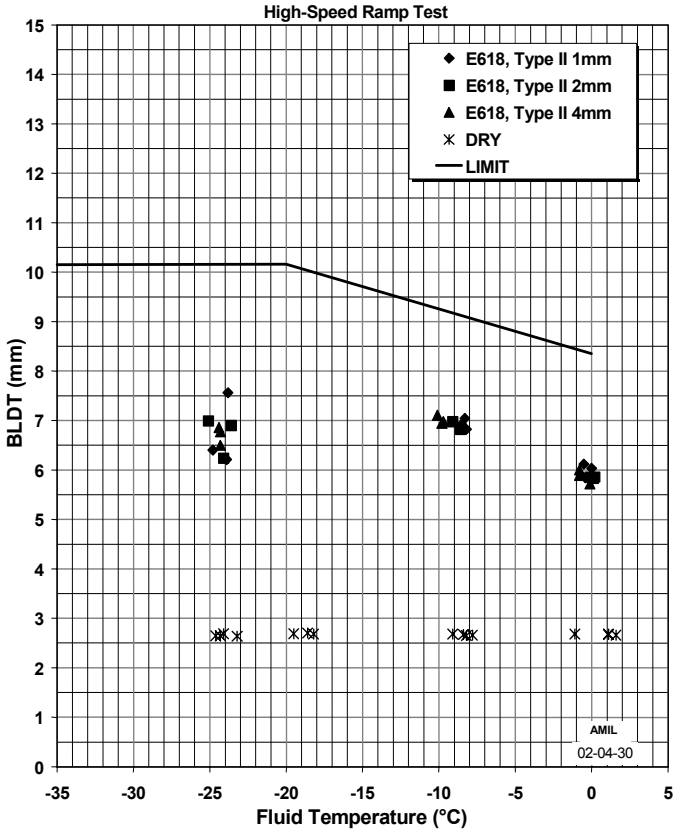

FIGURE 37. AERODYNAMIC TEST RESULTS FOR CLARIANT SAFEWING MPII 1951 WITH THREE DIFFERENT INITIAL FLUID THICKNESSES

Figure 38 presents the fluid elimination as a percentage for Clariant Safewing MPII 1951. The graph shows a smaller elimination percentage for the 1-mm initial thickness followed by the 2-mm initial thickness, and then the 4-mm initial thickness. However, at -25°C the 2- and 1-mm thicknesses had about the same percentage elimination.

Figure 39 presents the final fluid thicknesses for the three different initial thicknesses. For this fluid, there is significant variation, but all values occur below 250 µm. Only at 0°C does the 1-mm initial thickness have a lower final thickness than the other two.

TABLE 9. AERODYNAMIC PERFORMANCE TEST DATA FOR CLARIANT SAFEWING MPII 1951

Fluid Code	Test Code	T_a (°C)	T_f (°C)	r.h. (%)	t_o [(1)] (µm)	t_{end} [(2)] (µm)	F.E. [(3)] (%)	W.C. [(4)] (%)	V [(5)] (m/s)	δ* (mm)	δ max (mm)	t [(6)] (sec)	Maximum Wave Height (mm)
E-618	FP-679	0.0	0.0	84.0	1058	196	81.5	0.55	67.1	6.03	13.28	14	3
E-618	FP-677	0.6	-0.4	84.3	1100	160	85.5	0.37	68.9	5.84	13.21	12	3
E-618	FP-678	-1.3	-0.5	76.3	1100	185	83.1	0.37	67.1	6.12	13.23	12	3
E-618	FP-695	-8.3	-8.2	74.4	959	211	78.0	1.10	66.9	6.82	12.89	13	3
E-618	FP-696	-9.8	-8.3	67.1	1016	196	80.8	0.18	66.9	7.04	12.96	14	3
E-618	FP-697	-9.5	-8.5	68.3	959	229	76.1	0.00	67.2	6.92	12.63	13	3
E-618	FP-723	-25.3	-23.8	52.7	1016	185	81.8	-0.37	67.0	7.56	12.70	13	4
E-618	FP-714	-24.7	-23.9	63.0	1100	102	90.8	-0.92	66.9	6.21	12.42	13	3
E-618	FP-713	-26.9	-24.8	55.4	1058	102	90.4	0.00	66.8	6.40	12.73	14	3
E-618	FP-681	0.7	0.2	82.8	1975	236	88.0	0.55	67.5	5.86	16.21	12	5
E-618	FP-682	-0.4	0.1	79.0	2000	221	89.0	0.18	67.3	5.83	16.10	13	5
E-618	FP-680	0.1	-0.1	83.5	1975	221	88.8	-0.18	67.5	5.85	16.23	12	5
E-618	FP-698	-9.5	-8.6	72.4	1975	203	89.7	0.37	66.7	6.85	16.32	12	5
E-618	FP-700	-8.7	-8.6	77.1	1975	229	88.4	0.73	67.2	6.82	16.33	11	5
E-618	FP-699	-10.5	-9.1	67.4	2000	196	90.2	0.00	66.6	6.98	16.25	12	5
E-618	FP-724	-25.6	-23.6	52.1	1975	178	91.0	-1.10	66.6	6.90	16.01	14	5
E-618	FP-718	-24.9	-24.1	56.8	2000	127	93.7	0.00	66.9	6.24	15.46	10	4
E-618	FP-717	-27.5	-25.1	50.1	1975	160	91.9	0.00	66.8	6.99	16.71	12	4
E-618	FP-683	0.8	-0.1	85.0	4000	236	94.1	0.55	67.2	5.72	20.33	11	9
E-618	FP-684	-1.4	-0.8	75.4	4000	246	93.8	0.00	67.1	6.00	21.40	11	9
E-618	FP-685	-0.1	-0.8	82.0	4000	221	94.5	0.37	66.9	5.89	20.55	11	10
E-618	FP-701	-9.8	-9.7	70.4	4000	203	94.9	-0.37	67.0	6.98	21.19	11	9
E-618	FP-703	-9.6	-9.8	71.8	4000	229	94.3	0.18	66.4	6.94	20.62	12	7
E-618	FP-702	-9.8	-10.1	70.0	4000	203	94.9	0.18	66.9	7.11	20.79	10	8
E-618	FP-721	-25.7	-24.3	52.5	4000	127	96.8	-2.20	66.6	6.50	19.66	11	7
E-618	FP-720	-25.1	-24.3	57.2	4000	135	96.6	-2.01	66.4	6.77	19.37	12	8
E-618	FP-722	-26.3	-24.4	49.4	4000	145	96.4	-2.20	66.7	6.86	19.48	n.m.	7

n.m. = not measured

Acceptance Criteria for Type II Fluid Series: D_0 = 8.34 mm, D_{-10} = 9.25 mm, D_{-15} = 9.70 mm, D_{-20} = 10.16 mm

(1) Thickness of the fluid measured at the beginning of the test.
(2) Thickness of the fluid measured at the end of the test.
(3) Fluid Elimination.
(4) Water Change.
(5) Air velocity 30 seconds after the beginning of the test.
(6) Time of maximum wave height.

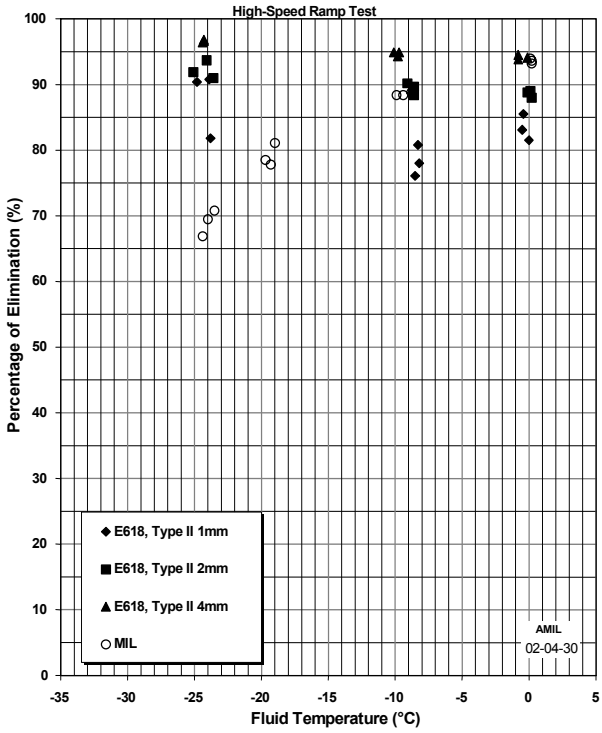

FIGURE 38. PERCENTAGE FLUID ELIMINATION FOR CLARIANT SAFEWING MPII 1951

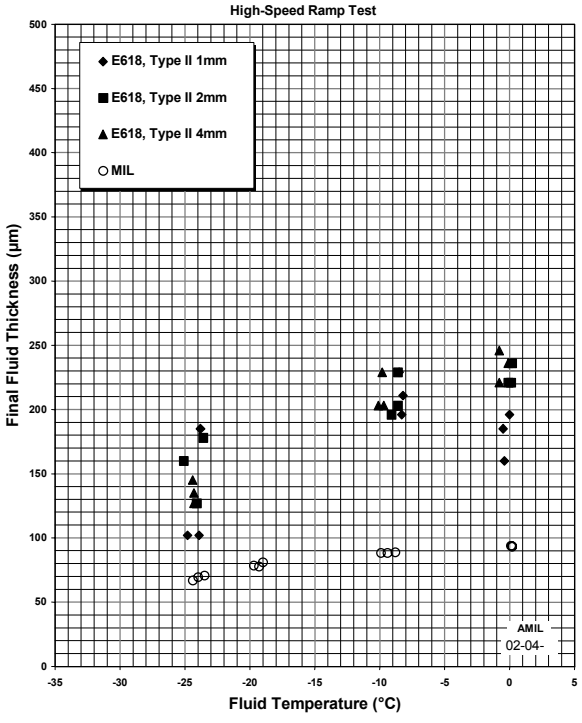

FIGURE 39. FINAL FLUID THICKNESS FOR CLARIANT SAFEWING MPII 1951

3.2.3 Octagon Process MaxFlight.

The results of FPET testing for different initial thicknesses of Octagon Process MaxFlight are presented in table 10. The table shows that the maximum wave heights are highest for the 4-mm initial thickness followed by the 2- and 1-mm thicknesses. Despite this, the BLDT measurements at 30 sec. are all relatively the same as seen in figure 40, which presents the BLDT measurements as a function of temperature with respect to the acceptance criteria. The graph shows that BLDT measurements are nearly equal at each temperature interval despite the different thicknesses.

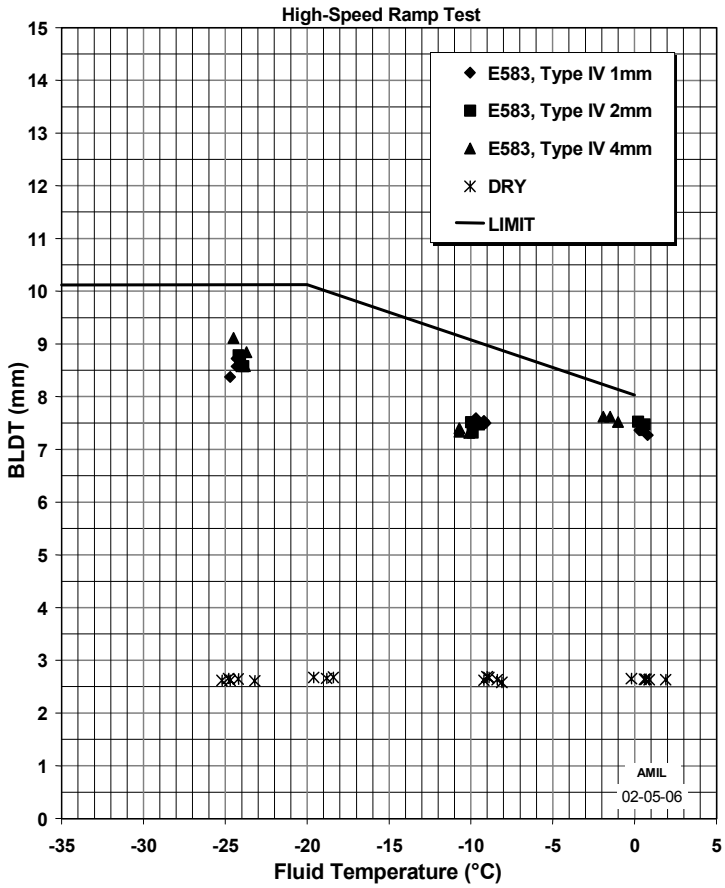

FIGURE 40. AERODYNAMIC TEST RESULTS FOR OCTAGON PROCESS MAXFLIGHT WITH THREE DIFFERENT INITIAL FLUID THICKNESS

Figure 41 presents the percentage of fluid elimination for the Octagon Process MaxFlight with the different initial thicknesses. The graph shows that the 4-mm initial thickness had the highest percentage elimination followed by the 2- and the 1-mm thicknesses. However, when the final thickness is examined (figure 42), the values are all in the same range within 50 μm, with more fluid elimination, or less final thickness, at the higher temperatures.

TABLE 10. AERODYNAMIC PERFORMANCE TEST DATA FOR OCTAGON PROCESS MAXFLIGHT

Fluid Code	Test Code	T_a (°C)	T_f (°C)	r.h. (%)	t_o[(1)] (μm)	t_{end}[(2)] (μm)	F.E.[(3)] (%)	W.C.[(4)] (%)	V[(5)] (m/s)	δ* (mm)	δ max (mm)	t[(6)] (sec)	Maximum Wave Height (mm)
E-583	FP-737	0.7	0.8	85.4	1058	170	83.9	1.89	66.6	7.27	13.21	13	2
E-583	FP-738	-1.2	0.4	77.1	1100	178	83.8	1.20	66.9	7.36	13.18	13	2
E-583	FP-736	-0.5	0.3	81.4	1058	178	83.2	1.89	66.8	7.36	13.07	13	2
E-583	FP-763	-10.1	-9.1	73.9	1016	211	79.3	0.86	66.8	7.50	13.03	11	3
E-583	FP-765	-9.7	-9.2	74.3	1016	236	76.8	0.00	66.5	7.54	12.90	11	3
E-583	FP-764	-11.6	-9.7	66.5	1058	236	77.7	0.17	67.0	7.59	13.25	13	3
E-583	FP-793	-27.4	-24.3	51.2	1058	229	78.4	-0.17	66.3	8.57	12.89	15	3
E-583	FP-792	-27.2	-24.3	53.9	1016	211	79.3	0.00	66.8	8.72	12.63	10	3
E-583	FP-791	-27.1	-24.7	56.8	975	203	79.2	0.17	66.9	8.37	12.70	11	2
E-583	FP-739	0.0	0.6	83.9	1975	160	91.9	1.38	67.0	7.48	16.13	13	5
E-583	FP-741	0.4	0.5	85.2	1975	196	90.1	1.03	67.0	7.42	16.21	12	4
E-583	FP-740	-1.0	0.2	78.8	1975	185	90.6	0.86	66.8	7.53	16.31	n.m.	n.m.
E-583	FP-767	-9.4	-9.5	73.8	2000	196	90.2	0.52	67.2	7.48	16.22	12	5
E-583	FP-768	-10.8	-9.9	65.8	1975	196	90.1	0.34	66.9	7.32	16.47	13	6
E-583	FP-766	-11.5	-10.0	65.7	1975	211	89.3	0.86	67.1	7.52	16.33	12	5
E-583	FP-796	-26.6	-23.9	53.2	2000	221	89.0	0.00	67.0	8.58	16.36	13	6
E-583	FP-795	-27.1	-24.1	51.3	2000	203	89.8	-0.17	66.8	8.76	15.85	13	6
E-583	FP-794	-27.6	-24.2	50.6	2000	211	89.5	0.00	66.9	8.79	16.16	13	5
E-583	FP-744	0.0	-1.0	88.9	4000	196	95.1	1.55	67.1	7.52	21.22	15	10
E-583	FP-743	-1.3	-1.5	86.6	4000	203	94.9	0.86	66.7	7.62	21.25	12	12
E-583	FP-742	-2.6	-1.9	80.5	4000	196	95.1	-0.69	66.8	7.62	21.91	12	10
E-583	FP-769	-9.2	-10.1	71.0	4000	196	95.1	1.38	66.6	7.31	21.05	10	10
E-583	FP-770	-10.6	-10.7	65.7	4000	178	95.6	0.69	66.9	7.40	21.11	11	11
E-583	FP-771	-9.5	-10.7	71.7	4000	221	94.5	0.69	67.1	7.33	21.40	14	11
E-583	FP-797	-26.8	-23.7	51.4	4000	246	93.8	-0.34	67.2	8.84	21.43	11	9
E-583	FP-799	-25.1	-23.8	59.6	4000	211	94.7	-0.17	66.7	8.58	20.12	15	9
E-583	FP-798	-27.8	-24.5	50.9	4000	203	94.9	-0.17	66.7	9.11	20.45	15	10

n.m. = not measured

Acceptance Criteria for Type IV Fluid Series: $D_0 = 8.03$ mm, $D_{-10} = 9.08$ mm, $D_{-15} = 9.60$ mm, $D_{-20} = 10.12$ mm

(1) Thickness of the fluid measured at the beginning of the test.
(2) Thickness of the fluid measured at the end of the test.
(3) Fluid Elimination.
(4) Water Change.
(5) Air velocity 30 seconds after the beginning of the test.
(6) Time of maximum wave height.

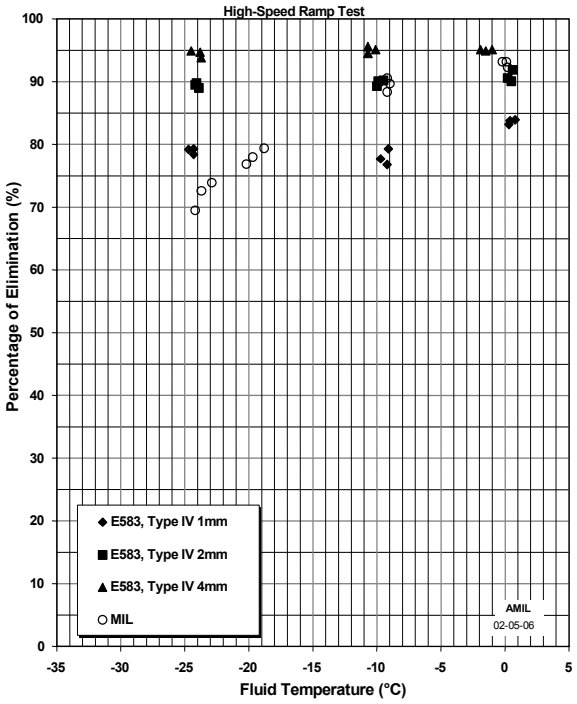

FIGURE 41. PERCENTAGE FLUID ELIMINATION FOR OCTAGON PROCESS MAXFLIGHT

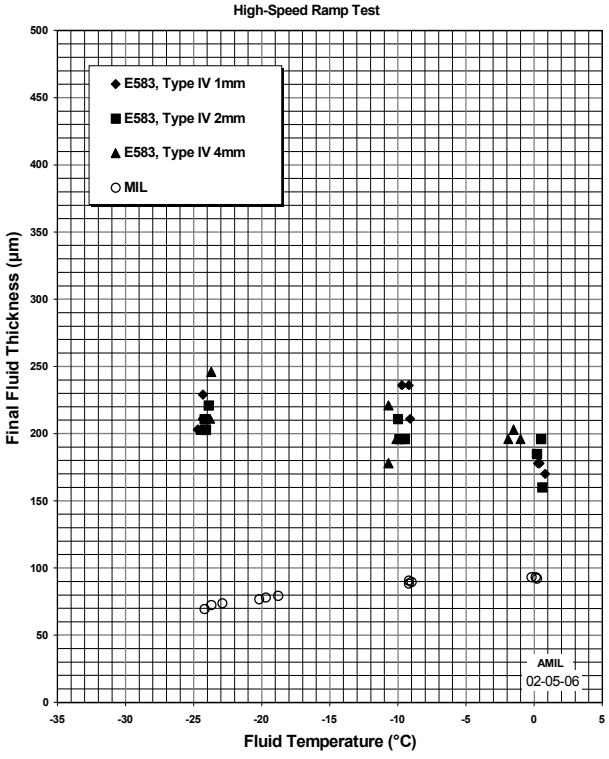

FIGURE 42. FINAL FLUID THICKNESS FOR OCTAGON PROCESS MAXFLIGHT

3.2.4 SPCA AD-480.

The results of FPET for different initial thicknesses of SPCA AD-480 are presented in table 11. The table shows that the maximum wave heights are highest for the 4–mm initial thickness followed by the 2- and 1-mm thicknesses. Despite this, the BLDT measurements at 30 sec. are all relatively the same (figure 43), which presents the BLDT measurements as a function of temperature with respect to the acceptance criteria. The graph shows that BLDT measurements are relatively the same at each temperature interval, no clear difference can be seen with respect to the different initial fluid thicknesses.

TABLE 11. AERODYNAMIC PERFORMANCE TEST DATA FOR SPCA AD-480

Fluid Code	Test Code	T_a (°C)	T_f (°C)	r.h. (%)	t_o[(1)] (μm)	t_{end}[(2)] (μm)	F.E.[(3)] (%)	W.C.[(4)] (%)	V[(5)] (m/s)	δ* (mm)	δ max (mm)	t[(6)] (sec)	Maximum Wave Height (mm)
E-007	FP-727	-0.2	-0.5	80.8	974	160	83.6	1.86	66.9	6.76	12.58	13	3
E-007	FP-728	0.4	-0.6	83.3	974	185	81.0	1.53	67.5	6.55	12.61	13	3
E-007	FP-729	-1.1	-0.9	78.3	1058	152	85.6	1.36	66.9	6.76	13.03	21	3
E-007	FP-755	-9.0	-8.7	74.7	1016	211	79.3	0.00	67.0	7.51	12.69	15	3
E-007	FP-754	-10.9	-9.1	65.8	1058	203	80.8	0.34	66.4	7.65	12.33	13	2
E-007	FP-756	-10.5	-9.1	64.7	1016	221	78.3	0.17	66.4	7.68	12.77	n.m.	n.m.
E-007	FP-784	-27.2	-23.9	51.2	1016	185	81.8	-0.68	67.0	8.07	12.82	13	n.m.
E-007	FP-783	-27.1	-24.1	51.3	1016	196	80.8	0.00	67.0	8.07	12.54	n.m.	3
E-007	FP-782	-26.9	-24.4	53.8	973	185	80.9	-0.17	67.3	7.91	12.76	n.m.	n.m.
E-007	FP-732	0.6	0.4	85.4	2000	178	91.1	0.68	67.4	6.28	16.26	12	6
E-007	FP-731	-0.6	-0.2	79.7	1975	196	90.1	0.85	67.4	6.38	16.38	13	6
E-007	FP-730	0.1	-0.2	83.1	1975	203	89.7	1.36	66.6	6.38	16.12	13	5
E-007	FP-759	-11.3	-10.3	70.6	1975	229	88.4	0.17	66.9	7.97	16.12	14	5
E-007	FP-758	-10.2	-10.3	75.2	1975	229	88.4	0.17	67.1	8.02	15.97	14	6
E-007	FP-757	-11.2	-10.5	74.1	1975	262	86.8	0.51	66.5	8.37	15.80	15	5
E-007	FP-787	-26.6	-23.6	52.5	1975	185	90.6	-0.85	67.0	8.14	15.76	13	4
E-007	FP-786	-25.9	-23.8	57.4	1975	185	90.6	-0.51	66.8	7.99	15.68	10	4
E-007	FP-785	-28.2	-24.7	52.2	1975	185	90.6	-0.34	66.8	8.33	15.52	14	4
E-007	FP-733	-1.5	-0.1	75.1	4000	178	95.6	0.68	67.2	6.37	21.10	12	9
E-007	FP-735	0.5	-0.1	85.1	4000	203	94.9	1.36	67.1	6.30	21.03	11	9
E-007	FP-734	-0.3	-0.2	83.1	4000	178	95.6	0.85	67.5	6.37	20.81	12	8
E-007	FP-760	-9.5	-9.9	78.7	4000	246	93.8	0.85	66.6	8.08	21.25	12	9
E-007	FP-761	-11.2	-10.3	68.8	4000	287	92.8	0.17	66.7	8.35	21.52	13	10
E-007	FP-762	-9.4	-10.3	78.9	4000	229	94.3	0.00	66.6	6.79	21.04	12	8
E-007	FP-790	-26.4	-23.4	53.3	4000	203	94.9	0.17	66.9	8.24	19.69	11	7
E-007	FP-789	-25.7	-23.7	59.0	4000	185	95.4	-0.17	67.0	8.10	19.85	15	7
E-007	FP-788	-28.5	-24.8	50.0	3333	196	94.1	0.17	66.6	8.85	20.44	13	7

n.m. = not measured

Acceptance Criteria for Type IV Fluid Series: $D_0 = 8.03$ mm, $D_{-10} = 9.08$ mm, $D_{-15} = 9.60$ mm, $D_{-20} = 10.12$ mm

(1) Thickness of the fluid measured at the beginning of the test.
(2) Thickness of the fluid measured at the end of the test.
(3) Fluid Elimination.
(4) Water Change.
(5) Air velocity 30 seconds after the beginning of the test.
(6) Time of maximum wave height.

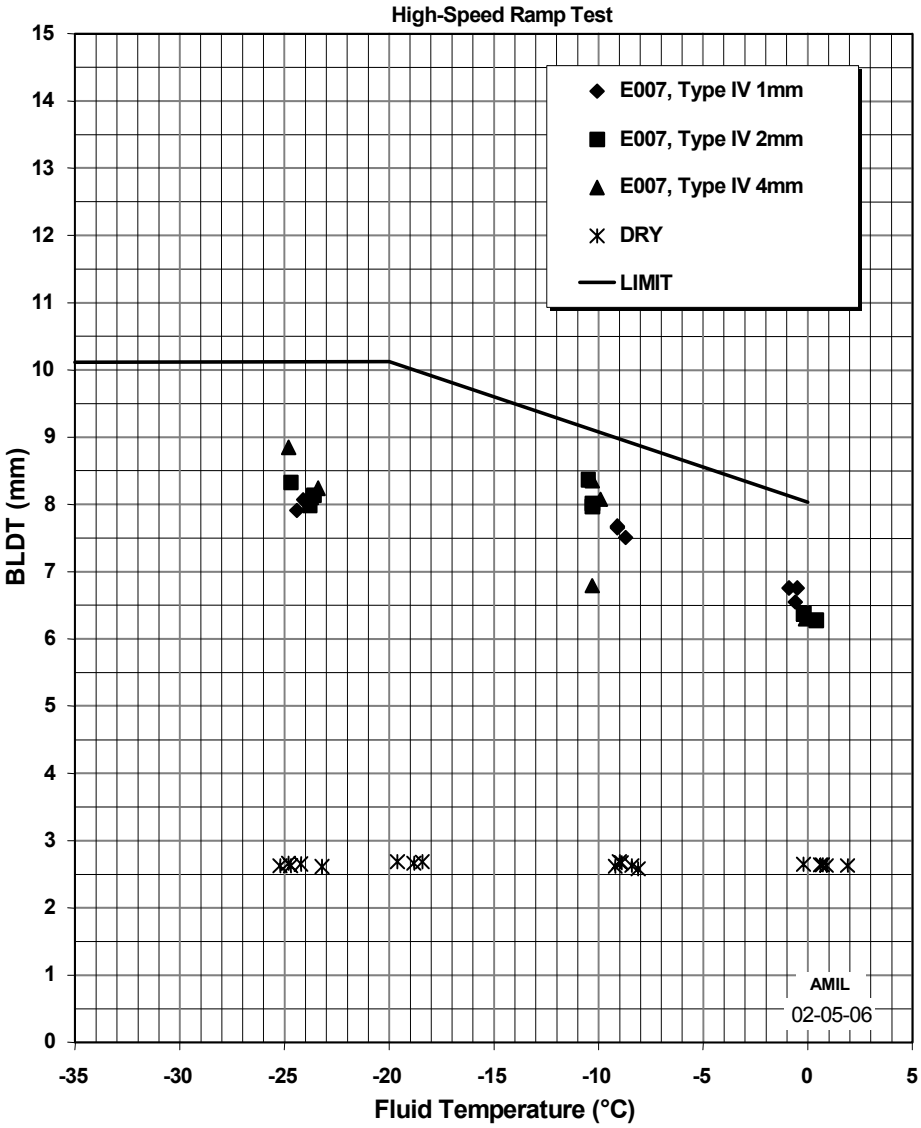

FIGURE 43. AERODYNAMIC TEST RESULTS FOR SPCA AD-480 WITH THREE DIFFERENT INITIAL FLUID THICKNESSES

Figure 44 presents the percentage elimination as a function of temperature for the FPET with the different initial fluid thicknesses. The graph shows that the 4-mm initial thickness had the highest percentage elimination followed by the 2- and the 1-mm thicknesses. However, when the final thickness is examined (figure 45), no clear difference is apparent between the initial thicknesses. Tests at -10°C show the most scatter and those at -25°C show the least.

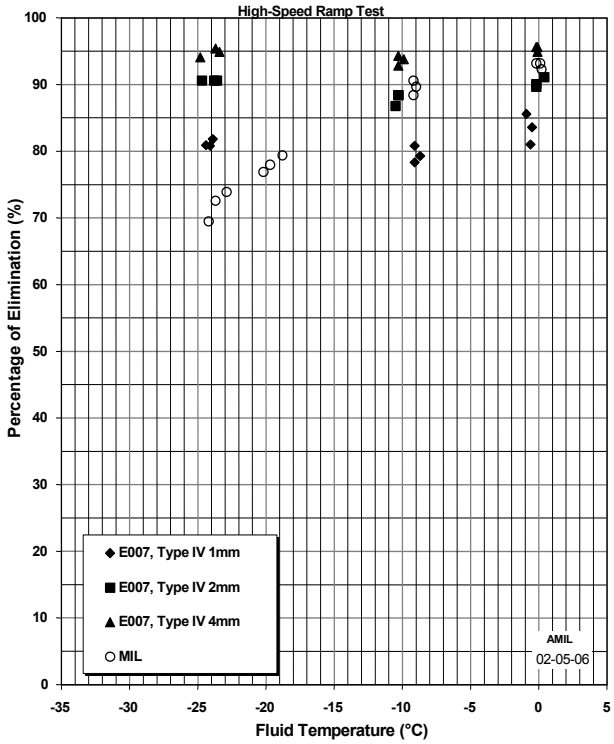

FIGURE 44. PERCENTAGE FLUID ELIMINATION FOR SPCA AD-480

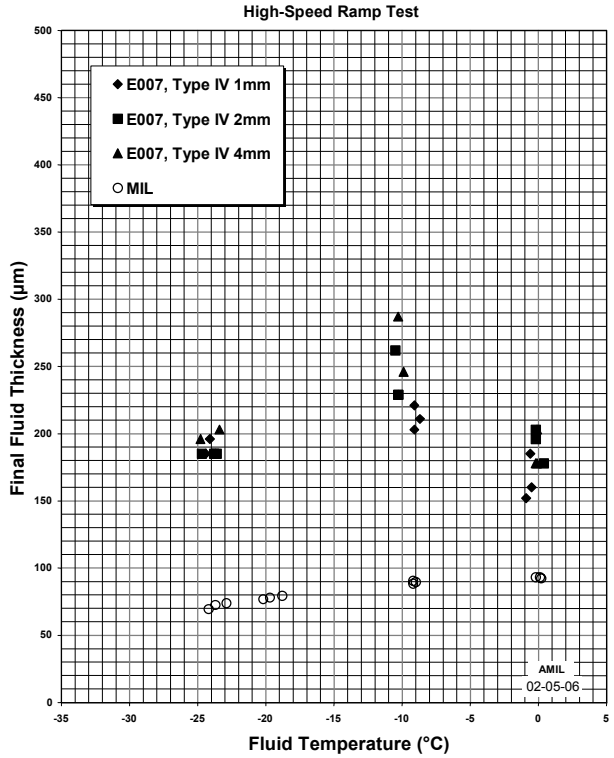

FIGURE 45. FINAL FLUID THICKNESS FOR SPCA AD-480

3.2.5 Dow Ultra+.

The results of FPET for different initial thicknesses of Dow Ultra+ are presented in table 12. The table shows that the maximum wave heights are highest for the 4-mm initial thickness followed by the 2- and 1-mm thicknesses. Figure 46 presents the BLDT measurements as a function of temperature with respect to the acceptance criteria. The graph shows that BLDT measurements are relatively the same at the 0° and -10°C temperature intervals. However, at -25°C, the 1-mm initial thickness points are well below the acceptance criteria, while the 4-mm points are above and the 2 mm around the acceptance criteria. This seems to be the only fluid tested where the initial thickness appears to have an effect on the BLDT measurements. This may be partially due to the fact that the fluid is normally certified, or passes just above -25°C. Therefore, this fluid is being tested around its limit of acceptability, a point at which there is normally more variation in the BLDT compared to tests at higher temperatures from their limit. Therefore, the initial fluid thickness may only have an effect on the fluid at critical temperatures, near where the fluid is acceptable.

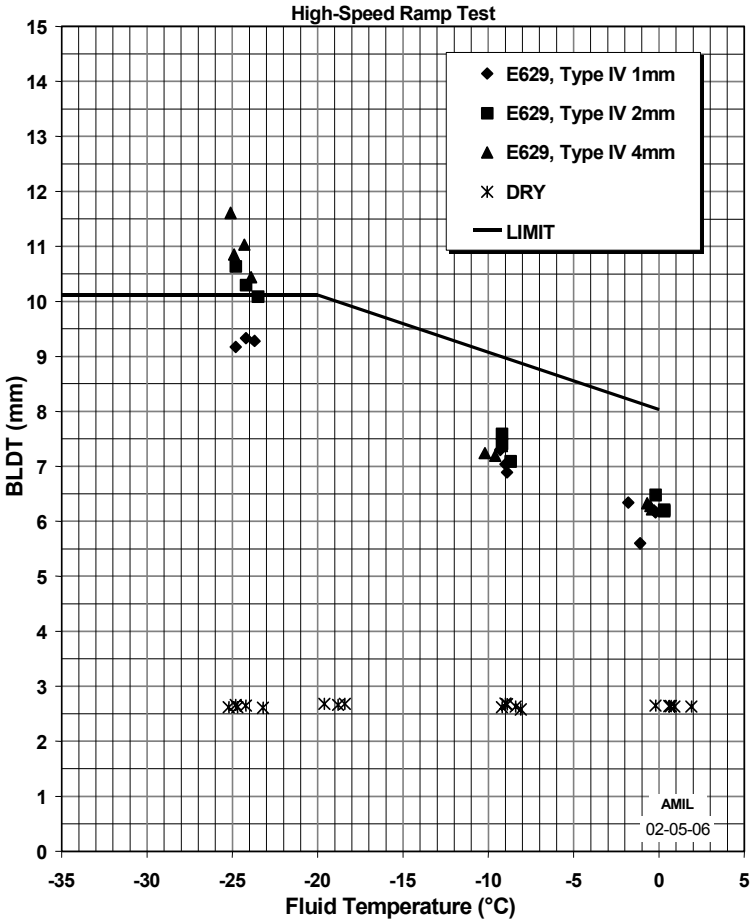

FIGURE 46. AERODYNAMIC TEST RESULTS FOR DOW ULTRA+ WITH THREE DIFFERENT INITIAL FLUID THICKNESSES

TABLE 12. AERODYNAMIC PERFORMANCE TEST DATA FOR DOW ULTRA+

Fluid Code	Test Code	T_a (°C)	T_f (°C)	r.h. (%)	t_o[1] (µm)	t_{end}[2] (µm)	F.E.[3] (%)	W.C.[4] (%)	V[5] (m/s)	δ* (mm)	δ max (mm)	t[6] (sec)	Maximum Wave Height (mm)
E-629	FP-746	0.3	-0.2	84.0	1100	196	82.2	4.52	67.4	6.16	12.89	13	3
E-629	FP-747	-1.2	-0.3	75.7	1100	178	83.8	2.56	67.4	6.20	13.00	14	3
E-629	FP-745	-1.1	-1.1	80.6	1143	135	88.2	4.52	75.6	5.60	12.88	14	2
E-629	FP-781	-2.5	-1.8	93.9	1100	185	83.1	3.61	67.4	6.34	12.98	13	4
E-629	FP-774	-9.4	-8.9	73.7	1058	236	77.7	1.20	66.9	6.89	11.93	12	3
E-629	FP-772	-9.6	-9.0	71.3	1100	246	77.6	1.51	67.1	7.04	11.73	11	2
E-629	FP-773	-11.2	-9.3	62.7	1100	221	79.9	1.20	67.2	7.30	11.77	10	3
E-629	FP-802	-26.6	-23.7	49.0	1058	279	73.6	0.30	66.1	9.28	11.56	13	2
E-629	FP-801	-26.7	-24.2	48.7	1058	312	70.5	0.00	66.3	9.33	11.60	n.m.	2
E-629	FP-800	-27.8	-24.8	48.8	1016	254	75.0	0.45	66.9	9.17	11.61	12	2
E-629	FP-748	0.0	0.3	83.1	2000	178	91.1	3.46	67.9	6.19	16.89	13	4
E-629	FP-750	0.0	0.3	82.6	2000	178	91.1	3.31	68.1	6.21	16.29	14	5
E-629	FP-749	-1.5	-0.2	76.7	2000	196	90.2	2.56	68.5	6.48	17.02	14	4
E-629	FP-776	-9.0	-8.7	75.4	2000	185	90.7	1.66	67.2	7.09	16.54	13	5
E-629	FP-775	-10.9	-9.2	65.9	2000	196	90.2	1.20	67.3	7.59	16.24	12	4
E-629	FP-777	-10.7	-9.2	65.3	2000	203	89.8	1.20	67.5	7.41	16.30	15	5
E-629	FP-805	-26.1	-23.5	52.6	2000	297	85.1	0.15	66.8	10.09	15.12	11	3
E-629	FP-804	-26.7	-24.2	51.4	2000	305	84.8	0.30	65.9	10.30	14.96	14	3
E-629	FP-803	-28.1	-24.8	49.3	2000	272	86.4	0.30	65.2	10.64	14.79	n.m.	n.m.
E-629	FP-752	-0.1	-0.4	83.5	4000	160	96.0	3.01	68.0	6.22	22.54	14	12
E-629	FP-751	-1.6	-0.5	75.3	4000	185	95.4	2.86	66.9	6.28	22.16	14	10
E-629	FP-753	-1.3	-0.7	76.3	4000	185	95.4	1.81	67.4	6.33	22.71	12	11
E-629	FP-778	-9.2	-9.2	71.1	4000	236	94.1	1.51	67.3	7.37	22.05	12	8
E-629	FP-779	-10.5	-9.6	65.9	4000	211	94.7	1.66	68.2	7.19	22.08	12	10
E-629	FP-780	-9.6	-10.2	69.9	4000	229	94.3	1.36	68.0	7.24	21.98	12	10
E-629	FP-808	-26.4	-23.9	53.6	4000	356	91.1	0.45	67.3	10.44	21.10	13	6
E-629	FP-807	-26.7	-24.3	52.9	4000	348	91.3	0.00	66.7	11.03	21.11	14	6
E-629	FP-809	-28.2	-24.9	50.6	4000	356	91.1	0.45	67.3	10.85	20.85	12	6
E-629	FP-806	-28.0	-25.1	51.2	4000	323	91.9	0.15	66.0	11.61	21.27	15	6

n.m. = not measured

Acceptance Criteria for Type IV Fluid Series: D_0 = 8.03 mm, D_{-10} = 9.08 mm, D_{-15} = 9.60 mm, D_{-20} = 10.12 mm

[1] Thickness of the fluid measured at the beginning of the test.
[2] Thickness of the fluid measured at the end of the test.
[3] Fluid Elimination.
[4] Water Change.
[5] Air velocity 30 seconds after the beginning of the test.
[6] Time of maximum wave height.

Figure 47 presents the percentage elimination as a function of temperature for the FPETs with the different initial fluid thicknesses. The graph shows that the 4-mm initial thickness had the highest percentage of elimination followed by the 2- and the 1-mm thicknesses. Figure 48 presents the final fluid thicknesses as a function of temperature. This graph shows, although there is much scatter at 0° and -10°C, that there is no clear difference between the initial fluid thicknesses. However, at -25°C, the 4-mm initial thickness clearly left more residue than the 2- and 1-mm thicknesses, neither showed a clear difference.

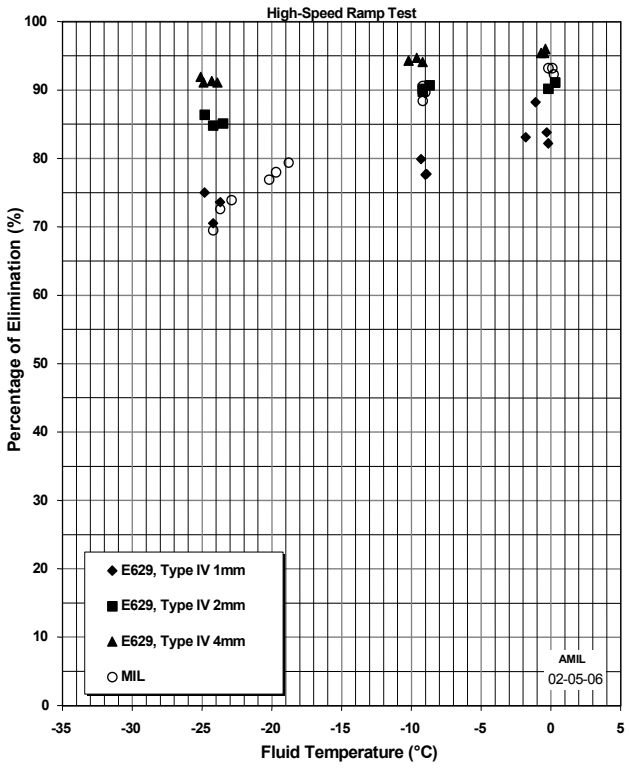

FIGURE 47. PERCENTAGE FLUID ELIMINATION FOR DOW ULTRA+

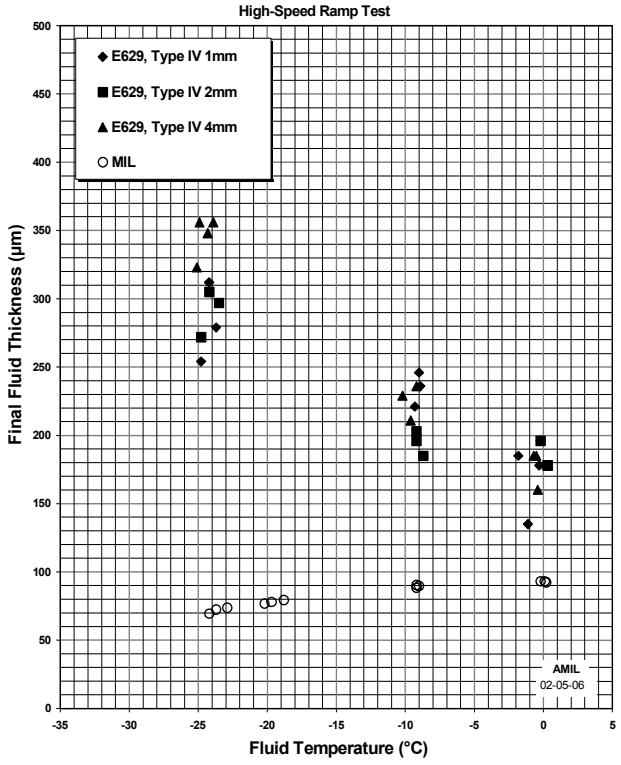

FIGURE 48. FINAL FLUID THICKNESS FOR DOW ULTRA+

3.3 MAXIMUM WAVE HEIGHT.

The maximum wave heights, as a function of temperature for all fluids at 1-, 2-, and 4-mm initial fluid thicknesses, are presented in figures 49 through 51 respectively. In all graphs, the Type II fluids are represented by the solid symbols, and the open symbols represent the Type IV fluids. All three graphs show no clear differences in maximum wave height between Type II and Type IV fluids.

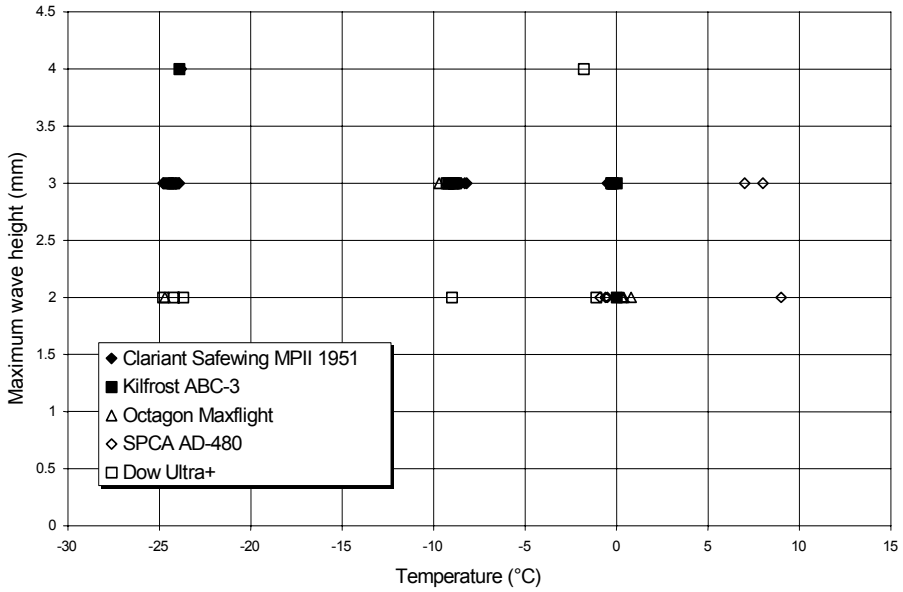

FIGURE 49. MAXIMUM WAVE HEIGHT FOR 1-mm INITIAL FLUID THICKNESS

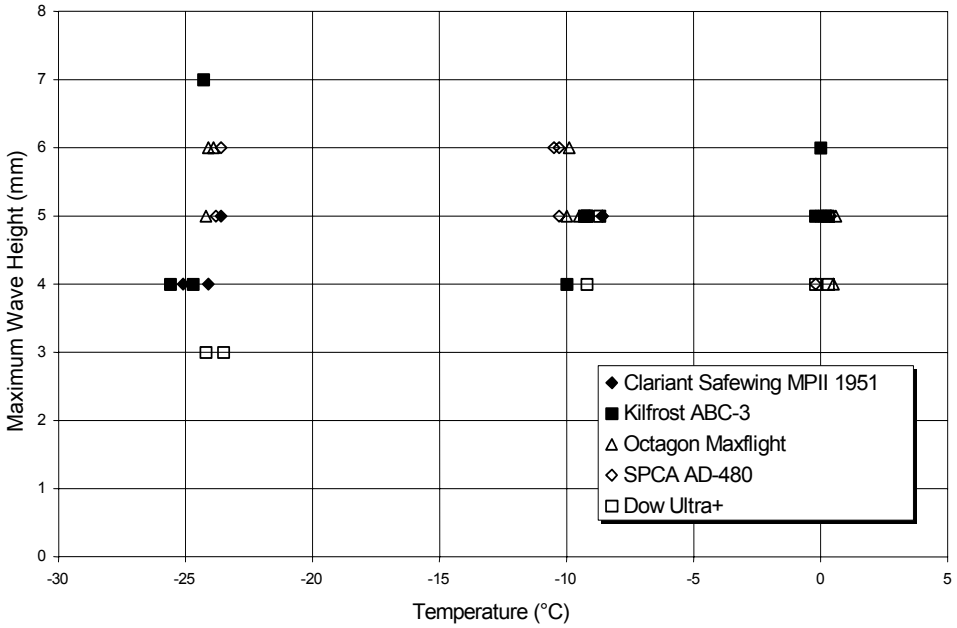

FIGURE 50. MAXIMUM WAVE HEIGHT FOR 2-mm INITIAL FLUID THICKNESS

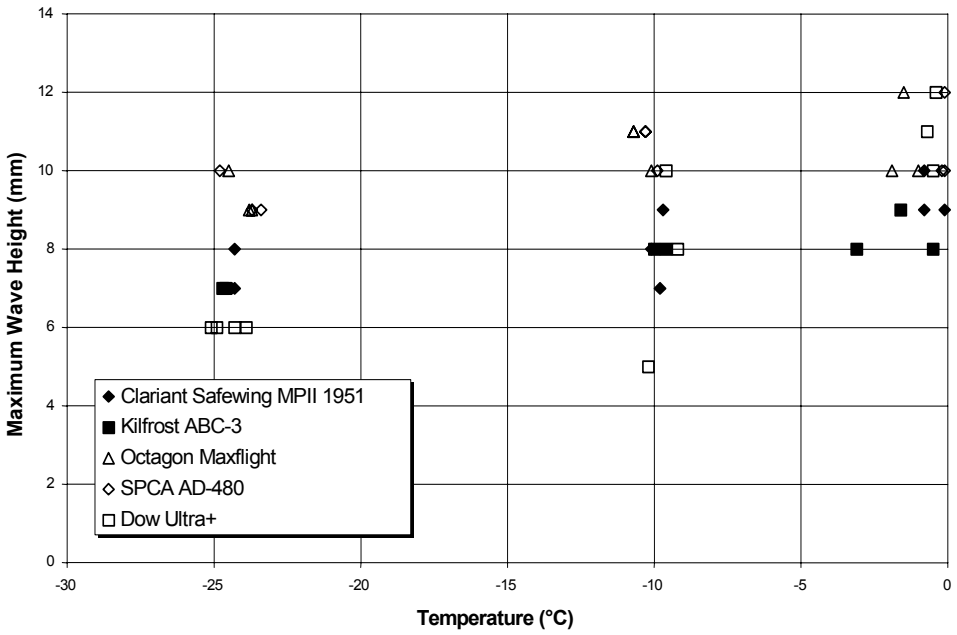

FIGURE 51. MAXIMUM WAVE HEIGHT FOR 4-mm INITIAL FLUID THICKNESS

3.4 DIFFERENT INITIAL FLUID THICKNESSES—CONCLUSION.

Examination of BLDT and elimination data from FPET on two Type II and three Type IV commercial fluids with initial fluid thicknesses of 1, 2, and 4 mm showed that for four of the five fluids the initial fluid thickness had little or no effect on the BLDT and fluid elimination. However, for one of the Type IV fluids, there was some difference with the 4-mm initial thickness at -25°C. It was noted that there were higher BLDT measurements and more fluid remained on the test section floor following the test. These higher BLDT values may be partially due to the fact that, for this fluid, -25°C is very near to its acceptable limit, a point where all fluids tended to show much variation in BLDT measurements. Therefore, the initial fluid thickness may only have an effect on a fluid at critical temperatures, near where the fluid is acceptable.

4. TASK 3: ENERGY REQUIRED.

Currently, during a certification FPET, the speed of the fan is initially adjusted to obtain a 5 m/s initial air speed over the test section for 5 minutes. Then the frequency is increased to obtain a linear wind speed acceleration of 2.6 m/s² for 25 sec., leveling off at 65 m/s for 30 sec. more (figure 1). To obtain this acceleration profile on fluids with different viscosities as well as dry without fluid, the acceleration of the fan frequency (speed) was adjusted, depending on the fluid and temperature.

This task consisted of two parts:

a. Determining the power and energy required to eliminate different fluids, depending on the fan frequency (speed).

b. Determining whether, if the same fan acceleration profile is used for all fluids, the same peak BLDT is obtained.

4.1 ENERGY DEPENDING ON THE FAN FREQUENCY.

To measure the power used by the motor to drive the wind tunnel fan, a power transducer was placed between the current input and the variable-speed drive that controls the motor for the fan. This transducer was able to measure the apparent power (in Volt-amperes) used by the drive. When the active power was measured between the drive and the motor, interferences with the current were observed. Therefore, it was decided to measure the apparent power since the only difference between apparent and active power would be the loss of power in the drive, and the loss would be relatively low, about the same for each fluid. Moreover, and more importantly, it is the relative difference in power that is needed and not absolute power measurements.

4.1.1 Equations.

The energy used to push the fluid in the test box section was evaluated using two parameters. The first parameter was the wind tunnel energy, which is the motor power integrated over a time period, and the second parameter was the energy factor that takes into consideration the energy loss in the wind tunnel.

The wind tunnel energy is the integration of the motor power as a function of time.

$$E = \int_0^t P_m(t) \cdot dt \tag{13}$$

Where

E = wind tunnel energy, J
P_m = motor power as measured by the transducer, Volt-Amperes
T = time, s

AMIL's Luan Phan refrigerated wind tunnel (figure 18) in which the tests were run has a larger test section (0.5 x 1.5 m) than that required to run FPET, according to AMS 1428. Therefore, a test section box and convergent and divergent cones were inserted into the tunnel test section (figure 17). For any given test run, a portion of the air circulating in the tunnel goes outside the test section box. Therefore, an analysis of the energy factor was done to take into consideration the energy losses outside the test section, using the methods of references 10 and 11. The energy factor is defined as the ratio of the wind tunnel energy measured by the transducer and the air energy theoretically in the test section box. The air energy in the test section box is the integration of the air power in the test section box over a time period. The power factor is the ratio of the power measured by the transducer over the theoretical power in the test section.

The air power (as measured by the transducer) in the test section box is

$$P_a(t) = \tfrac{1}{2} \cdot \rho_{air} \cdot A \cdot [U(t)]^3 \tag{14}$$

The power factor is

$$\lambda = \frac{P_m(t)}{\frac{1}{2} \cdot \rho_{air} \cdot A \cdot [U(t)]^3} \tag{15}$$

The energy factor is

$$\Lambda = \frac{\int_0^t P_m(t) \cdot dt}{\int_0^t \frac{1}{2} \cdot \rho_{air} \cdot A \cdot [U(t)]^3 \cdot dt} \tag{16}$$

Where

P_a = air power, w
A = cross sectional area at the test section box input, m^2
E = wind tunnel energy, J
t = time, s
U = velocity measured in the test section box, m/s
ρ_{air} = air density, kg/m^3

4.1.2 Dry (No Fluid) Test Data.

Figure 52 shows test data from the dry test data, where the velocity, BLDT, and fluid temperature are represented as a function of time. For the same test run, figure 52 shows the apparent power and power factor measured and calculated with the power transducer. The table in figure 53 shows the energy and energy factors calculated at 30 and 50 sec., considered as the area under the power curve.

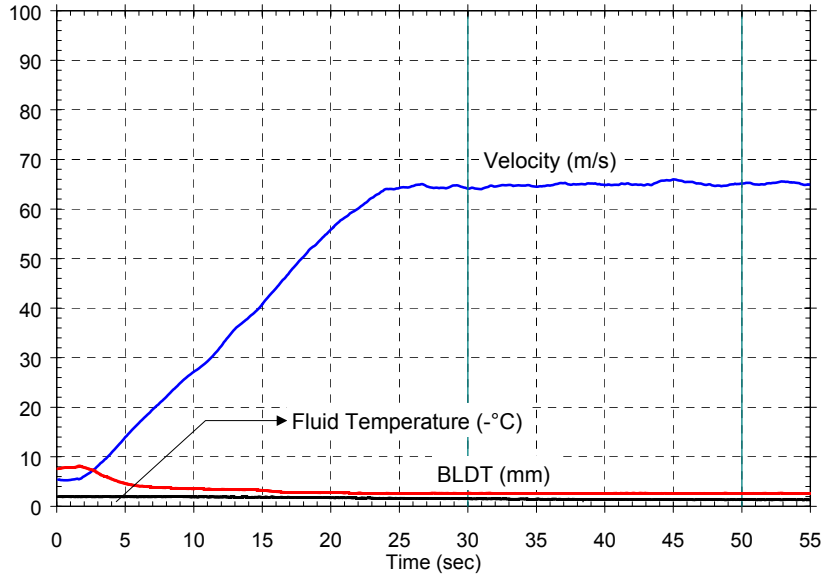

FIGURE 52. TEST DATA FROM A DRY TEST RUN

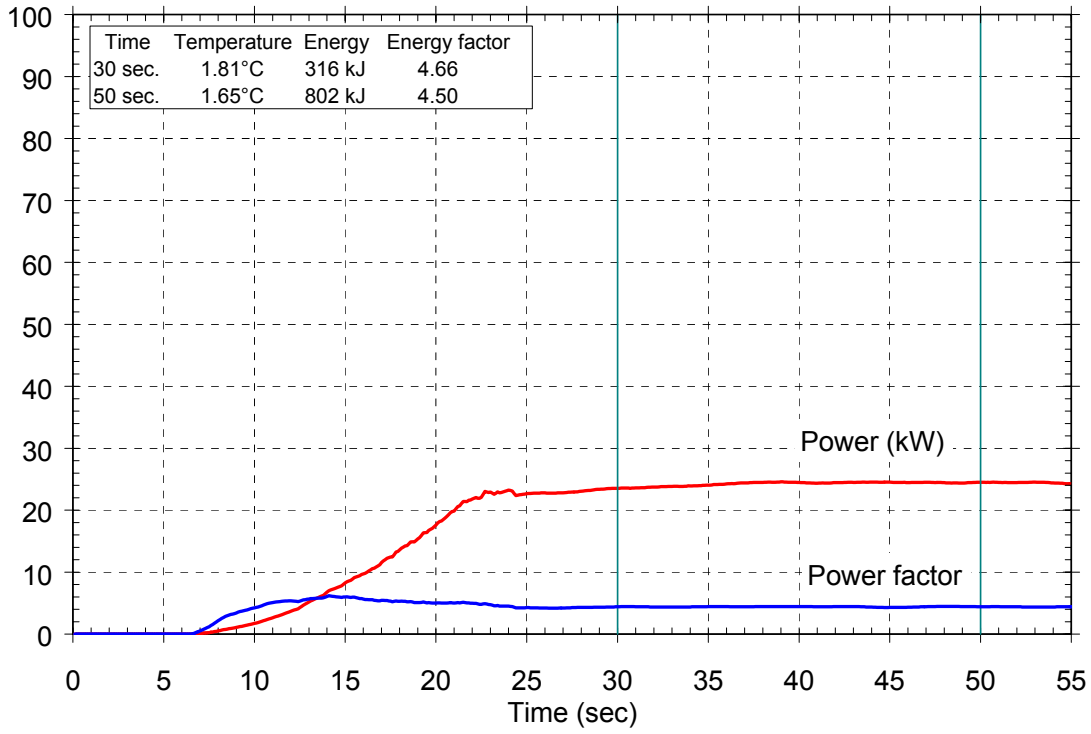

FIGURE 53. POWER AND ENERGY REQUIRED FOR THE DRY TEST (FIGURE 52)

4.1.3 Dry and Reference Military Fluid Test Data.

Figures 54 and 55 present the energy and energy factors after 30 sec. as a function of temperature for a dry test run (without fluid) as well as the reference military fluid. The graph of figure 54 shows that the dry value is in the 325 to 365 kJ range for the dry fluid with only a slight increase in energy with decreasing temperature. Figure 55 shows the energy factor for the same dry test run in the 4.3 to 4.5 range.

Figures 56 and 57 show the energy and energy factor as a function of temperature for the same test runs after 50 sec. Figure 56 shows that the energy input for the dry run is in the 800 to 920 kJ range, which increases with decreasing temperature. Figure 57 shows that the energy factor for the same test runs is in the 4.60- to 4.65-unit range and only increases slightly with decreasing temperature.

Figures 54 through 57 show the energy and energy factor values for the reference military fluid, MIL-A-7243, as a function of temperature after 30 and 50 sec. Figure 54 shows the energy input after 30 sec. is in the 780 kJ range at 0°C and increases to 1200 kJ at -25°C. Figure 55 shows the energy factor after 30 sec. in the 10.5-unit range, increasing linearly to 15 at -25°C. Figure 56 shows an energy input after 50 sec. in the 1500 kJ range at 0°C, increasing to 2800 kJ at -25°C. Figure 57 shows an energy factor after 50 sec. of 8 units at 0°C, which increases to 13.5 at -25°C.

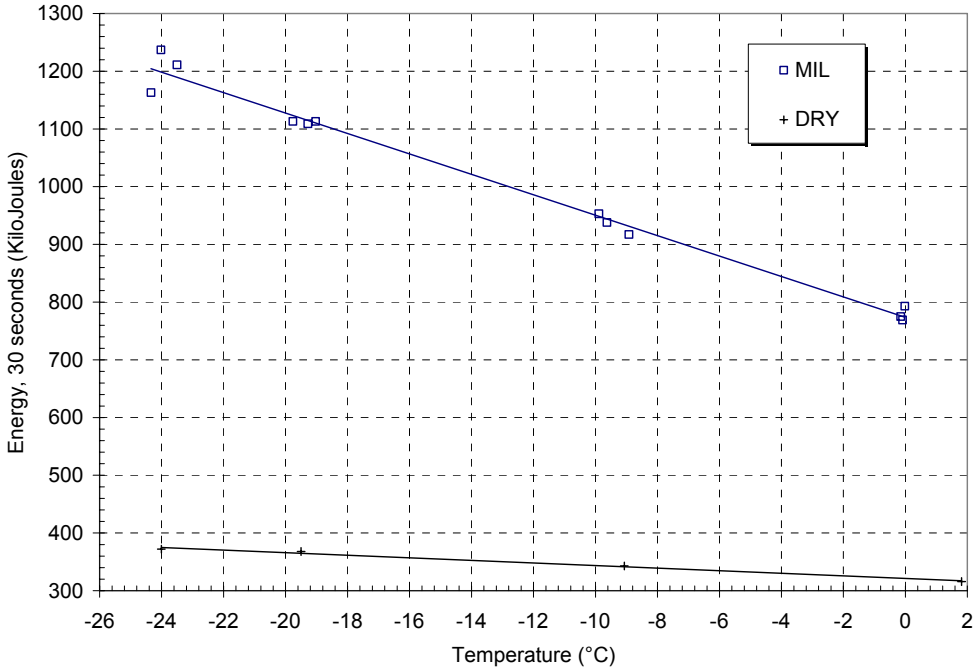

FIGURE 54. ENERGY AFTER 30 sec. FOR DRY RUN AND MILITARY FLUID

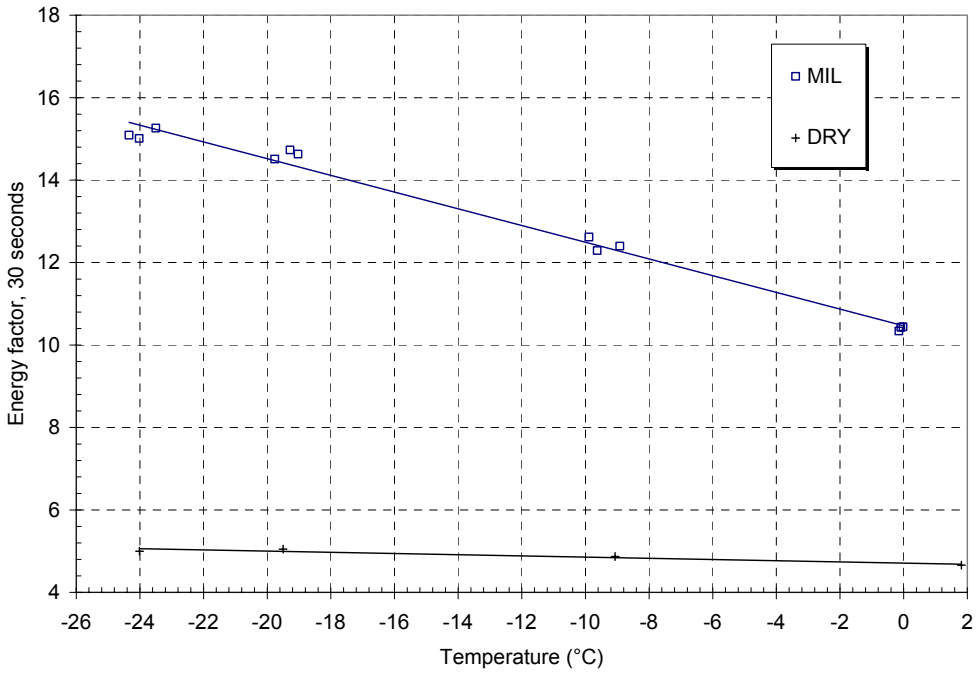

FIGURE 55. ENERGY FACTOR AFTER 30 sec. FOR DRY RUN AND MILITARY FLUID

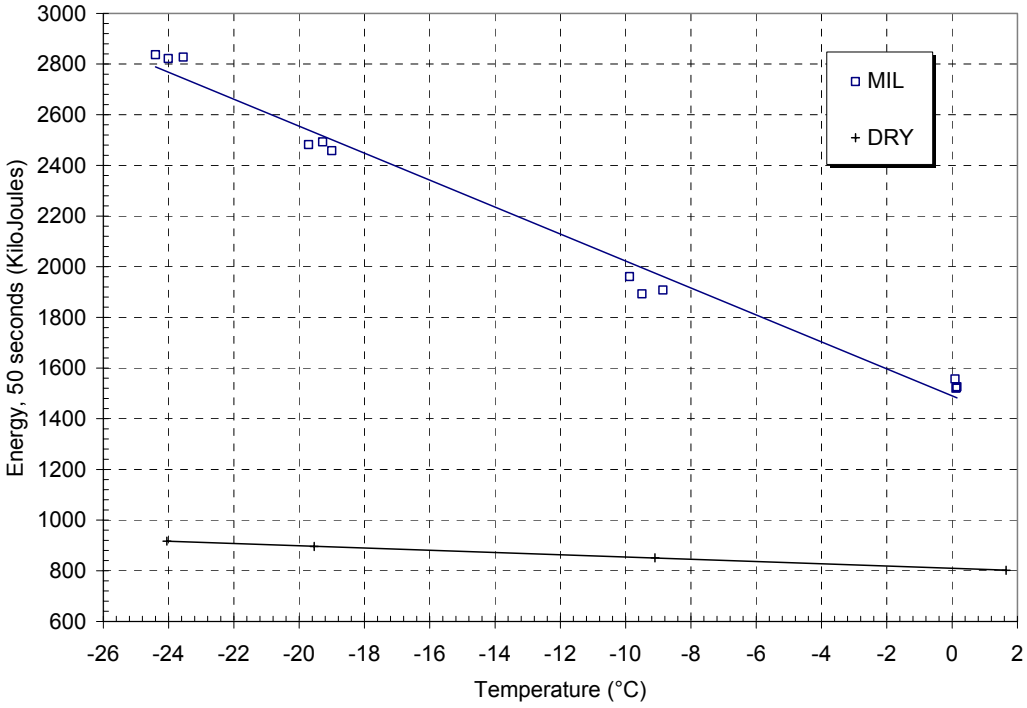

FIGURE 56. ENERGY AFTER 50 sec. FOR DRY RUN AND MILITARY FLUID

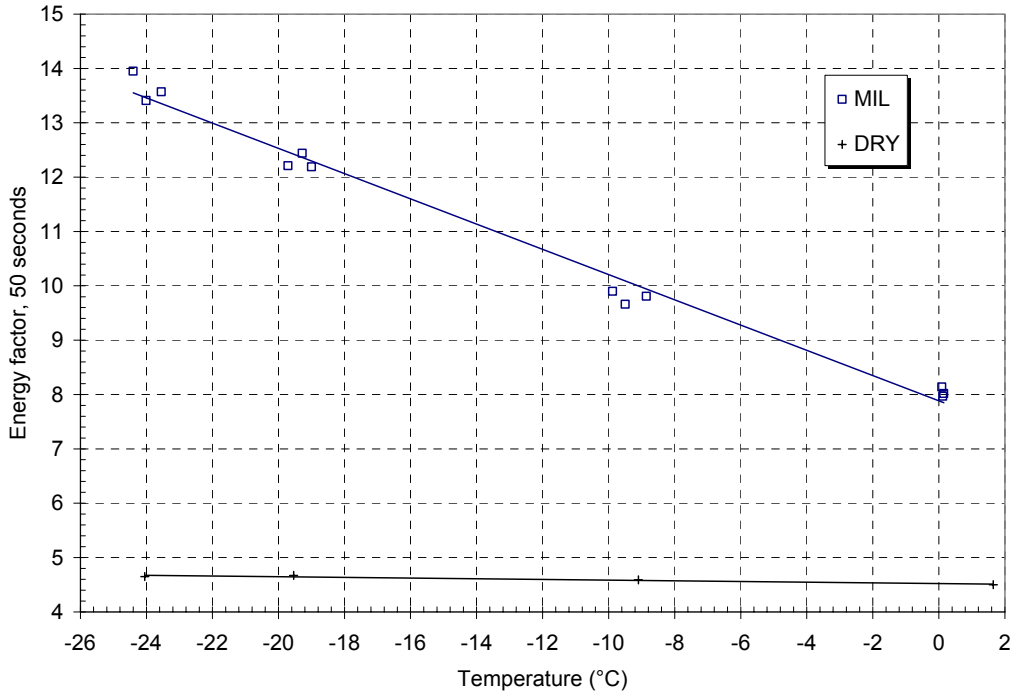

FIGURE 57. ENERGY FACTOR AFTER 50 sec. FOR DRY RUN AND MILITARY FLUID

4.1.4 Energy Input for Test Fluids.

Figures 58 through 61 show the energy input and energy factor after 30 and 50 sec. as a function of temperature for all the test fluids listed in table 5. For these graphs, the solid symbols represent the two Type II anti-icing fluids, while the open symbols represent the Type IV fluids.

Figure 58 shows the energy input after 30 sec. with about a 150 kJ variation for all fluids at each temperature interval. Dow Ultra+ appears to have the lowest energy requirements at all temperature intervals tested, while the Type II fluids and Octagon Process MaxFlight seem to have the highest energy requirements. Moreover, Octagon Process MaxFlight seems to have similar energy requirements as a Type II fluid. As a whole, the Type II energy requirements are more similar than Type IV fluids, whose data shows more scatter. Similar observations can be made for the energy input after 50 sec. (figure 59). Type II and Type IV best-fit curves are plotted in figures 58 and 59. The curves show higher energy requirements for Type II fluids compared to Type IV fluids. However, these curves would probably be even closer if the Dow Ultra+ Type IV fluid were not included. The graphs show about a 6% energy input difference after 30 sec., and a 2% difference after 50 sec. between the two fluid types.

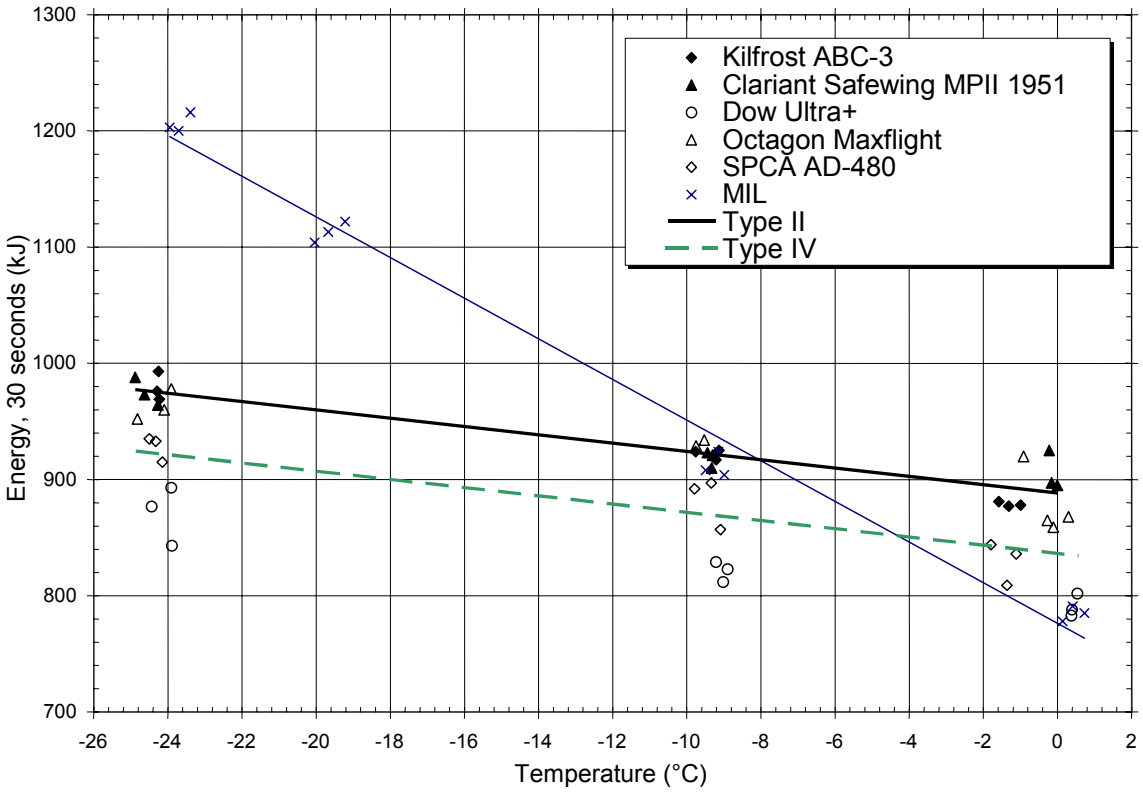

FIGURE 58. ENERGY INPUT AFTER 30 sec. FOR TEST FLUIDS

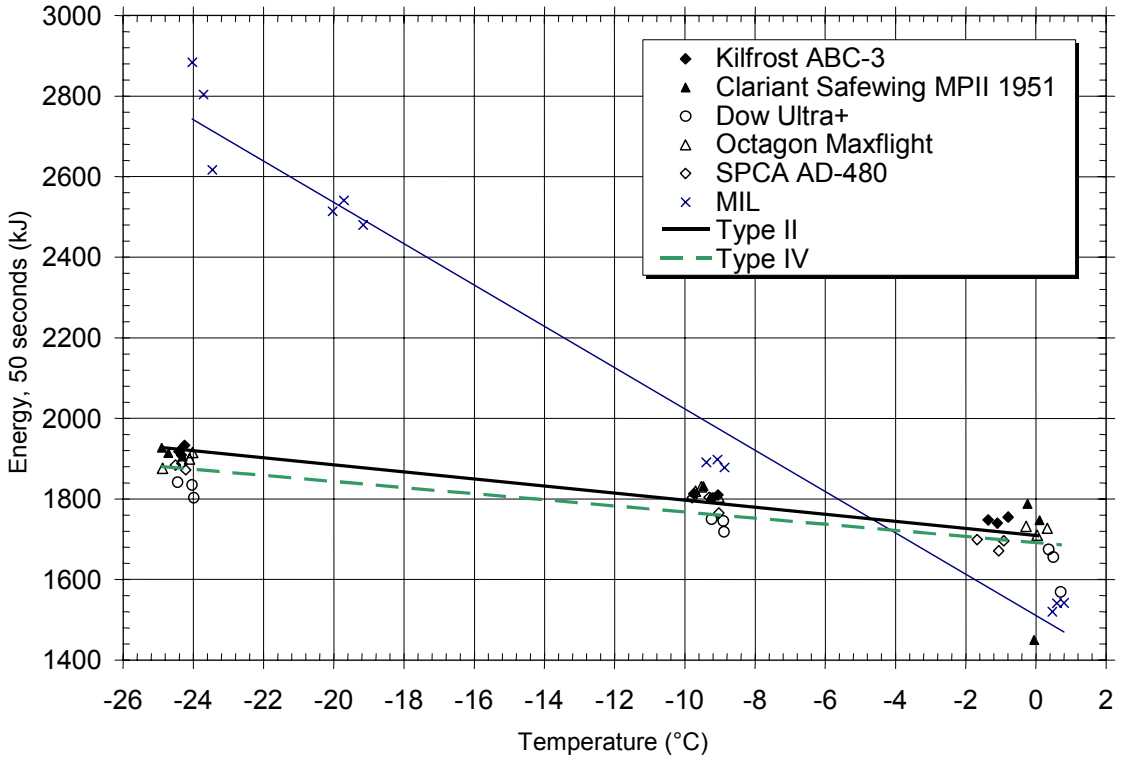

FIGURE 59. ENERGY INPUT AFTER 50 sec. FOR TEST FLUIDS

Figure 60 presents the energy factor after 30 sec. for the test fluids. The figure shows about a 2-unit variation between fluids at each temperature interval. Here, no fluid has a consistently higher or lower factor at each temperature interval. This is mirrored by the fact that the Type II and IV trends crossover at around -12°C. This crossover, seen in the energy factor and not in the energy, may be due to the fact that more energy is lost at colder temperatures, and the energy losses are only taken into account in the energy factor variable. In terms of the energy factor, Dow Ultra+ has the highest values of all fluids at -25°C and is amongst the lowest at 0°C. Similar relationships are seen in figure 61, comparing the energy factor after 50 sec.

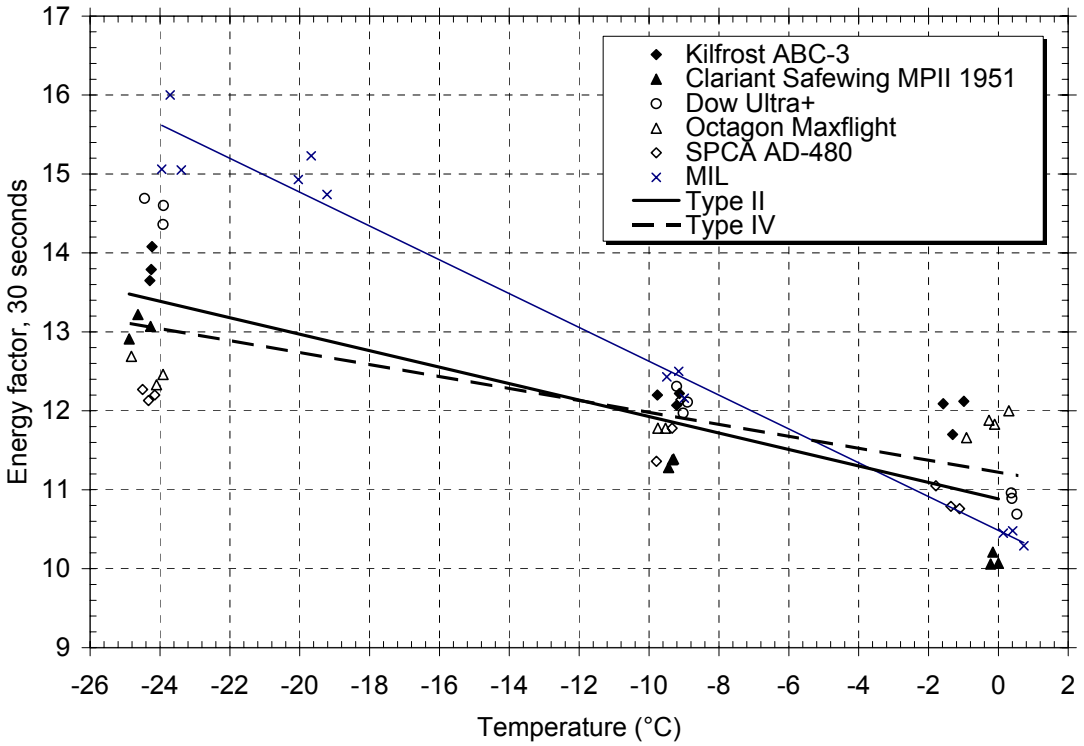

FIGURE 60. ENERGY FACTOR AFTER 30 sec. FOR TEST FLUIDS

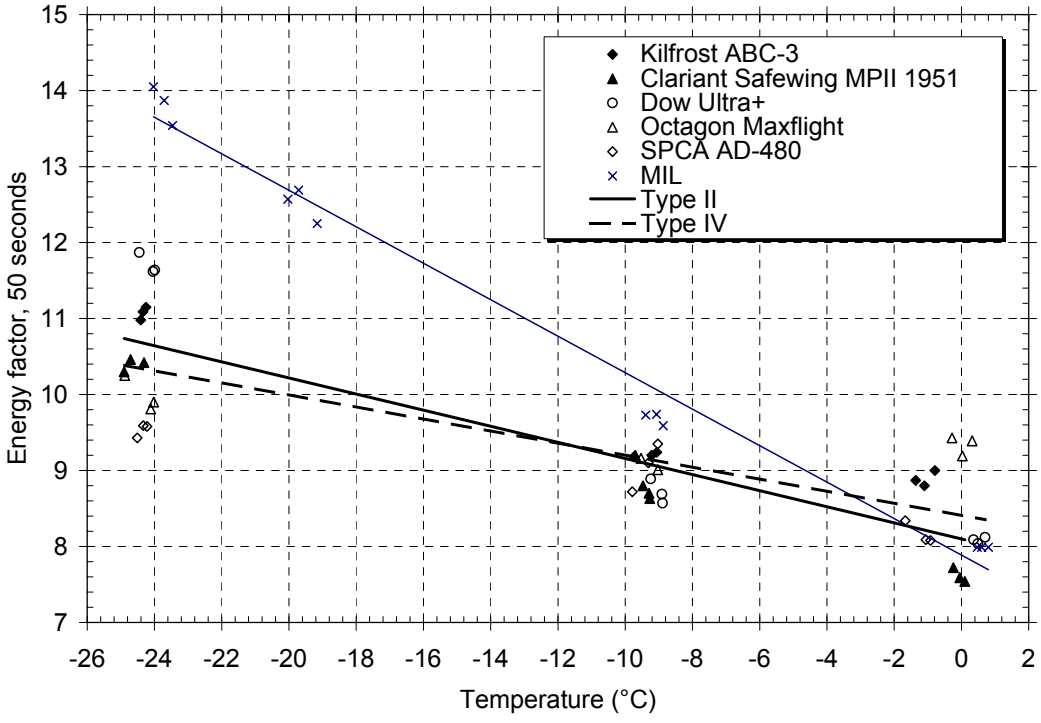

FIGURE 61. ENERGY FACTOR AFTER 50 sec. FOR TEST FLUIDS

4.1.5 Energy Input for Different Initial Fluid Thicknesses.

4.1.5.1 Kilfrost ABC-3.

The energy input after 30 and 50 sec. is presented in figures 62 and 63 respectively for different initial fluid thicknesses of Kilfrost ABC-3 as a function of temperature. The figures show slightly higher energy requirements for thicker initial fluid thicknesses with the 4 mm requiring about 5% more energy after 30 sec. and 2% more energy after 50 sec.

Figures 64 and 65 show the energy factor after 30 and 50 sec. respectively as a function of temperature for different initial fluid thicknesses of Kilfrost ABC-3. The figures show no difference between the energy factors at 0°C, but there is an increase in the difference with the decreasing temperature with the thicker fluid having a higher energy factor. In both cases, the energy factor difference between thicknesses is in the 5% range.

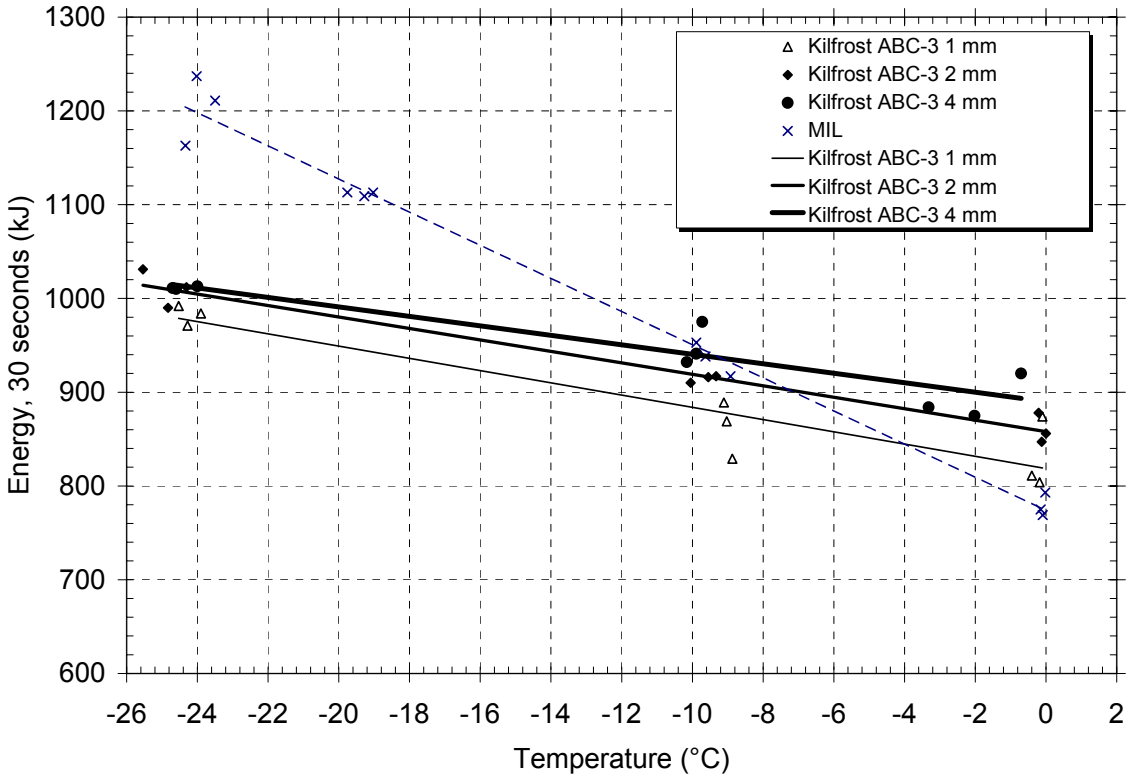

FIGURE 62. ENERGY INPUT AFTER 30 sec. FOR DIFFERENT INITIAL FLUID THICKNESSES OF KILFROST ABC-3

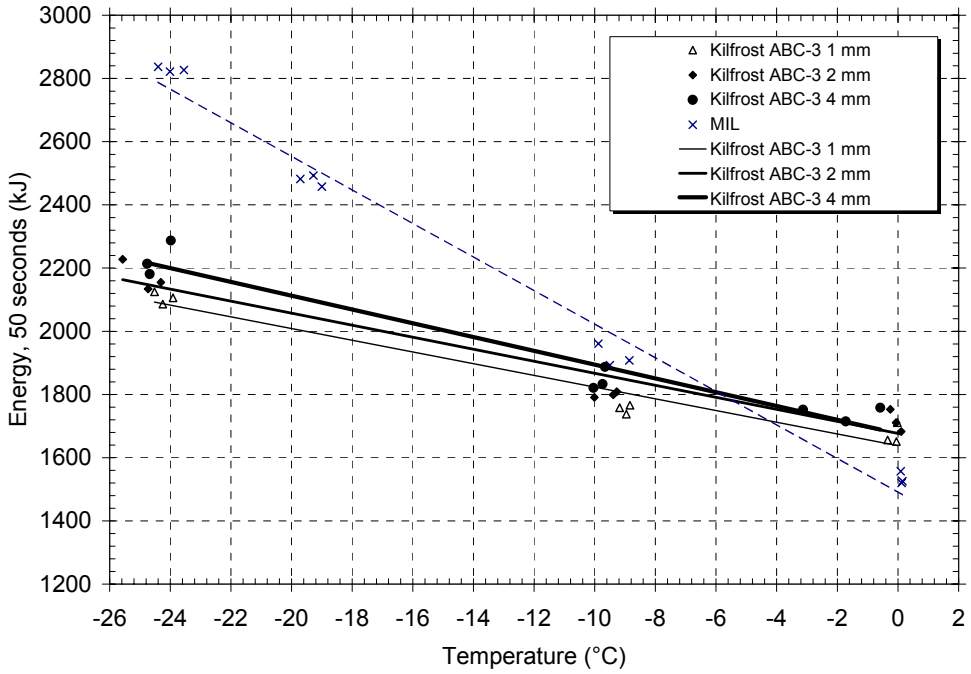

FIGURE 63. ENERGY INPUT AFTER 50 sec. FOR DIFFERENT INITIAL FLUID THICKNESSES OF KILFROST ABC-3

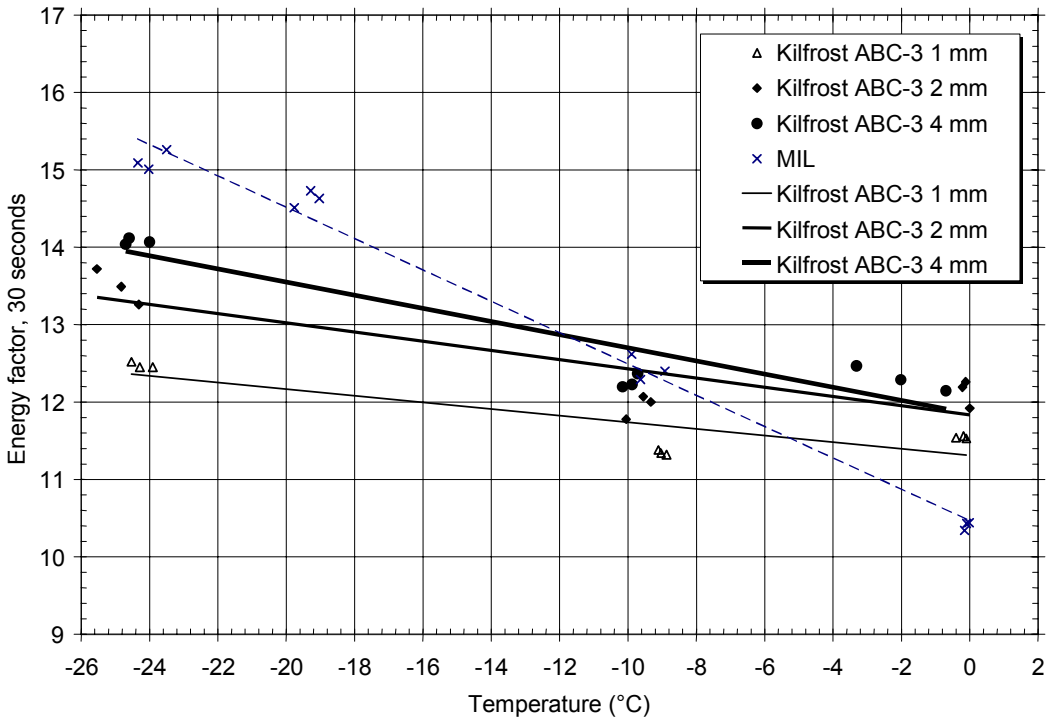

FIGURE 64. ENERGY FACTOR AFTER 30 sec. FOR DIFFERENT INITIAL FLUID THICKNESSES OF KILFROST ABC-3

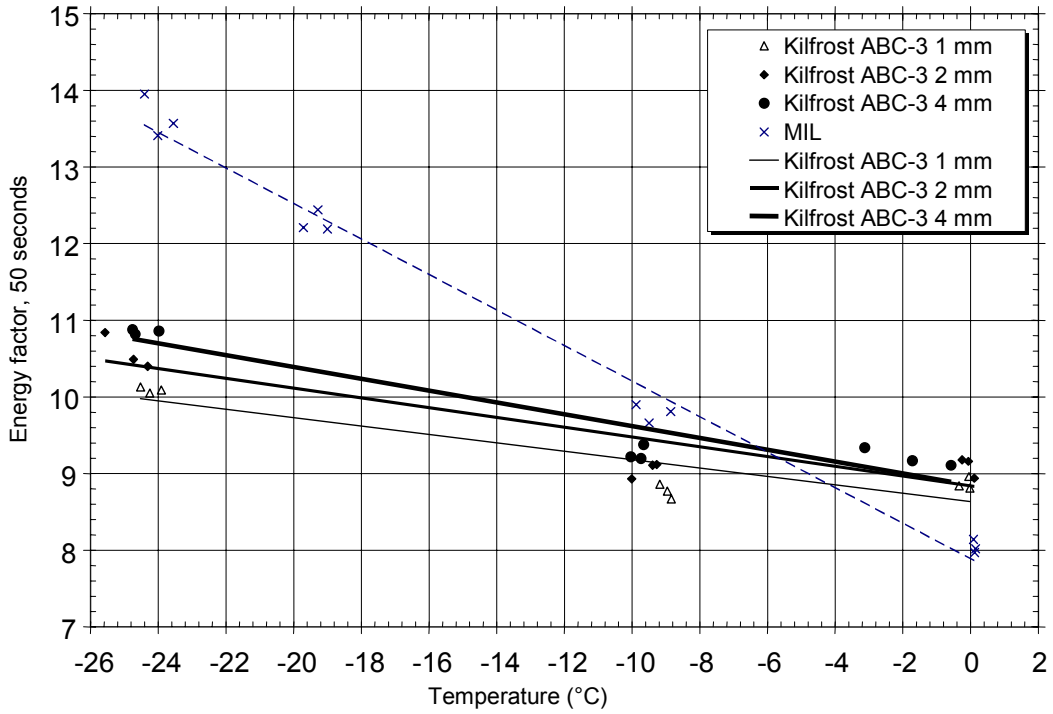

FIGURE 65. ENERGY FACTOR AFTER 50 sec. FOR DIFFERENT INITIAL FLUID THICKNESSES OF KILFROST ABC-3

4.1.5.2 Clariant Safewing MPII 1951.

The energy input after 30 and 50 sec. is presented in figures 66 and 67 respectively for different initial fluid thicknesses of Clariant Safewing MPII 1951 as a function of temperature. Figure 66 shows that at 0° and -10°C there is more energy required to move the fluid of 2-mm thickness than that of 4-mm thickness. Then at -25°C, all fluid thicknesses require about the same energy. The energy factor difference between thicknesses is in the 6% range.

Figure 67 shows that after 50 sec. all fluid thicknesses have about the same energy input. In terms of the energy factor presented in figure 68 for 30 sec. and figure 69 for 50 sec., there is little or no difference for the different initial fluid thicknesses.

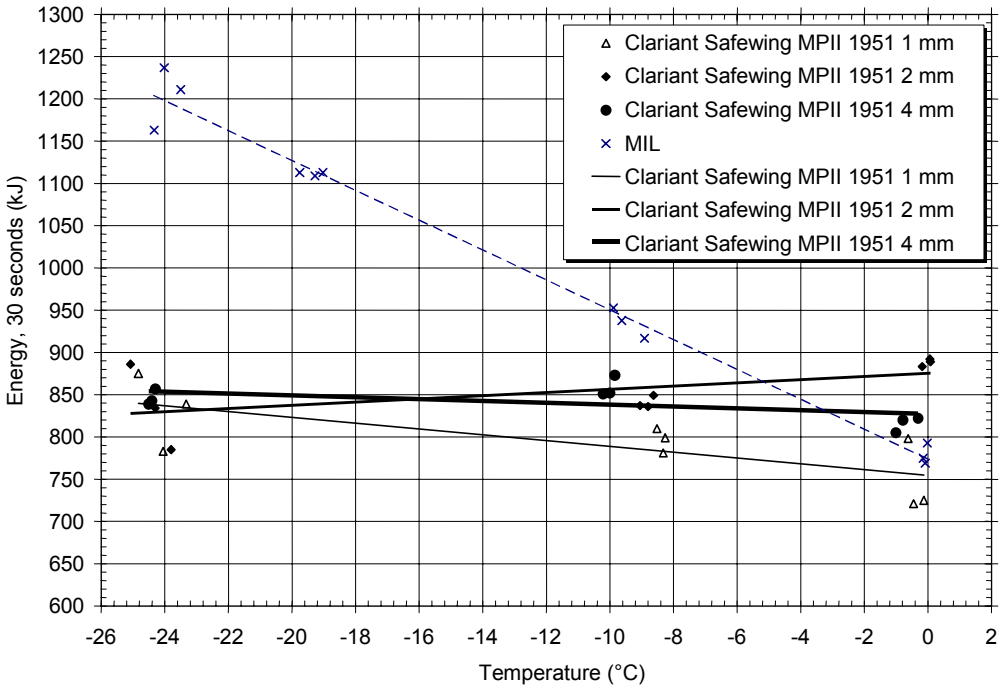

FIGURE 66. ENERGY INPUT AFTER 30 sec. FOR DIFFERENT INITIAL FLUID THICKNESSES OF CLARIANT SAFEWING MPII 1951

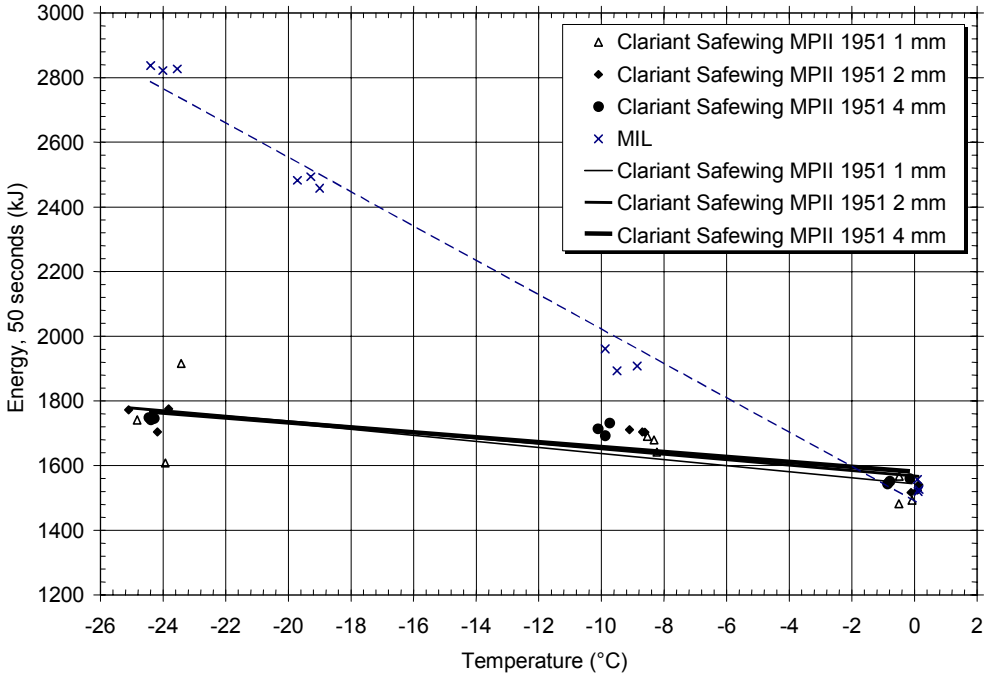

FIGURE 67. ENERGY INPUT AFTER 50 sec. FOR DIFFERENT INITIAL FLUID THICKNESSES OF CLARIANT SAFEWING MPII 1951

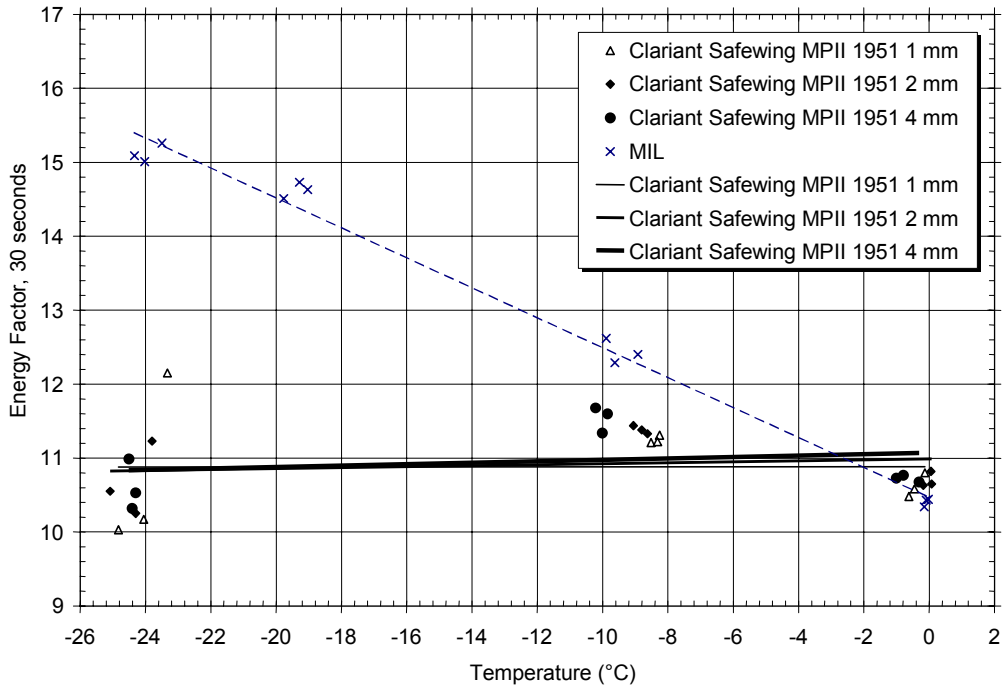

FIGURE 68. ENERGY FACTOR AFTER 30 sec. FOR DIFFERENT INITIAL FLUID THICKNESSES OF CLARIANT SAFEWING MPII 1951

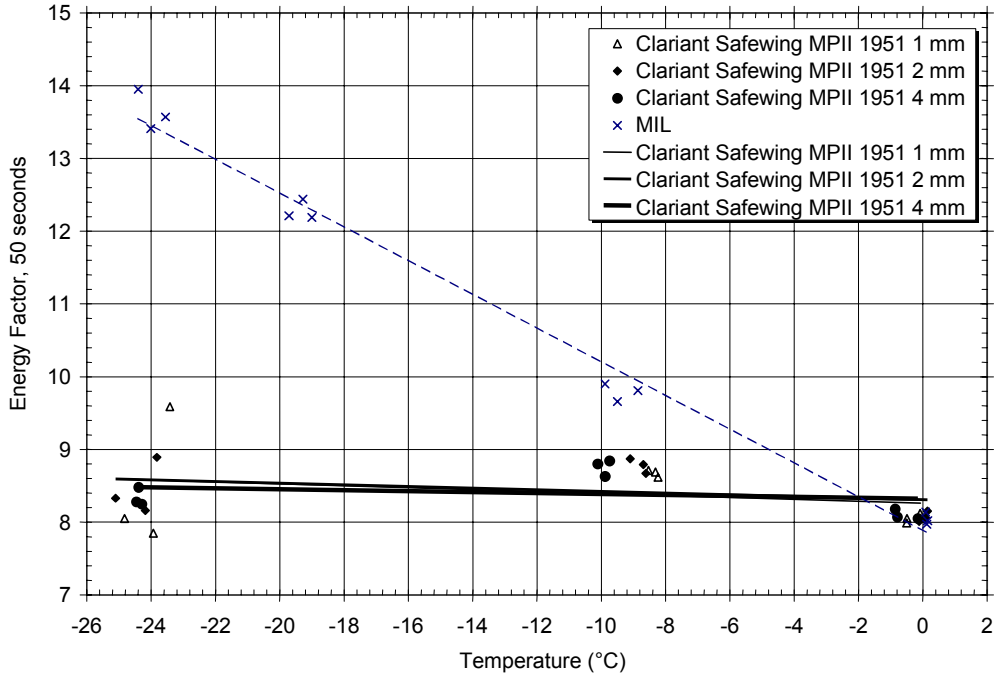

FIGURE 69. ENERGY FACTOR AFTER 50 sec. FOR DIFFERENT INITIAL FLUID THICKNESSES OF CLARIANT SAFEWING MPII 1951

4.1.5.3 Octagon Process MaxFlight.

The energy inputs after 30 and 50 sec. for different initial fluid thicknesses of Octagon Process MaxFlight are presented in figures 70 and 71 respectively. Figure 70 shows only a slightly higher energy requirement, about 2%, for the thicker fluid, while figure 71 shows that after 50 sec. the energy input is relatively the same for all fluids. The energy factor after 30 sec. (figure 72) shows greater differences between the different fluid thicknesses, about 5%, especially for the colder temperatures where the thicker fluids require more energy. Figure 73, showing the energy factor after 50 sec., reflects the small difference seen in figure 71.

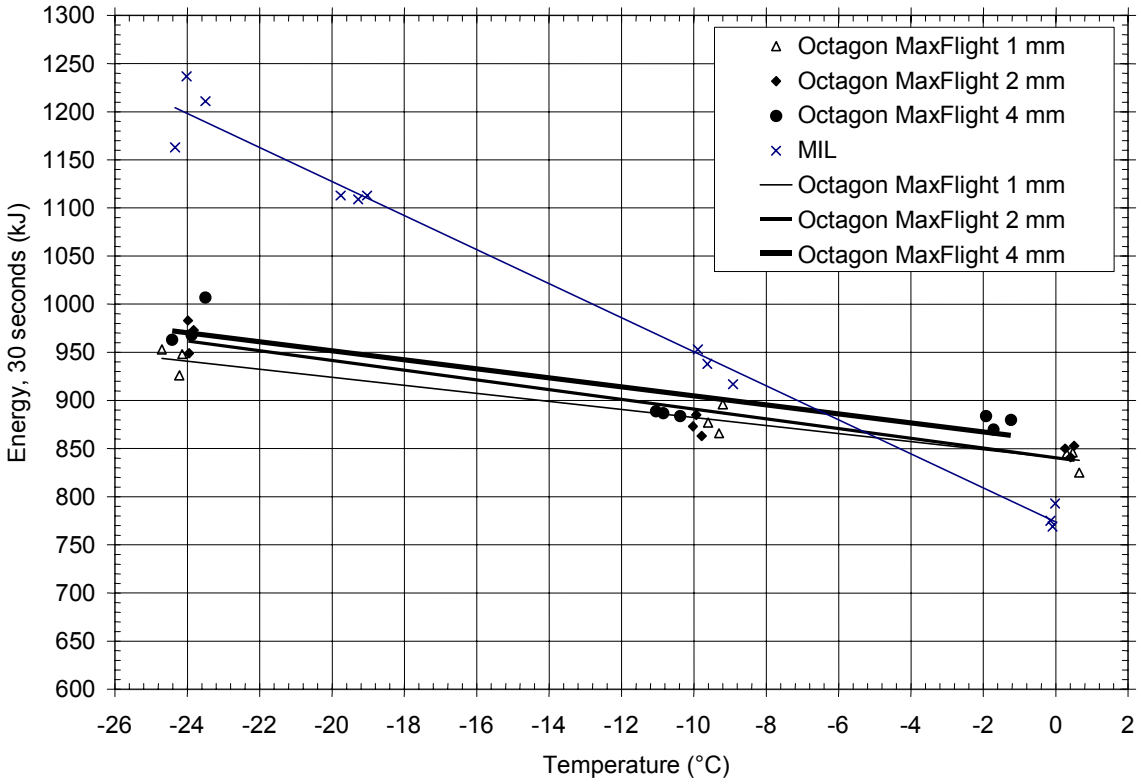

FIGURE 70. ENERGY INPUT AFTER 30 sec. FOR DIFFERENT INITIAL FLUID THICKNESSES OF OCTAGON PROCESS MAXFLIGHT

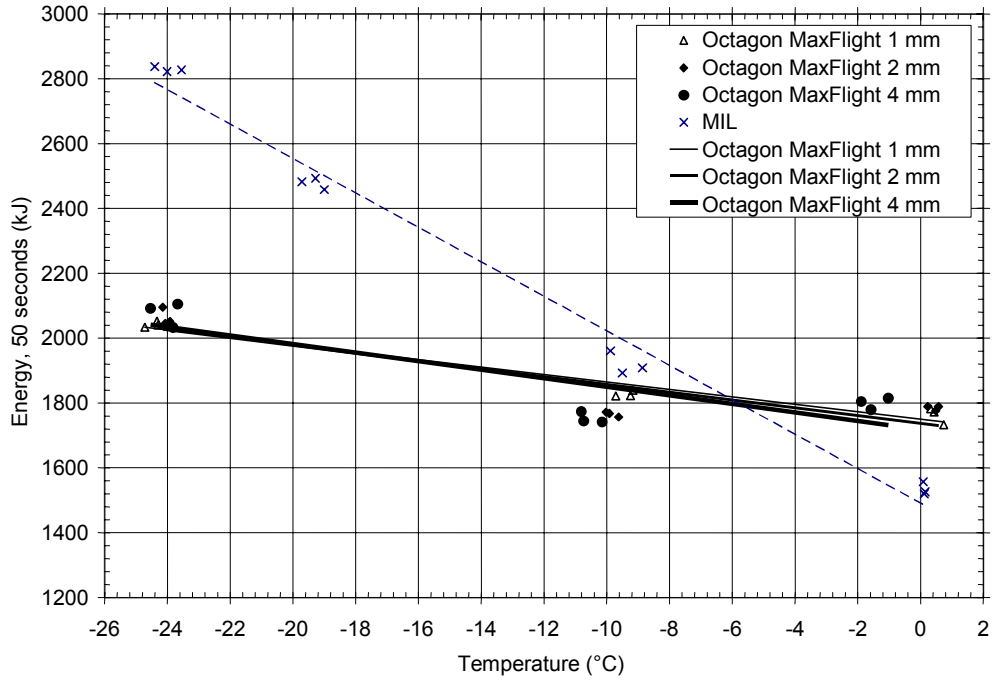

FIGURE 71. ENERGY INPUT AFTER 50 sec. FOR DIFFERENT INITIAL FLUID THICKNESSES OF OCTAGON PROCESS MAXFLIGHT

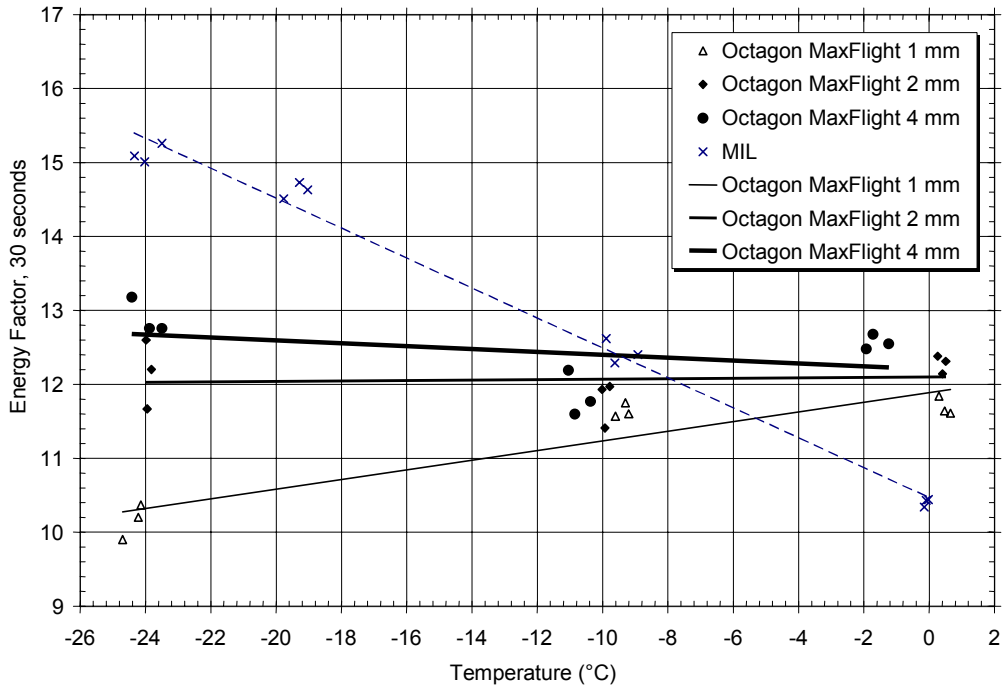

FIGURE 72. ENERGY FACTOR AFTER 30 sec. FOR DIFFERENT INITIAL FLUID THICKNESSES OF OCTAGON PROCESS MAXFLIGHT

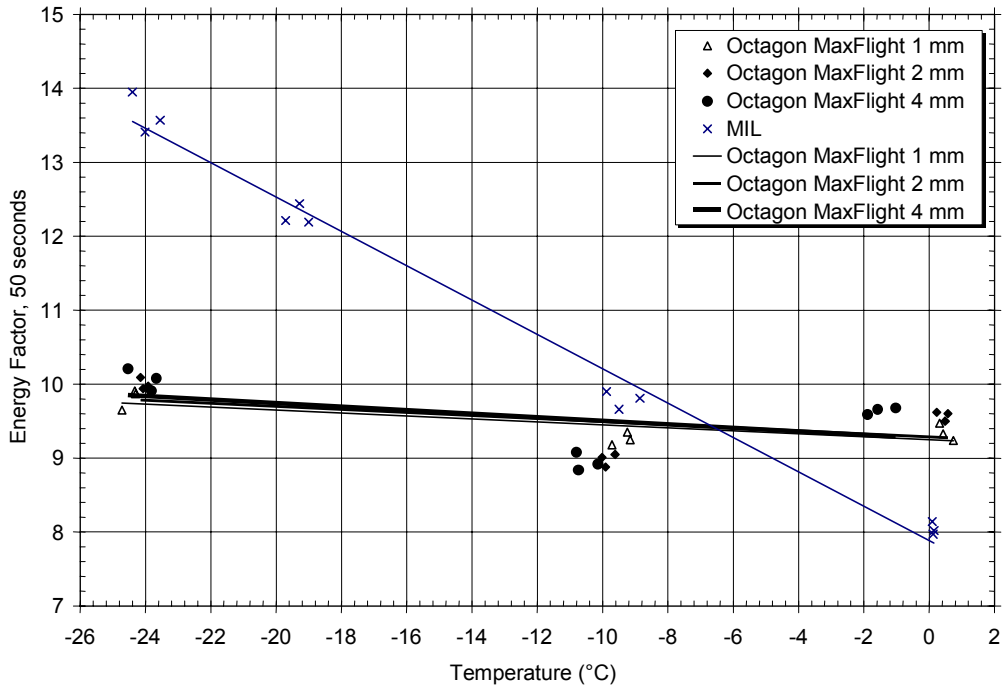

FIGURE 73. ENERGY FACTOR AFTER 50 sec. FOR DIFFERENT INITIAL FLUID THICKNESSES OF OCTAGON PROCESS MAXFLIGHT

4.1.5.4 SPCA AD-480.

Figures 74 through 77 show the energy input and factor after 30 and 50 sec. for different initial fluid thicknesses of SPCA AD-480. Figure 74, presenting the energy input after 30 sec., shows a greater energy required for the thicker fluids at 0°C, about 6%, less at -10°C, and no difference at -25°C. However, after 50 sec., the energy input difference is negligible (figure 75). Figure 76, which presents the energy factor after 30 sec., shows a more linear difference between the different initial fluid thicknesses with the thicker fluids requiring more. Figure 77 shows that after 50 sec., there is only a slightly lower energy factor at -25°C for the 1-mm initial fluid thickness; for the other temperature intervals, the energy factor is relatively the same.

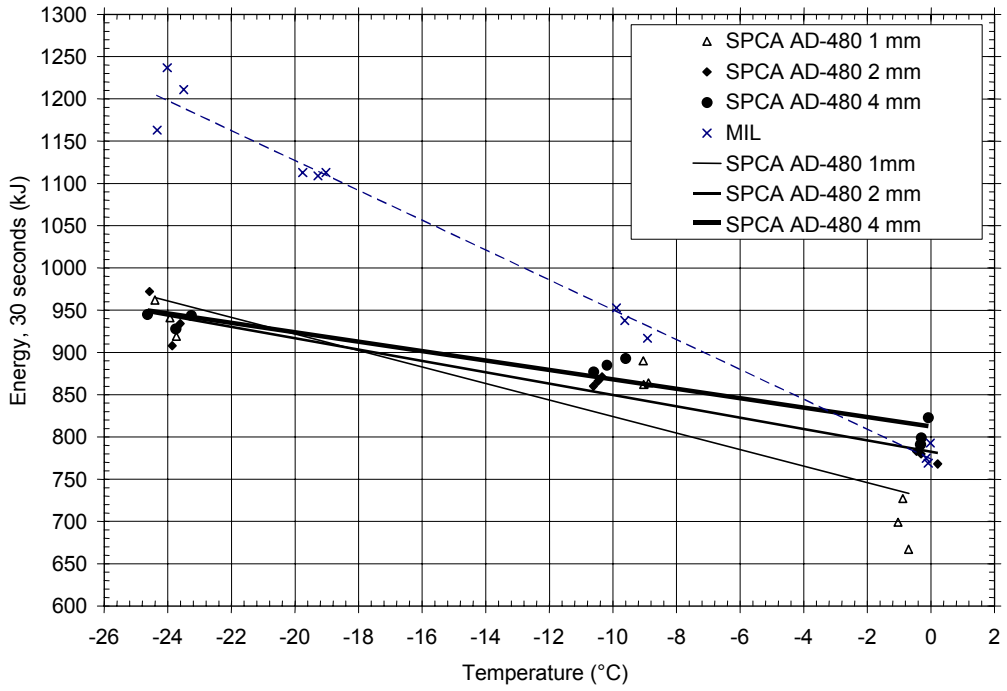

FIGURE 74. ENERGY INPUT AFTER 30 sec. FOR DIFFERENT INITIAL FLUID THICKNESSES OF SPCA AD-480

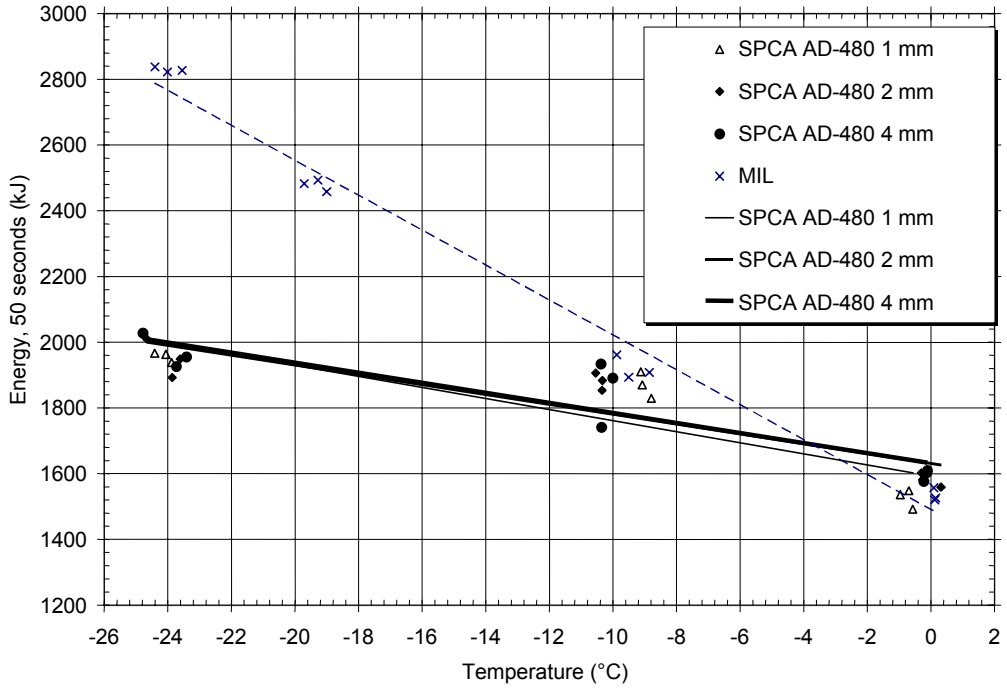

FIGURE 75. ENERGY INPUT AFTER 50 sec. FOR DIFFERENT INITIAL FLUID THICKNESSES OF SPCA AD-480

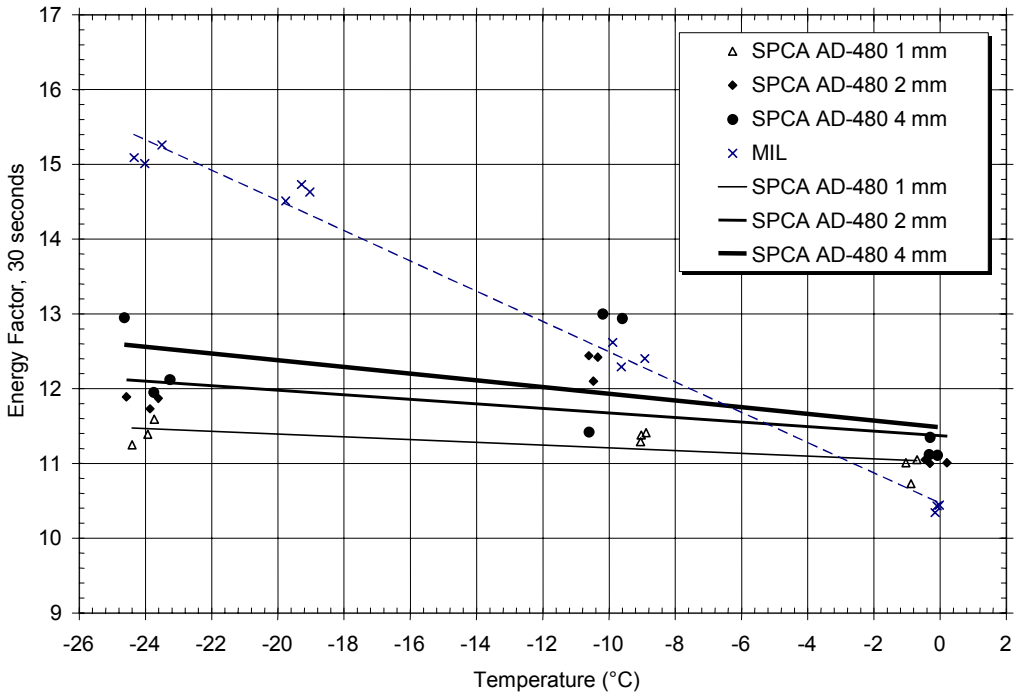

FIGURE 76. ENERGY FACTOR AFTER 30 sec. FOR DIFFERENT INITIAL FLUID THICKNESSES OF SPCA AD-480

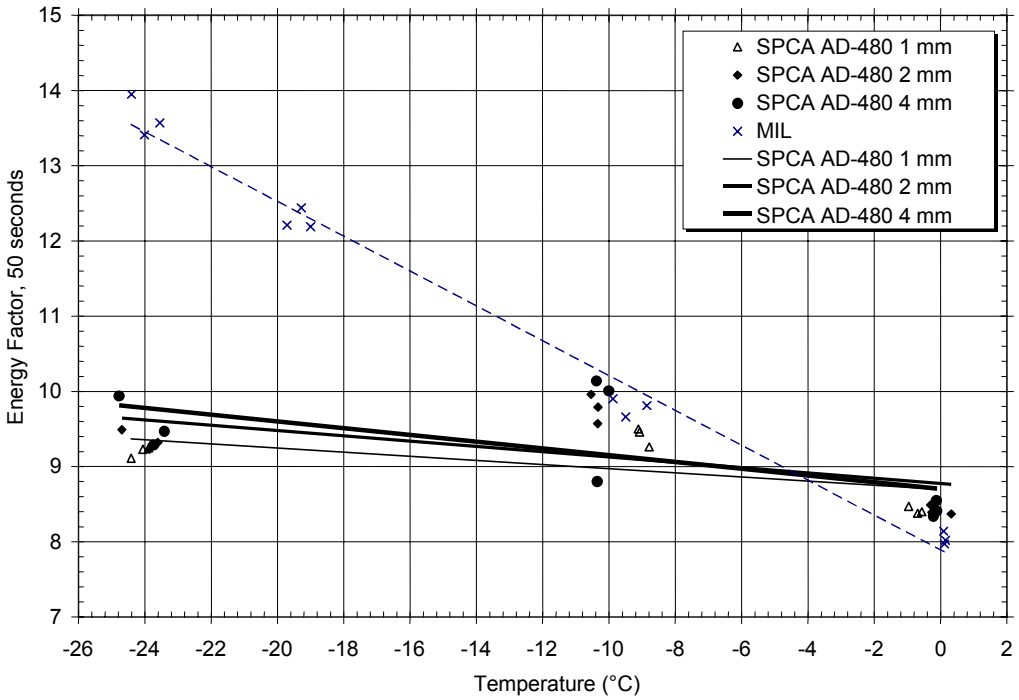

FIGURE 77. ENERGY FACTOR AFTER 50 sec. FOR DIFFERENT INITIAL FLUID THICKNESSES OF SPCA AD-480

4.1.5.5 Dow Ultra+.

Figures 78 through 81 show the energy input and factor after 30 and 50 sec. for the different initial fluid thicknesses of Dow Ultra+. The best-fit trends of the data have a slope closer to that of the military fluid, unlike the other fluids, with proportionally more energy required at the colder temperatures. Figure 78 shows that at 0°C there is more energy required to push the thicker fluids, about 5%, whereas at -10°C, the 1- and 2-mm thicknesses require the same. At -25°C, 1-mm thickness requires more energy than the 2-mm thickness, but less than the 4-mm thickness. After 50 sec., the different energy requirements of the different thicknesses are less and the thicker fluids require more energy, about 5% more (figure 79). The energy factor after 30 sec. (figure 80) shows a higher energy input for 4 mm of fluid than for the military fluid. It also shows that the thicker fluids require more energy, about 10%, a higher value compared to the other fluids tested. Figure 81, presenting the energy factor after 50 sec., shows higher values for the thicker fluids but not higher than the reference military fluid.

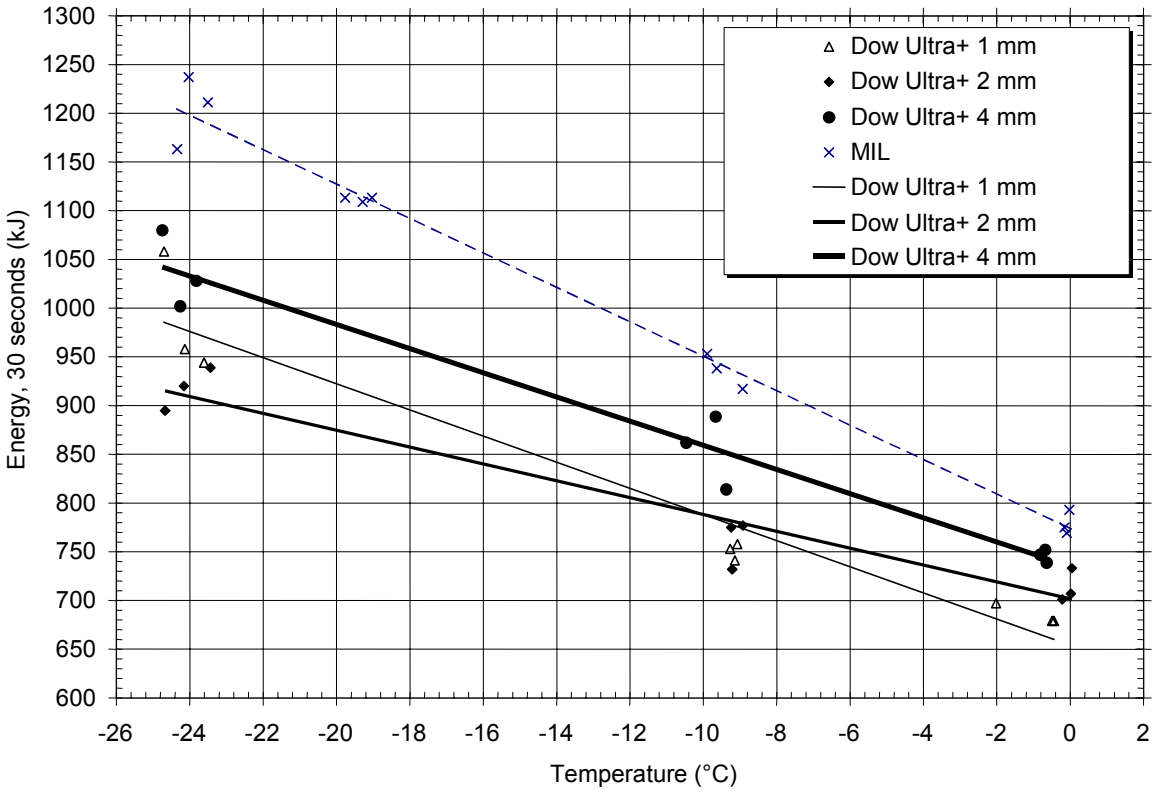

FIGURE 78. ENERGY INPUT AFTER 30 sec. FOR DIFFERENT INITIAL FLUID THICKNESSES OF DOW ULTRA+

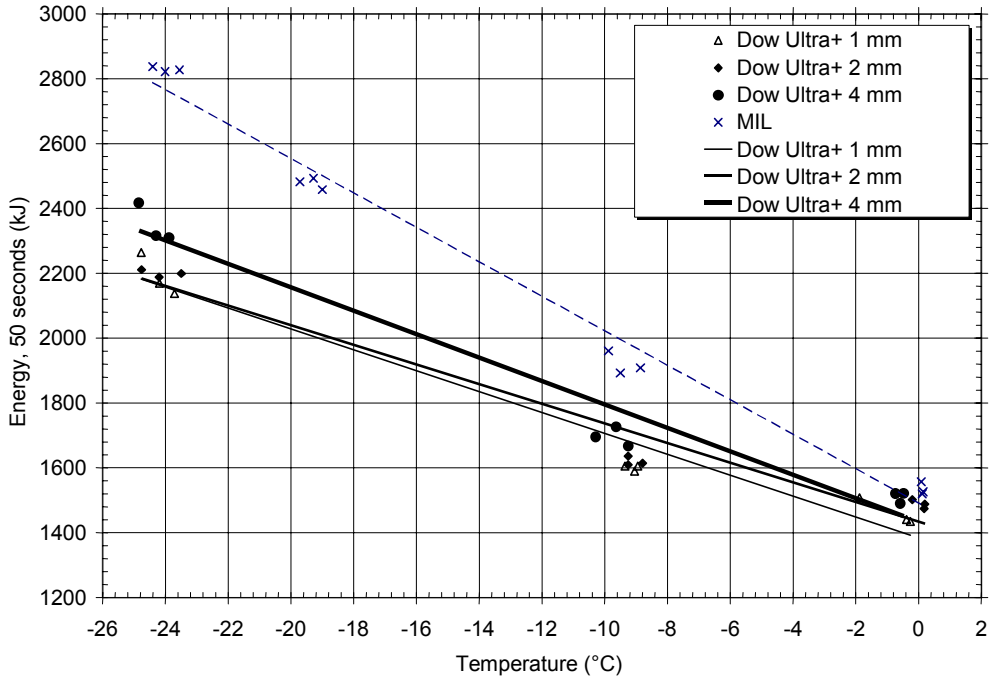

FIGURE 79. ENERGY INPUT AFTER 50 sec. FOR DIFFERENT INITIAL FLUID THICKNESSES OF DOW ULTRA+

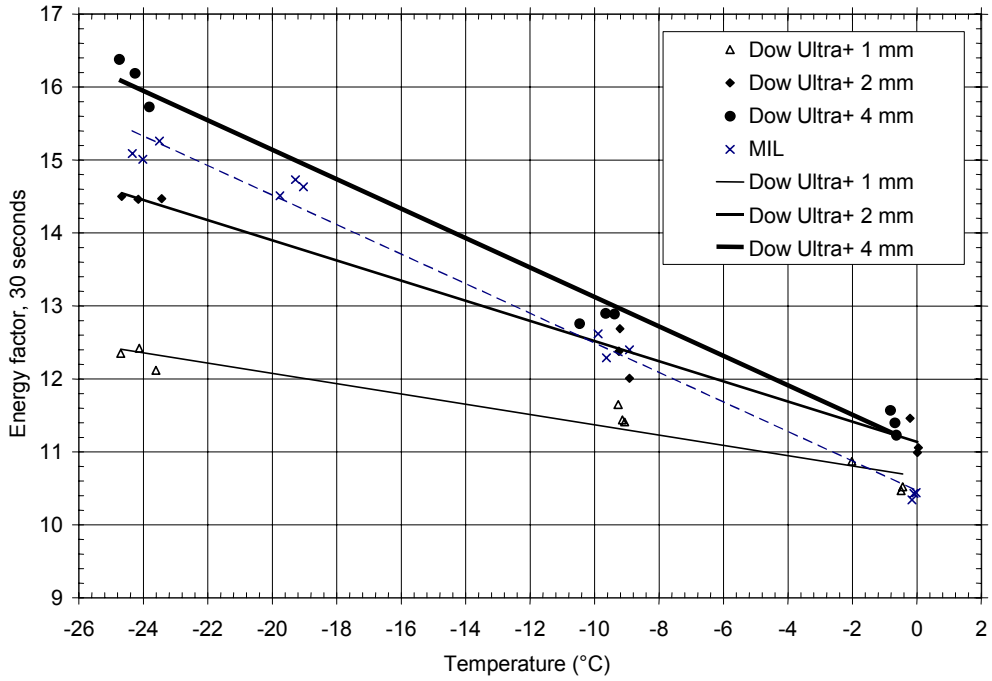

FIGURE 80. ENERGY FACTOR AFTER 30 sec. FOR DIFFERENT INITIAL FLUID THICKNESSES OF DOW ULTRA+

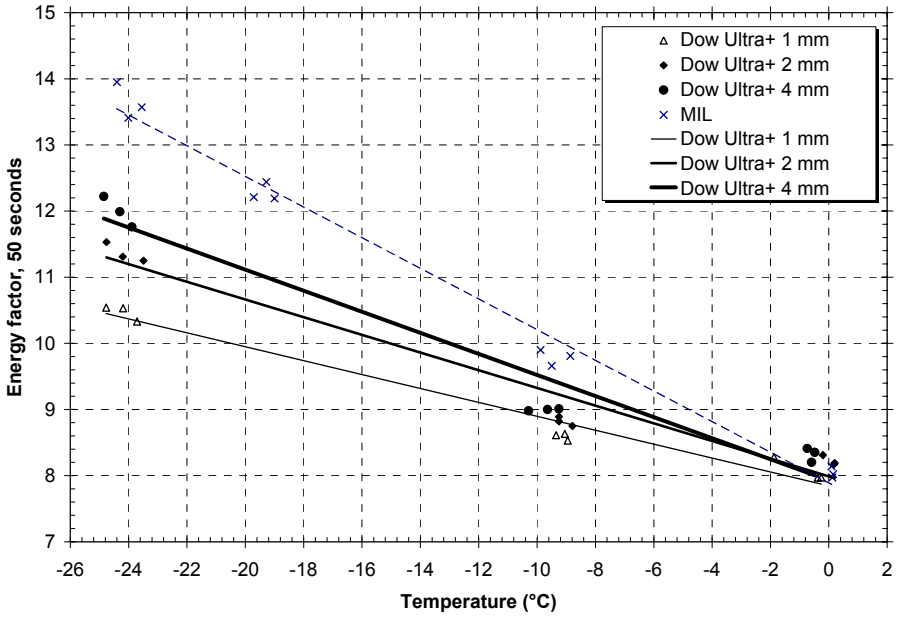

FIGURE 81. ENERGY FACTOR AFTER 50 sec. FOR DIFFERENT INITIAL FLUID THICKNESSES OF DOW ULTRA+

4.1.5.6 Energy Input for Different Initial Fluid Thicknesses—Summary.

Table 13 summarizes the relative energy requirements of the wind tunnel to push the different thicknesses of the fluids tested. The table shows which thicknesses required the most energy or energy factor followed by the percentage of how much. The table shows that in most cases, the 4-mm thickness required the most energy, although for some cases, there was no difference. In most cases, the 4-mm thickness required about 5% more energy, both for the Type II and Type IV fluids. The only exception was Dow Ultra+ that required a 10% higher energy factor at 30 sec.

TABLE 13. SUMMARY OF ENERGY AND ENERGY FACTOR FOR THE DIFFERENT THICKNESSES OF THE FLUIDS TESTED

Fluid	Type	Energy		Energy Factor	
		30 sec.	50 sec.	30 sec.	50 sec.
Kilfrost ABC-3	II	4 mm more 5%	4 mm more 2%	4 mm more 5%	4 mm more 5%
Clariant Safewing MPII 1951	II	2 mm more 6%	No	no	no
Octagon Process MaxFlight	IV	4 mm more 2%	No	4 mm more 5%	no
SPCA AD-480	IV	4 mm more 6%	4 mm more 2%	4 mm more 5%	4 mm more 4%
Dow Ultra+	IV	4 mm more 5%	4 mm more 5%	4 mm more 10%	4 mm more 5%

4.2 FIXED FAN ACCELERATION PROFILE.

For this section and test series, the fan accelerator profile was fixed, or set, at the same for all fluids and temperature intervals. In a normal certification FPET, the fan acceleration profile is adjusted, depending on the fluid and temperature, to ensure an acceleration profile that fits within the envelope presented in figure 1 to meet the requirements of Annex B of AMS1428 [3].

The fixed fan frequency profile selected is presented in figure 82. The profile chosen was that of Kilfrost ABC-3 at -10°C. The Kilfrost fluid was chosen because it was the only fluid in the test set which was part of the original Boeing report [5] that set the FPET test method; -10°C was chosen as an intermediate temperature range.

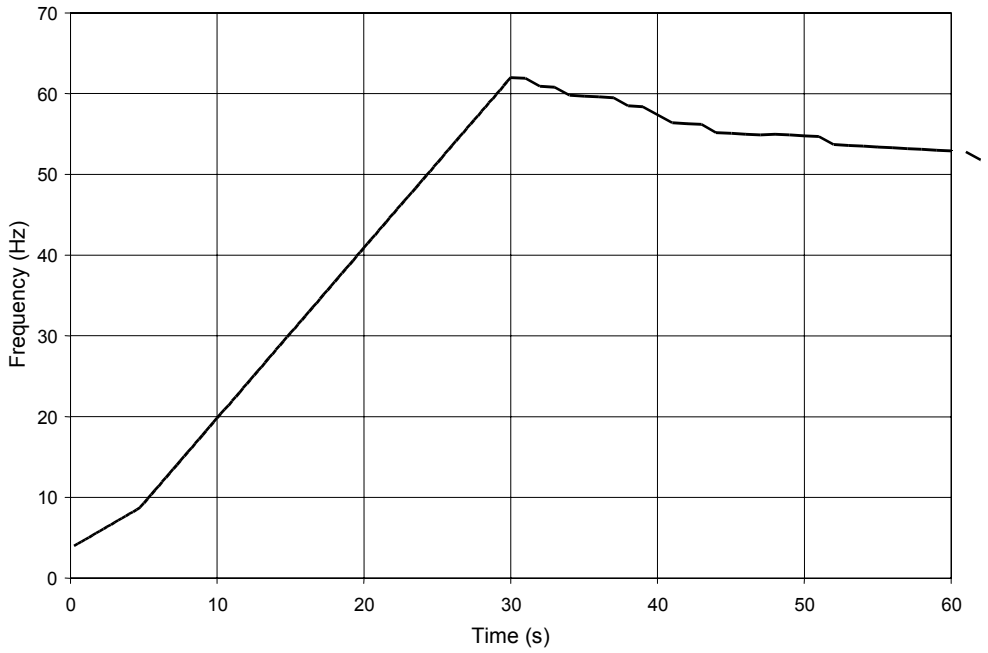

FIGURE 82. FAN ACCELERATION PROFILE FOR KILFROST ABC-3 AT -10°C

4.2.1 Kilfrost ABC-3.

Table 14 presents the aerodynamic acceptance test results of Kilfrost ABC-3 tested according to the fixed ramp of figure 82. Figure 83 compares the results with that of a normal certification ramp where the acceleration profile was adjusted according to temperature and fluid. In effect, these certification ramp tests are from the 2-mm initial thickness of section 3.2. Since the test runs were not performed simultaneously, both acceptance criteria limits are presented. The graph shows that relative to the respective acceptance criteria, there is no apparent difference between the results obtained with both ramps. However, this is to be expected, since the fixed ramp is based on this fluid at -10°C. Figure 84 presents the percentage fluid elimination for both ramps and shows no apparent difference. Figure 85 shows the maximum wave height for both ramp test series; it also shows no apparent difference in the values with both ramps.

TABLE 14. AERODYNAMIC PERFORMANCE TEST DATA WITH FIXED RAMP FOR KILFROST ABC-3

Fluid Code	Test Code	T_a (°C)	T_f (°C)	r.h. (%)	t_o [1] (µm)	t_{end} [2] (µm)	F.E. [3] (%)	W.C. [4] (%)	V [5] (m/s)	δ* (mm)	δ max (mm)	t [6] (sec)	Maximum Wave Height (mm)
E-607	FP-839	-0.1	-0.7	80.2	2000	178	91.1	2.08	68.1	7.04	16.43	11	5
E-607	FP-840	0.1	-1.0	80.2	2000	170	91.5	1.39	68.0	7.05	16.51	12	5
E-607	FP-841	0.2	-1.3	80.0	2000	185	90.7	2.26	68.3	7.11	16.42	13	5
E-607	FP-845	-9.8	-9.0	71.9	2000	229	88.6	0.35	66.9	7.34	16.21	11	5
E-607	FP-846	-10.5	-9.2	66.6	2000	221	89.0	0.52	66.9	7.41	16.46	12	5
E-607	FP-847	-10.7	-9.7	66.0	2000	196	90.2	-0.17	67.3	7.35	16.34	12	6
E-607	FP-853	-26.9	-24.3	49.4	1975	236	88.0	0.17	62.6	8.42	16.26	12	5
E-607	FP-851	-26.9	-24.4	51.5	1975	229	88.4	0.00	62.9	8.29	16.57	13	5
E-607	FP-852	-26.9	-24.4	49.3	1975	221	88.8	0.17	62.5	8.56	16.05	13	5

Acceptance Criteria for Type II Fluid Series: $D_0 = 8.44$ mm, $D_{-10} = 9.14$ mm, $D_{-15} = 9.49$ mm, $D_{-20} = 9.84$ mm

[1] Thickness of the fluid measured at the beginning of the test.
[2] Thickness of the fluid measured at the end of the test.
[3] Fluid Elimination.
[4] Water Change.
[5] Air velocity 30 seconds after the beginning of the test.
[6] Time of maximum wave height.

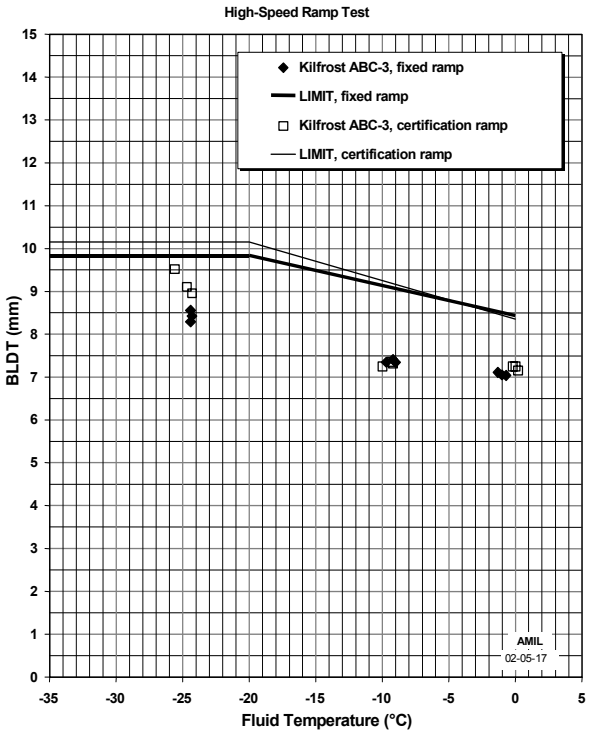

FIGURE 83. BOUNDARY LAYER DISPLACEMENT THICKNESS AERODYNAMIC PERFORMANCE FOR KILFROST ABC-3

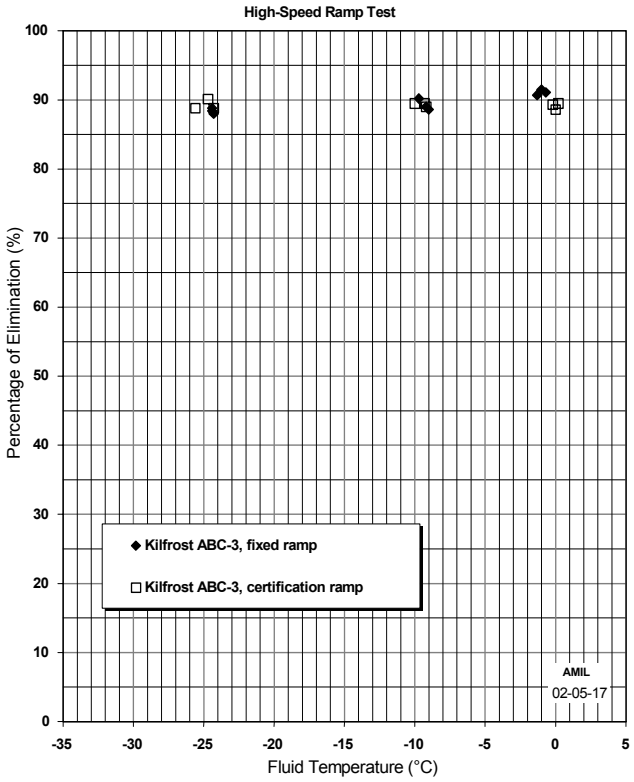

FIGURE 84. FLUID ELIMINATION FOR KILFROST ABC-3

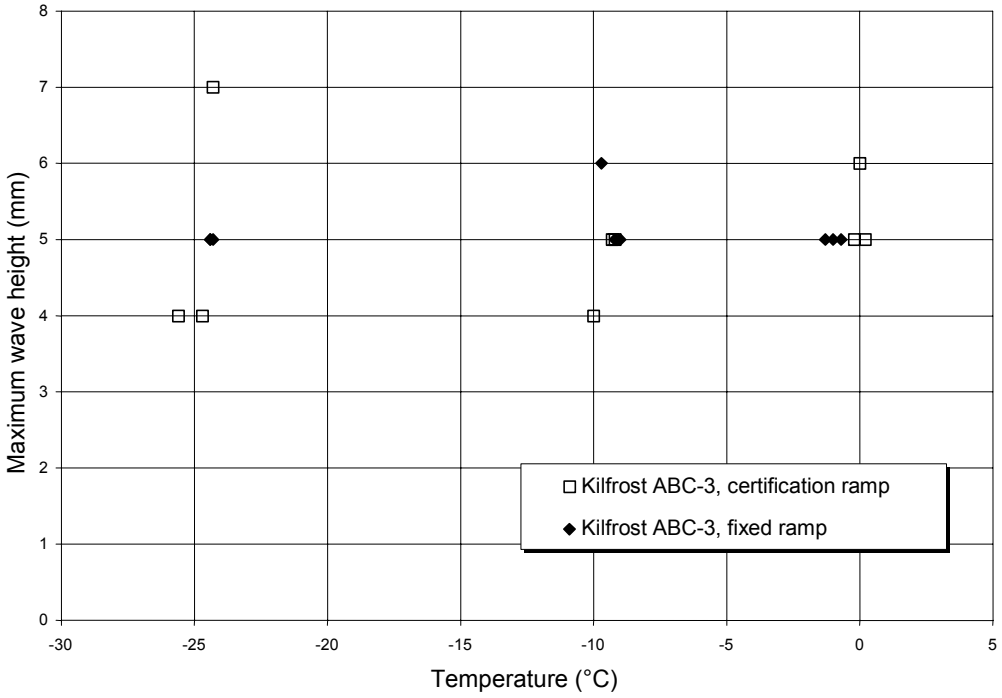

FIGURE 85. MAXIMUM WAVE HEIGHTS FOR BOTH RAMPS, KILFROST ABC-3

4.2.2 Clariant Safewing MPII 1951.

Table 15 presents the aerodynamic acceptance test results of Clariant Safewing MPII 1951 tested according to the fixed ramp of figure 82. Figure 86 compares the results with that of a normal certification ramp where the acceleration profiles were adjusted according to temperature and fluid. Since the test runs were not performed simultaneously, both acceptance criteria limits are presented. The graph shows that with the fixed ramp, the BLDT values are higher, at -25°C, relative to its acceptance limit. Figure 88 presents an example of an acceleration profile for Clariant Safewing MPII 1951 at 0°C, all of which are presented in the annexes. The graph shows how, with the fixed ramp, the wind speed increases to 70 m/s outside the acceptable limit. This effect may be giving more push to the fluid at 0°C. This is probably due to the high-energy requirements for Kilfrost ABC-3, as shown in figure 58. However, this figure also shows that Clariant Safewing MPII 1951 had similar energy requirements. The wind speed is within the envelope (figure 89) at -25°C, the temperature at which there is a difference in BLDTs. Figure 87 shows little or no difference in the fluid elimination percent values. Figure 90 shows similar wave heights for 0° and -10°C but higher maximum wave heights at -25°C for the fixed ramp.

TABLE 15. AERODYNAMIC PERFORMANCE TEST DATA WITH FIXED RAMP FOR CLARIANT SAFEWING MPII 1951

Fluid Code	Test Code	T_a (°C)	T_f (°C)	r.h. (%)	t_o [1] (µm)	t_{end} [2] (µm)	F.E. [3] (%)	W.C. [4] (%)	V [5] (m/s)	δ* (mm)	δ max (mm)	t [6] (sec)	Maximum Wave Height (mm)
E-618	FP-844	0.3	0.1	82.5	2000	196	90.2	1.65	72.4	5.68	16.27	12	6
E-618	FP-842	0.3	0.0	81.0	2000	196	90.2	1.28	71.9	5.64	16.13	12	6
E-618	FP-843	-1.2	-0.2	74.4	2000	196	90.2	0.55	71.9	5.69	16.18	11	5
E-618	FP-848	-10.1	-9.2	68.4	1975	178	91.0	0.37	68.8	6.78	16.43	12	5
E-618	FP-849	-10.3	-9.2	69.4	1975	185	90.6	0.18	68.7	6.78	16.16	12	5
E-618	FP-850	-10.9	-9.5	66.9	1975	203	89.7	0.18	68.8	6.86	16.74	11	6
E-618	FP-856	-26.5	-24.3	51.4	1975	229	88.4	0.18	64.0	7.65	16.66	12	7
E-618	FP-855	-26.9	-24.7	50.4	1975	211	89.3	0.00	63.6	7.78	16.64	13	7
E-618	FP-854	-27.1	-24.9	53.2	1975	196	90.1	0.37	64.0	7.51	16.55	n.m.	7

Acceptance Criteria for Type II Fluid Series: D_0 = 8.44 mm, D_{-10} = 9.14 mm, D_{-15} = 9.49 mm, D_{-20} = 9.84 mm

[1] Thickness of the fluid measured at the beginning of the test.
[2] Thickness of the fluid measured at the end of the test.
[3] Fluid Elimination.
[4] Water Change.
[5] Air velocity 30 seconds after the beginning of the test.
[6] Time of maximum wave height.

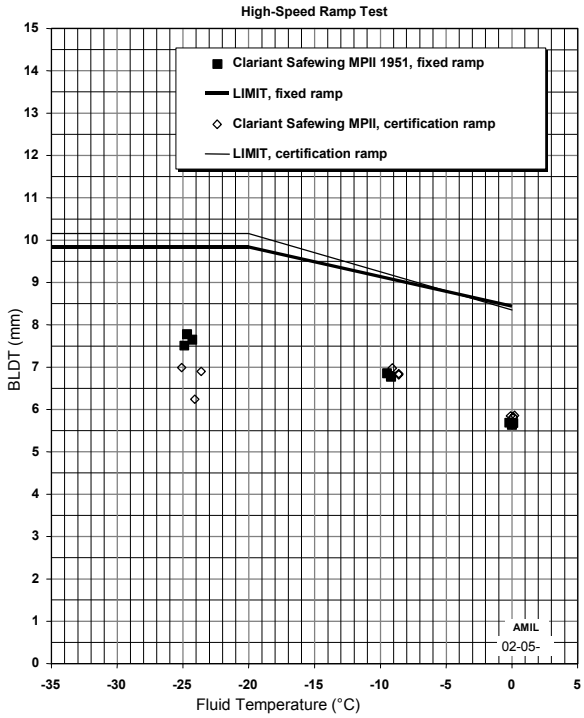

FIGURE 86. BOUNDARY LAYER DISPLACEMENT THICKNESS AERODYNAMIC PERFORMANCE FOR CLARIANT SAFEWING MPII 1951

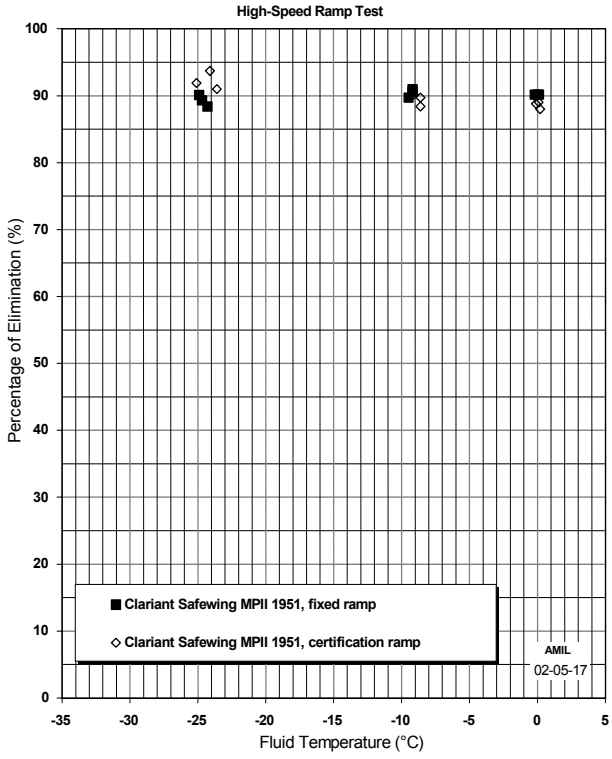

FIGURE 87. FLUID ELIMINATION FOR CLARIANT SAFEWING MPII 1951

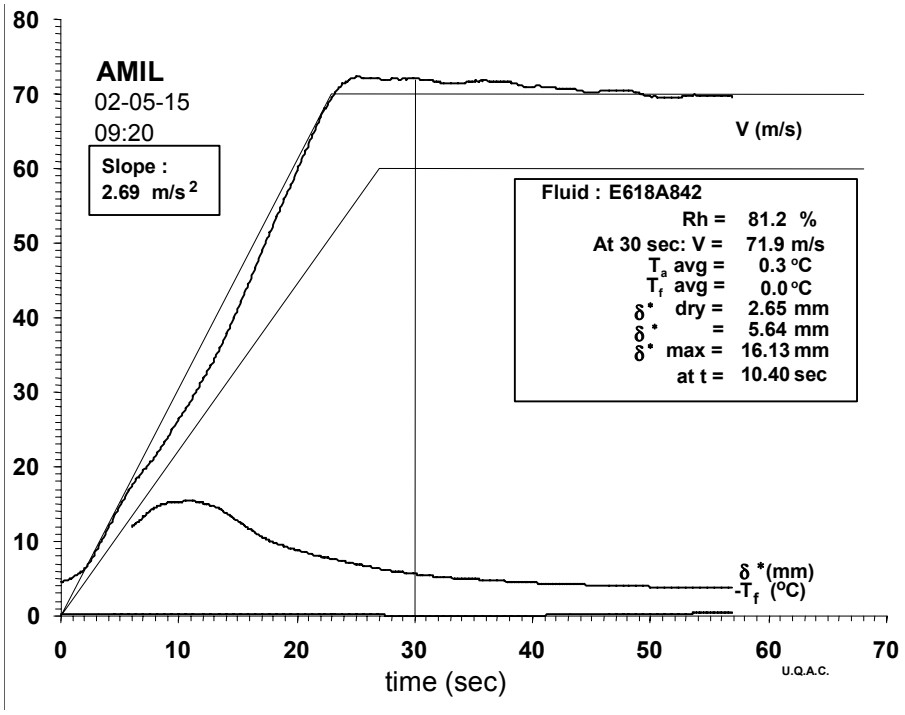

FIGURE 88. EXAMPLE OF FIXED RAMP TEST AT 0°C—CLARIANT SAFEWING MPII 1951

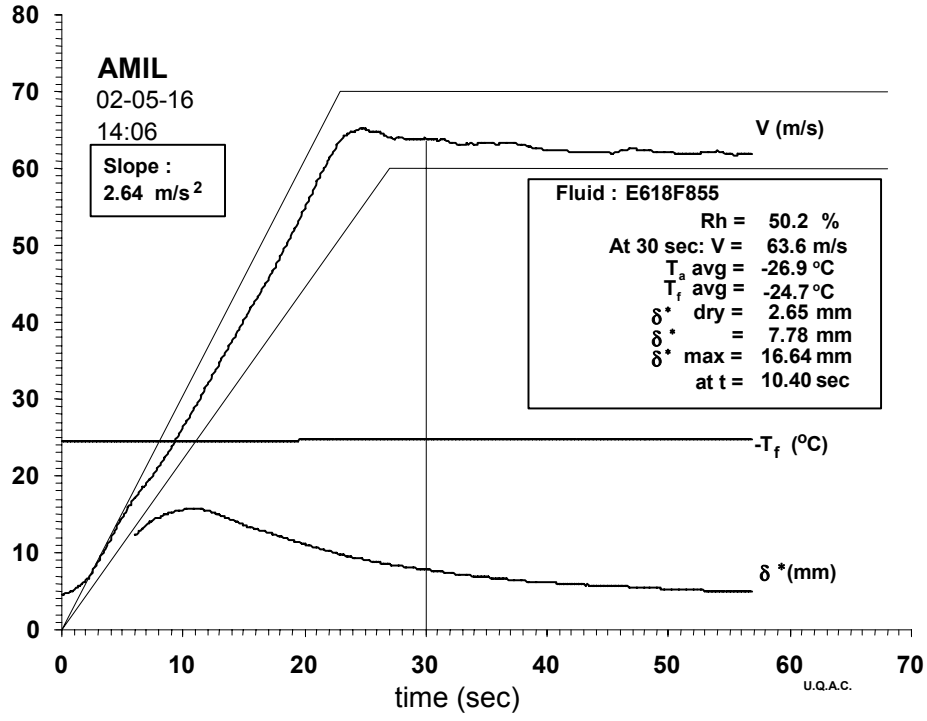

FIGURE 89. EXAMPLE OF FIXED RAMP TEST AT -25°C—CLARIANT SAFEWING MPII 1951

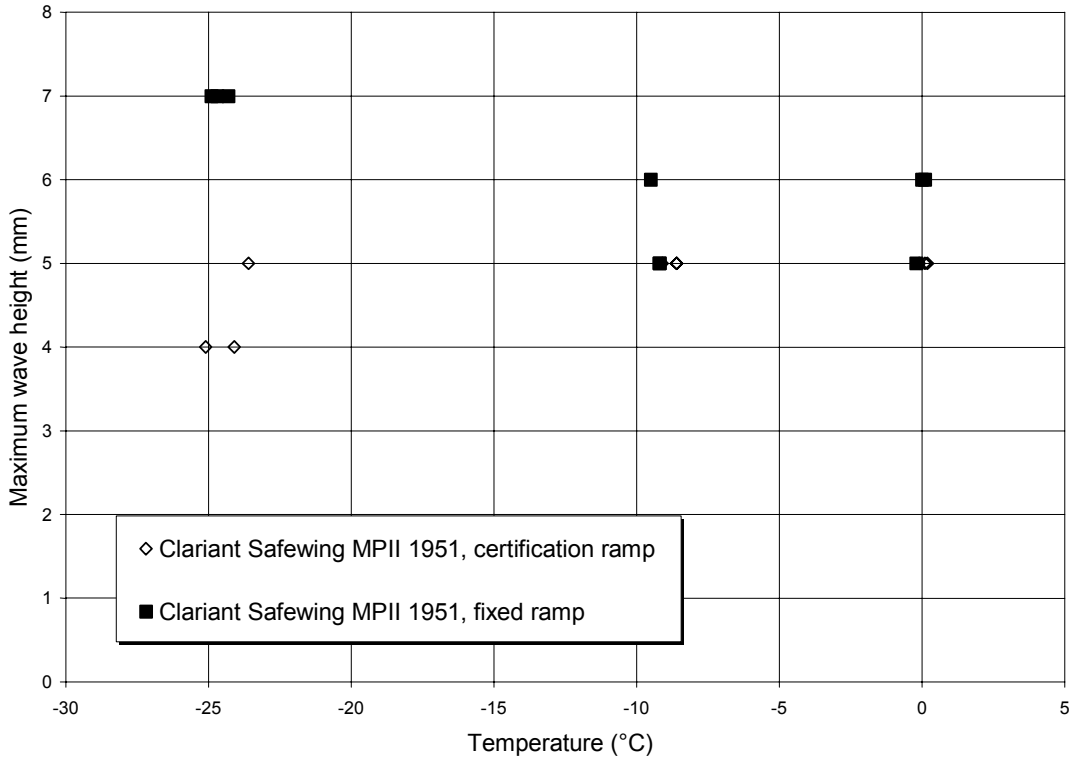

FIGURE 90. MAXIMUM WAVE HEIGHTS FOR BOTH RAMPS, CLARIANT SAFEWING MPII 1951

4.2.3 Octagon Process MaxFlight.

Table 16 presents the aerodynamic acceptance test results of Octagon Process MaxFlight tested according to the fixed ramp of figure 82. Figure 91 compares the results with a normal certification ramp where the acceleration profile was adjusted according to temperature and fluid. Since the test runs were not performed simultaneously, both acceptance criteria limits are presented; however, in this case and for all the Type IV fluids, the limits are essentially the same. The graph shows that there is little or no significant difference between the values obtained with both ramps. Figure 92 presents the fluid elimination data and shows no apparent difference between the values obtained with both ramps. Figure 93 shows that there is no apparent difference in the maximum wave heights for both ramps.

TABLE 16. AERODYNAMIC PERFORMANCE TEST DATA WITH FIXED RAMP FOR OCTAGON PROCESS MAXFLIGHT

Fluid Code	Test Code	T_a (°C)	T_f (°C)	r.h. (%)	t_o [1] (μm)	t_{end} [2] (μm)	F.E. [3] (%)	W.C. [4] (%)	V [5] (m/s)	δ* (mm)	δ max (mm)	t [6] (sec)	Maximum Wave Height (mm)
E-583	FP-819	-0.6	0.3	82.7	2000	185	90.7	1.72	67.0	7.35	16.45	13	6
E-583	FP-814	0.3	0.1	90.3	1975	160	91.9	2.24	67.5	7.38	16.31	14	5
E-583	FP-815	-1.2	-0.3	80.3	2000	178	91.1	1.72	66.9	7.51	16.83	14	6
E-583	FP-824	-9.1	-9.0	72.6	2000	229	88.6	1.55	68.1	7.11	16.26	14	6
E-583	FP-825	-10.6	-9.5	67.3	2000	229	88.6	0.86	67.4	7.20	16.70	11	7
E-583	FP-826	-10.3	-9.7	69.3	2000	262	86.9	0.17	67.4	7.26	16.96	13	6
E-583	FP-834	-26.9	-24.0	52.6	2000	203	89.8	0.17	65.2	8.56	16.31	12	4
E-583	FP-833	-26.5	-24.1	55.8	1975	160	91.9	-0.17	65.0	8.38	16.31	12	4
E-583	FP-835	-27.9	-24.9	47.7	2000	203	89.8	0.17	64.0	8.73	16.02	11	5

Acceptance Criteria for Type II Fluid Series: $D_0 = 7.97$ mm, $D_{-10} = 9.00$ mm, $D_{-15} = 9.52$ mm, $D_{-20} = 10.03$ mm

[1] Thickness of the fluid measured at the beginning of the test.
[2] Thickness of the fluid measured at the end of the test.
[3] Fluid Elimination.
[4] Water Change.
[5] Air velocity 30 seconds after the beginning of the test.
[6] Time of maximum wave height.

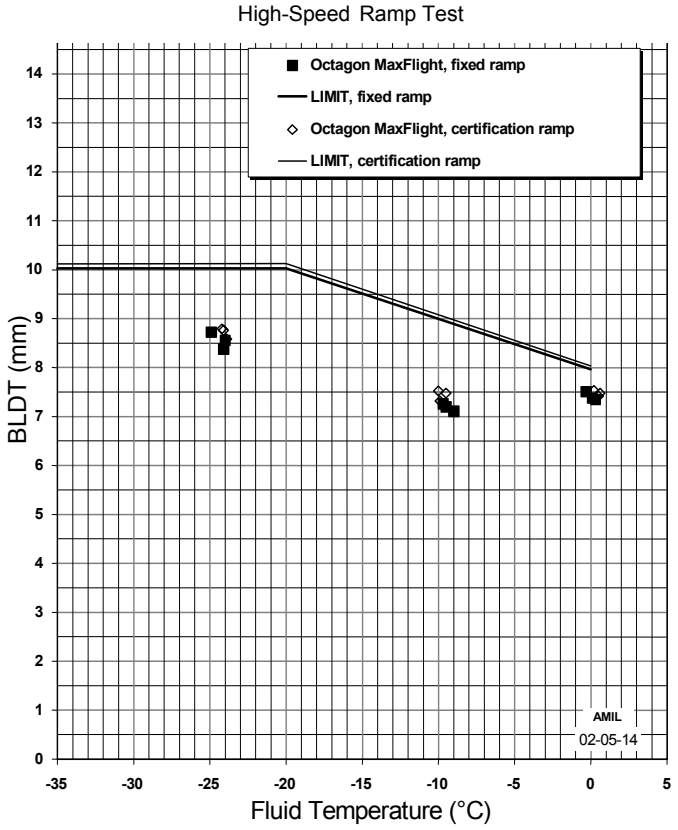

FIGURE 91. BOUNDARY LAYER DISPLACEMENT THICKNESS AERODYNAMIC PERFORMANCE FOR OCTAGON PROCESS MAXFLIGHT

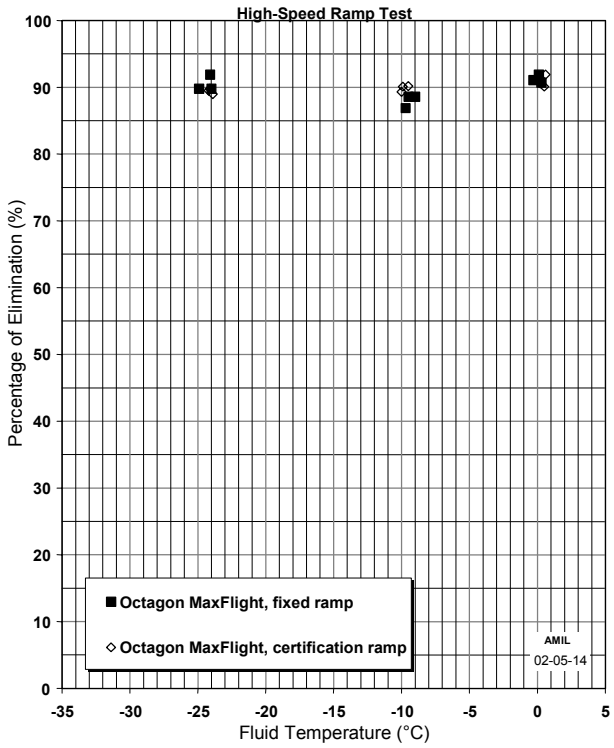

FIGURE 92. FLUID ELIMINATION FOR OCTAGON PROCESS MAXFLIGHT

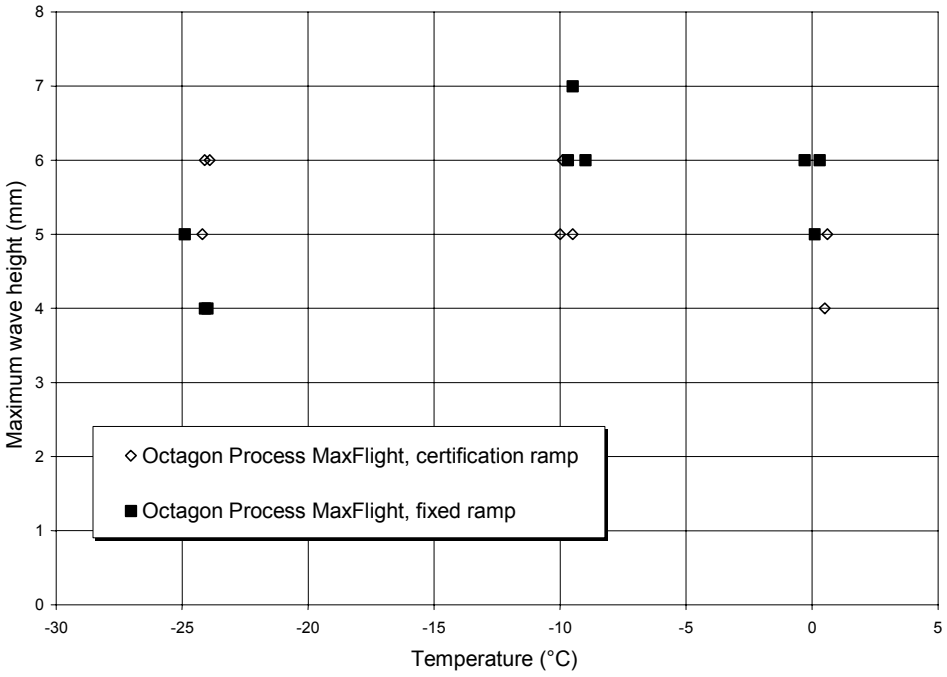

FIGURE 93. MAXIMUM WAVE HEIGHTS FOR BOTH RAMPS, OCTAGON PROCESS MAXFLIGHT

4.2.4 SPCA AD-480.

Table 17 presents the aerodynamic acceptance test results of SPCA AD-480 tested according to the fixed ramp of figure 82. Figure 94 compares the results with a normal certification ramp where the acceleration profile was adjusted according to temperature and fluid. The figure shows similar results at 0° and -25°C for both ramps but somewhat higher BLDT at -10°C for the certification ramp; however, this may be within the error. Figure 96 presents the test data for a fixed ramp test run of SPCA AD-480 at -10°C. The graph shows an acceleration profile near the upper limit of the acceptable envelope, which may explain the slight differences at -10°C for SPCA AD-480. Figure 95 shows little or no apparent difference between the fluid elimination values for both ramps. Figure 97 shows no apparent difference in the maximum wave heights for both ramps.

TABLE 17. AERODYNAMIC PERFORMANCE TEST DATA WITH FIXED RAMP FOR SPCA AD-480

Fluid Code	Test Code	T_a (°C)	T_f (°C)	r.h. (%)	t_o [1] (µm)	t_{end} [2] (µm)	F.E. [3] (%)	W.C. [4] (%)	V [5] (m/s)	δ* (mm)	δ max (mm)	t [6] (sec)	Maximum Wave Height (mm)
E-007	FP-810	-0.1	-0.8	87.1	2000	152	92.4	2.71	69.6	6.42	16.35	13	5
E-007	FP-811	0.9	-0.9	90.3	2000	211	89.5	2.71	69.8	6.41	16.34	14	6
E-007	FP-812	-1.4	-1.6	79.8	2000	178	91.1	1.69	69.1	6.60	16.22	15	7
E-007	FP-821	-9.6	-9.0	71.4	2000	203	89.8	0.85	66.7	7.71	16.37	14	6
E-007	FP-822	-10.1	-9.3	68.7	2000	203	89.8	0.17	67.8	7.42	16.24	14	5
E-007	FP-823	-10.8	-9.8	66.4	1975	203	89.7	0.17	68.5	7.05	16.29	15	5
E-007	FP-832	-26.7	-24.2	53.3	1975	185	90.6	-0.68	66.3	8.20	15.48	14	5
E-007	FP-831	-27.2	-24.3	53.7	1975	196	90.1	-0.17	66.0	8.39	15.54	14	5
E-007	FP-830	-26.8	-24.5	55.4	1975	185	90.6	0.00	66.0	8.25	15.43	13	4

Acceptance Criteria for Type II Fluid Series: D_0 = 7.97 mm, D_{-10} = 9.00 mm, D_{-15} = 9.52 mm, D_{-20} = 10.03 mm

[1] Thickness of the fluid measured at the beginning of the test.
[2] Thickness of the fluid measured at the end of the test.
[3] Fluid Elimination.
[4] Water Change.
[5] Air velocity 30 seconds after the beginning of the test.
[6] Time of maximum wave height.

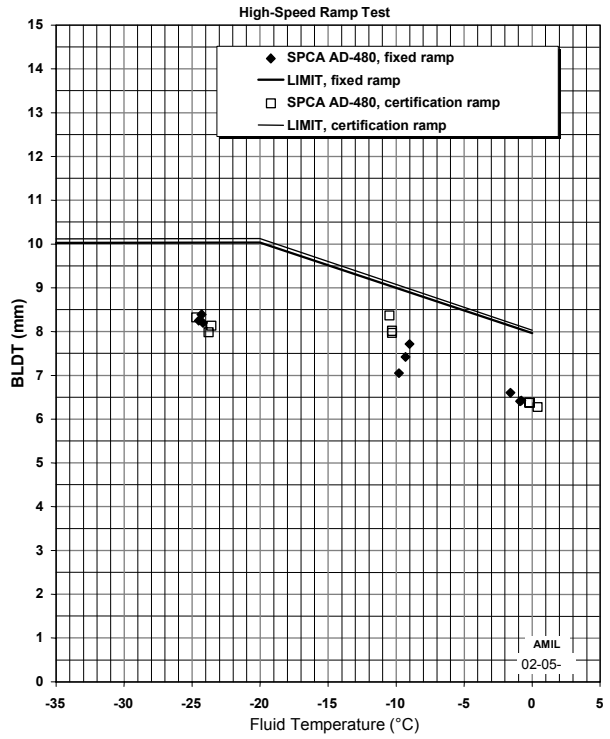

FIGURE 94. BOUNDARY LAYER DISPLACEMENT THICKNESS AERODYNAMIC PERFORMANCE FOR SPCA AD-480

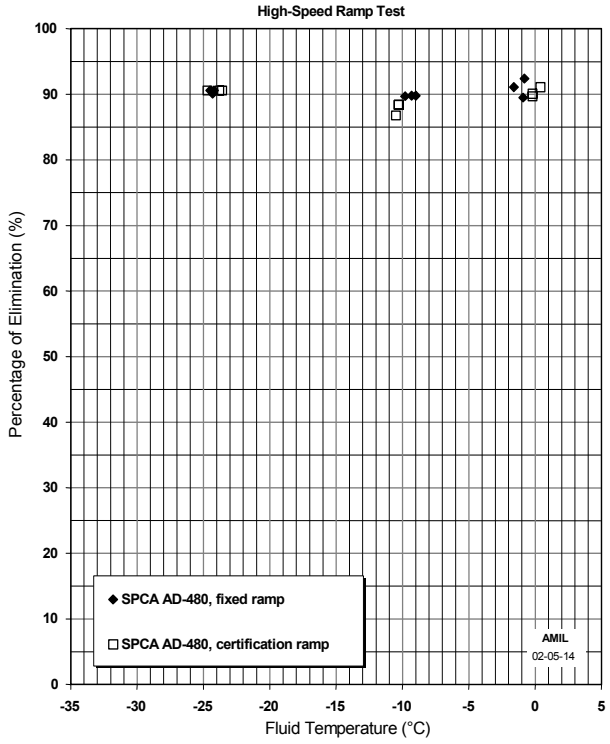

FIGURE 95. FLUID ELIMINATION FOR SPCA AD-480

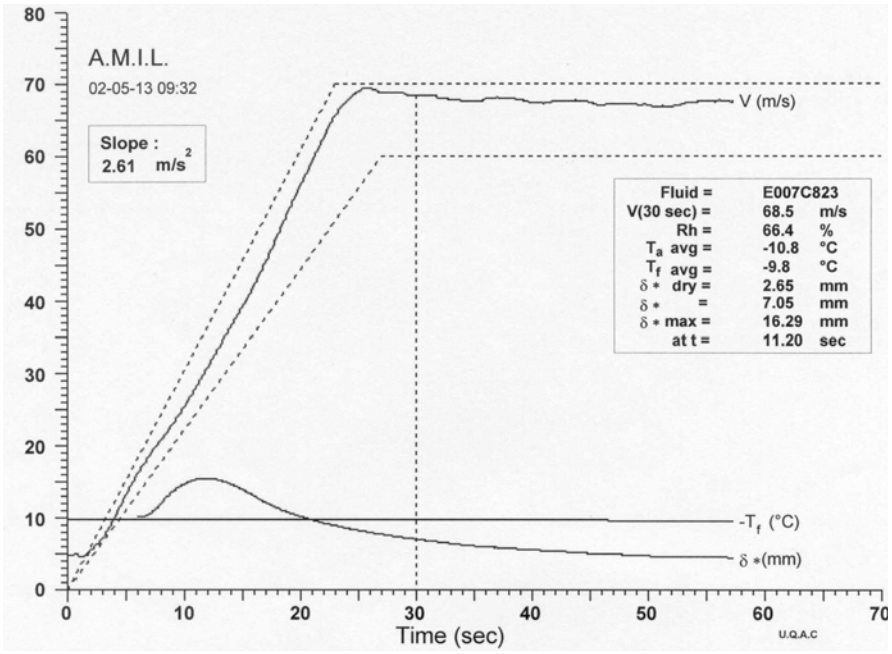

FIGURE 96. EXAMPLE OF FIXED RAMP TEST AT 0°C—SPCA AD-480

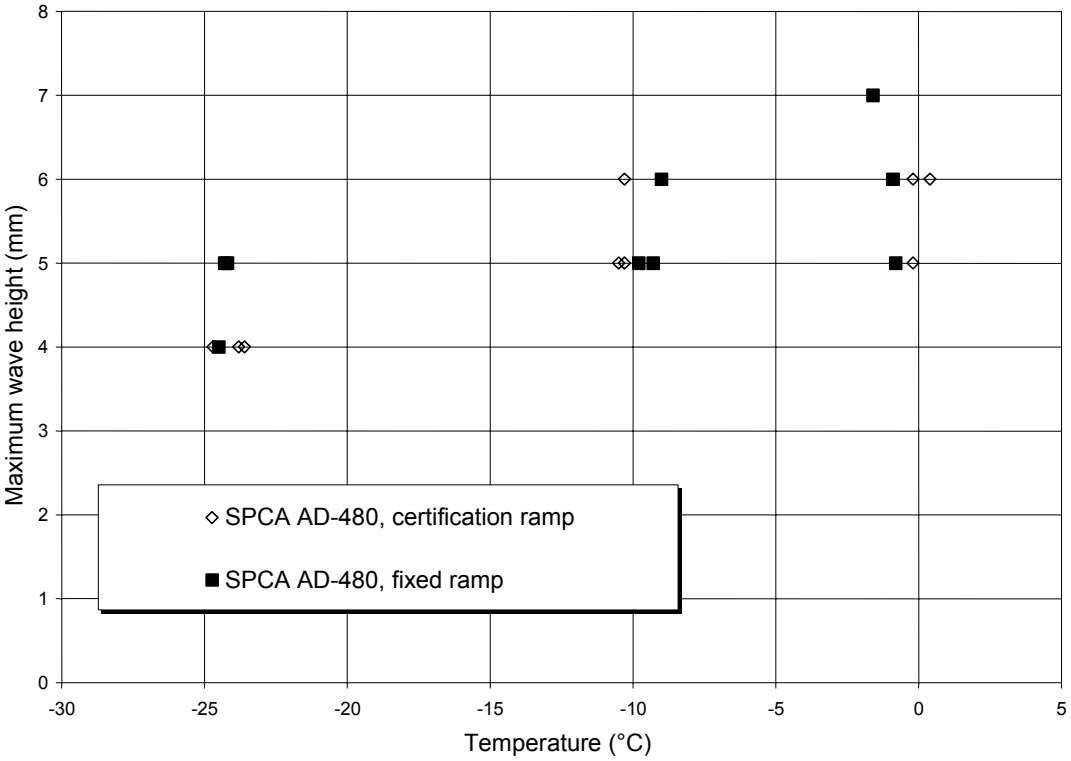

FIGURE 97. MAXIMUM WAVE HEIGHTS FOR BOTH RAMPS, SPCA AD-480

4.2.5 Dow Ultra+.

Table 18 presents the aerodynamic acceptance test results of Dow Ultra+ tested according to the fixed ramp of figure 82. Figure 98 compares the results with a normal certification ramp where the acceleration profile was adjusted according to temperature and fluid. The graph shows more scatter for the fixed ramp values but the certification values occur within the scatter of fixed ramp values. Figure 99 presents the fluid elimination percentage as a function of temperature for both ramps. The figure shows no apparent difference at 0°C but an increasing difference at -10°C with the fixed ramp eliminating more. Figure 100 shows the maximum wave heights as a function of temperature for both ramps. The graph shows that there is no clear difference between the values obtained with both ramps.

TABLE 18. AERODYNAMIC PERFORMANCE TEST DATA WITH FIXED RAMP FOR DOW ULTRA+

Fluid Code	Test Code	T_a (°C)	T_f (°C)	r.h. (%)	t_o[(1)] (µm)	t_{end}[(2)] (µm)	F.E.[(3)] (%)	W.C.[(4)] (%)	V[(5)] (m/s)	δ* (mm)	δ max (mm)	t[(6)] (sec)	Maximum Wave Height (mm)
E-629	FP-820	0.8	1.2	86.7	2000	178	91.1	4.82	72.3	6.06	16.76	14	4
E-629	FP-816	0.6	0.8	90.3	2000	203	89.8	4.52	70.8	6.02	16.78	14	5
E-629	FP-818	-0.2	0.5	84.9	2000	178	91.1	4.22	71.6	6.15	16.67	14	5
E-629	FP-817	-1.5	0.4	79.2	2000	178	91.1	3.46	71.3	6.14	17.04	14	5
E-629	FP-827	-9.2	-8.8	74.4	2000	229	88.6	1.81	69.2	7.01	16.23	15	4
E-629	FP-828	-10.3	-8.9	69.1	2000	236	88.2	1.66	68.7	7.07	16.51	16	3
E-629	FP-829	-10.8	-9.2	67.4	2000	236	88.2	1.20	67.8	7.15	16.26	15	4
E-629	FP-837	-27.1	-24.0	50.3	2000	363	81.8	0.45	61.4	10.25	14.86	19	3
E-629	FP-838	-27.3	-24.1	49.1	1975	389	80.3	-0.45	61.0	10.06	14.54	19	4
E-629	FP-836	-26.9	-24.4	52.8	1975	373	81.1	0.30	61.2	10.13	14.62	19	3

Acceptance Criteria for Type IV Fluid Series: D_0 = 7.97 mm, D_{-10} = 9.00 mm, D_{-15} = 9.52 mm, D_{-20} = 10.03 mm

(1) Thickness of the fluid measured at the beginning of the test.
(2) Thickness of the fluid measured at the end of the test.
(3) Fluid Elimination.
(4) Water Change.
(5) Air velocity 30 seconds after the beginning of the test.
(6) Time of maximum wave height.

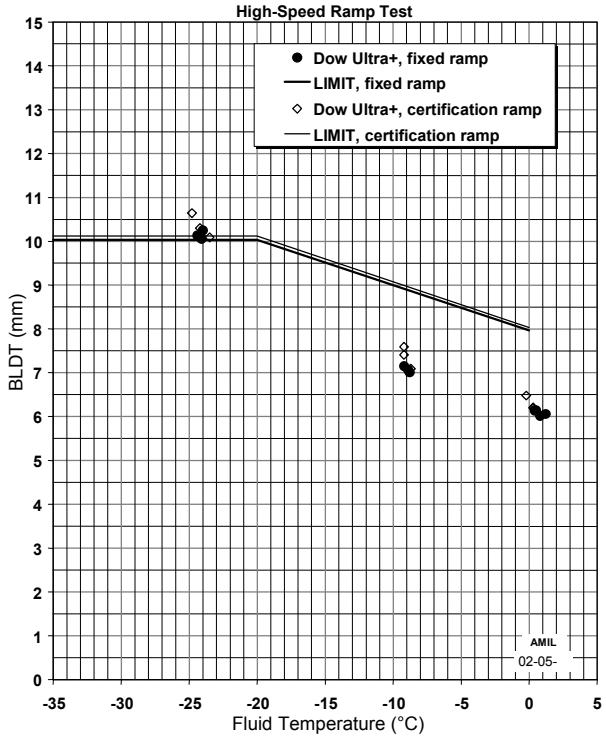

FIGURE 98. BOUNDARY LAYER DISPLACEMENT THICKNESS AERODYNAMIC PERFORMANCE FOR DOW ULTRA+

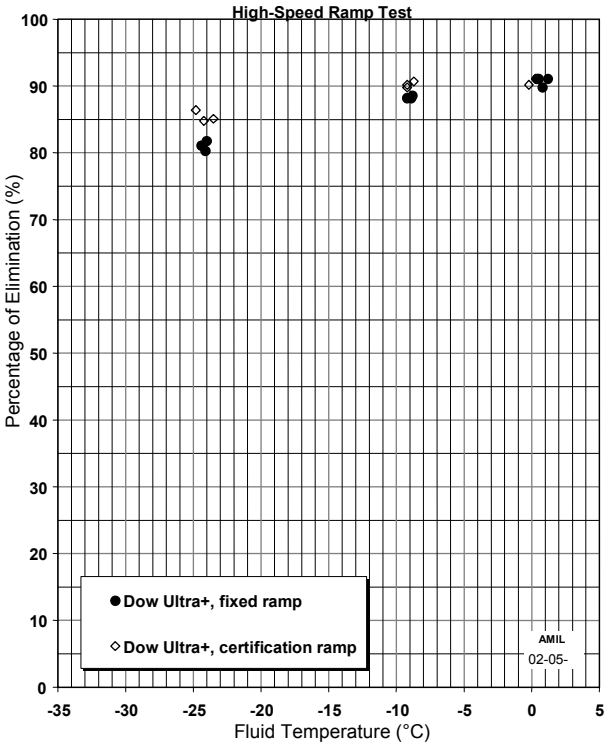

FIGURE 99. FLUID ELIMINATION FOR DOW ULTRA+

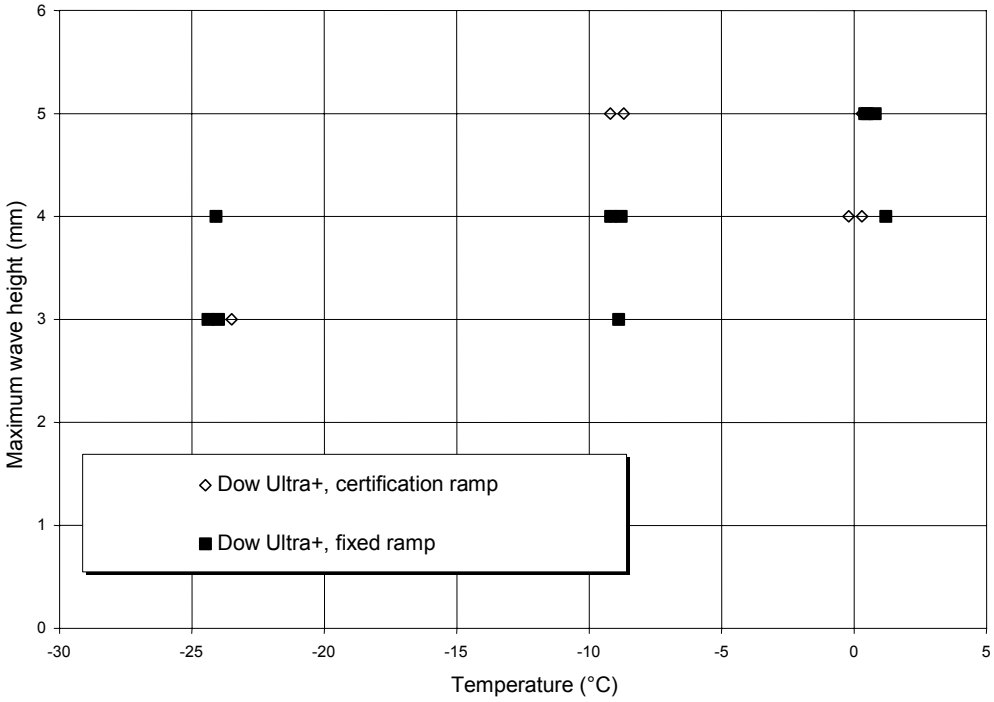

FIGURE 100. MAXIMUM WAVE HEIGHTS FOR BOTH RAMPS, DOW ULTRA+

4.2.6 Fixed Fan Acceleration Profile—Summary.

For the five fluids tested with the fixed ramp, there was little difference seen in the BLDT at 30 sec. Fluid elimination and maximum wave heights when compared to a certification ramp where the fan frequency (velocity) was adjusted, depending on fluid and temperature to obtain the same acceleration profile, were unremarkable. For Kilfrost ABC-3, Octagon Process MaxFlight, and Dow Ultra+, there was no difference. For Clariant Safewing MPII 1951, the fixed ramp resulted in higher BLDT values at -25°C. For SPCA AD-480, at -10°C, the certification ramp had somewhat higher values but possibly within the error of the test.

5. CONCLUSIONS.

5.1 BOUNDARY LAYER DISPLACEMENT THICKNESS COMPARISONS.

Comparisons of the (1) Boundary Layer Displacement Thickness (BLDT) at 30 sec,. (2) BLDT at 30 sec. (with respect to the acceptance criteria limit), (3) maximum BLDT, (4) time of maximum BLDT, (5) fluid elimination, and (6) BLDT at 50 sec. showed no clear difference between Type II and Type IV fluids.

A parallel study done on the merging of the upper and lower boundary layers showed that for a sample fluid the test section merges at 1.16 m from its entry. The study also showed that at station 3 where the BLDT is measured for a certification FPET, 1.55 m from the entry, the maximum BLDT that can be measured was 17 mm. So that the boundary layer thicknesses do

not merge, the required box height at the output would be 117.42 mm, 8 mm higher than it currently is. However, to measure the BLDT at 30 sec. for a certification FPET, which is usually below about 10 mm to be acceptable, the current box height is more than adequate.

5.2 DIFFERENT INITIAL FLUID THICKNESSES.

The examination of BLDT and elimination data from the FPET on two Type II fluids and three Type IV fluids with initial fluid thicknesses of 1, 2, and 4 mm showed that for four of the five fluids the initial fluid thickness had little or no effect on the BLDT and fluid elimination. However, for one of the Type IV fluids, there was some difference with the 4-mm initial thickness at -25°C, where higher BLDT measurements and more fluid remaining on the test section floor following the test were noted. These higher BLDT values may be partially due to the fact that for this fluid -25°C is very near to its acceptable limit, a point at which all fluids tend to show much variation in BLDT measurements. Therefore, the initial fluid thickness may only have an effect on a fluid at critical temperatures, near where the fluid begins to fail.

5.3 ENERGY REQUIRED.

A comparison was made between the amount of energy and the energy factor, which takes into account the energy lost outside the test section, between Type II and Type IV fluids. The results showed that more energy was required to move the Type II fluids compared to the Type IV fluids.

The energy required to move the test fluids with three different initial thicknesses was calculated. The data showed that in most cases it was the 4-mm thickness that required the most energy. For some cases there was no difference. In most cases the 4-mm thickness required about 5% more energy. The only exception was one Type IV fluid, which required 10% more energy factor at 30 sec.

FPET were run using the same fan acceleration profile for all fluids at all temperatures. For three of the five fluids tested with the fixed ramp, there was little difference seen in the BLDT at 30 sec., the fluid elimination, and the maximum wave heights when compared to a test with a certification ramp, where the fan frequency was adjusted, depending on fluid and temperature to obtain the same acceleration profile. The two other fluids had slightly higher BLDT values for the fixed ramp, possibly within error.

6. RECOMMENDATIONS.

a. Given the fact that BLDT and fluid elimination data are similar and Type II fluids require more energy to move them, no need is seen for a different certification process of Type IV fluids compared to Type II fluids.

b. The energy requirements needed to certify the aerodynamic acceptance of new fluids should be measured to ensure that they present similar levels of performance to the existing Type II and Type IV fluids.

c. The preliminary testing does not indicate a need for full-scale or model airfoil testing on Type IV fluids.

A study is recommended to investigate testing with a modified test section box where the boundary layers do not merge.

7. REFERENCES.

1. Bakken, R., "De/Anti-icing Type II/IV Fluid Effects on MD-80 and DC-9 Aircraft," Presentation From the SAE G-12 Fluids Subcommittee Minutes, New Orleans, May 2001.

2. Bakken, R., Jacobsen, U., Jensen, E., and Aalvik, M., "Videotaping Thickened Fluids Flow-Off Characteristics - Test Results SAS - Report # TK-10442-Test Results," 2001.

3. SAE Aerospace, "Material Specifications AMS1428D Fluid Aircraft De/Anti-Icing, Non Newtonian (pseudo-plastic) SAE Type II, Type III and Type IV," February 2002.

4. Aerospace Standard AS5900, "Standard Test Method for Aerodynamic Acceptance of SAE AMS1424 and SAE AMS1428 Aircraft De/Anti-Icing Fluids," Proposed Draft G-12 Committee Meeting, Frankfurt, June 2002.

5. Hill, E.G., "Aerodynamic Acceptance Test for Aircraft Ground Deicing/Anti-Icing Fluids," Boeing Document D6-55573, October 1990.

6. Laforte, J.-L., Bouchard, G., and Louchez, P.R., "Aerodynamic Acceptance Testing of Aircraft Ground De/Anti-Icing Fluids Flat Plate Elimination Tests," prepared for Transportation Development Centre, Transport Canada, TP11078E, 1991.

7. Laforte, J.-L., Bouchard, G., and Louchez, P.R., "A Proposal of Aerodynamic Acceptance Test for Aircraft Ground De-Icing/Anti-Icing Fluids," prepared for Transportation Development Centre, Transport Canada, TP11170E, 1992.

8. Minutes of the SAE G-12 Fluids Subcommittee Aerodynamics Working Group, Montreal, November 2001.

9. White, F., *Fluid Mechanics 3rd ed.* McGraw-Hill Inc., USA, 1994, p. 402.

10. Pankhurst, R.C. and Holder, D.W., *Wind Tunnel Technique, an Account of Experimental Methods in Low and High Speed Wind Tunnels*, Sir Isaac Pitman & Sons Ltd., London, 1968.

11. Mehta, R.D. and Bradshaw, P. "Design Rules for Small Low Speed Wind Tunnels," in *Aeronautical Journal of the Royal Aeronautical Society*, November 1979, pp. 443-449.